Title 40 CFR Part 191
Compliance Certification
Application
for the
Waste Isolation Pilot Plant

Appendix SOTERM

United States Department of Energy
Waste Isolation Pilot Plant

Carlsbad Area Office
Carlsbad, New Mexico

Source Term

CONTENTS

ACRONYMS ..... SOTERM-v

APPENDIX SOTERM SOTERM-1

SOTERM.1 Introduction SOTERM-1

SOTERM.2 Conceptual Framework of Chemical Conditions SOTERM-2
SOTERM.2.1 Ambient Geochemical Conditions SOTERM-2
SOTERM.2.2 Repository Chemical Conditions SOTERM-2
SOTERM.2.2.1 Brine SOTERM-3
SOTERM.2.2.2 Microbial Degradation of Organic Materials SOTERM-4
SOTERM.2.2.3 Corrosion of Steels and Other Metals SOTERM-19
SOTERM.2.2.4 Other Effects SOTERM-20
SOTERM.2.2.5 Summary SOTERM-21

SOTERM.3 Prediction of Dissolved Actinide Solubility SOTERM-21
SOTERM.3.1 Previous Approaches to Estimating Actinide Solubility in the WIPP SOTERM-21
SOTERM.3.2 Selection of the Pitzer Activity Coefficient Model SOTERM-22
SOTERM.3.3 The FMT Computer Code SOTERM-23
SOTERM.3.4 Overview of the Experimental Data SOTERM-25
SOTERM.3.4.1 The III Actinides: Am(III), Pu(III), Cm (III) and the Lanthanide Analog Nd(III) SOTERM-25
SOTERM.3.4.2 The IV Actinides: Th (IV), U(IV), Pu(IV), Np(IV) SOTERM-26
SOTERM.3.4.3 The V Actinides: Np(V) SOTERM-27
SOTERM.3.4.4 The VI Actinides: U(VI) SOTERM-27
SOTERM.3.5 Calculations of Actinide Solubility Using the FMT Computer Code SOTERM-28
SOTERM.3.6 Use of FMT Results in Performance Assessment SOTERM-28

SOTERM.4 Oxidation State Distribution of the Actinides in Solution SOTERM-33
SOTERM.4.1 Thorium SOTERM-33
SOTERM.4.2 Uranium SOTERM-33
SOTERM.4.3 Neptunium SOTERM-34
SOTERM.4.4 Americium SOTERM-34
SOTERM.4.5 Curium SOTERM-35
SOTERM.4.6 Plutonium SOTERM-35
SOTERM.4.7 Summary of Oxidation State Distribution SOTERM-36

SOTERM.5 The Role of Organic Ligands SOTERM-36

CONTENTS (Continued)

SOTERM.6 Mobile Colloidal Actinide Source Term SOTERM-41
SOTERM.6.1 Introduction SOTERM-41
SOTERM.6.1.1 Formation and Behavior of Colloidal Particles .. SOTERM-42
SOTERM.6.1.2 Definition of Colloidal Particle Types SOTERM-44
SOTERM.6.2 Performance Assessment Implementation SOTERM-45
SOTERM.6.3 Development of Parameter Values SOTERM-45
SOTERM.6.3.1 Mineral Fragment Colloids SOTERM-46
SOTERM.6.3.2 Actinide Intrinsic Colloids SOTERM-51
SOTERM.6.3.3 Humic Substances SOTERM-58
SOTERM.6.3.4 Microbes SOTERM-65
SOTERM.6.3.5 Summary of Parameter Values SOTERM-69
SOTERM.6.4 Summary SOTERM-69

SOTERM.7 Use of the Actinide Source Term in Performance Assessment ... SOTERM-70
SOTERM.7.1 Simplifications SOTERM-70
SOTERM.7.1.1 Elements and Isotopes Modeled SOTERM-70
SOTERM.7.1.2 Use of Brine End Members SOTERM-71
SOTERM.7.1.3 Sample Uncertain Parameters SOTERM-72
SOTERM.7.1.4 Combining the Transport of Dissolved and Colloidal Species in the Salado Formation SOTERM-73
SOTERM.7.2 Construction of Source Term SOTERM-74

REFERENCES SOTERM-80

ATTACHMENTS SOTERM-91

FIGURES

SOTERM-1. The pmH Changes of Salado Brine in the Absence of Added MgO as the Disposal Room is Pressurized with CO_2 Generated by Microbial Reactions SOTERM-7

SOTERM-2. The pmH Changes of Castile Brine in the Absence of Added MgO as the Disposal Room Is Pressurized with CO_2 Generated by Microbial Reactions SOTERM-9

SOTERM-3. EQ3/6 Titration of Hydrated MgO into Salado Brine (Brine A) . SOTERM-11

SOTERM-4. EQ3/6 Titration of Hydrated MgO into Castile Brine (ERDA-6) . SOTERM-13

SOTERM-5a. Chemical-Buffer Distribution for Salado Brine (Brine-A) as a Function of CO_2 Produced and $Mg(OH)_2$[+$Ca(OH)_2$] Added per Kilogram of Water SOTERM-15

SOTERM-5b. Chemical-Buffer Distribution for Castile Brine (ERDA-6) as a Function of CO_2 Produced and $Mg(OH)_2$[+$Ca(OH)_2$] Added per Kilogram of Water SOTERM-17

SOTERM-6. Deviation of 150 Experimental Log Solubilities from the Model-Predicted Values. SOTERM-29

SOTERM-7. Distribution of Actinide Solubility Uncertainty Utilized by Performance Assessment. SOTERM-31

SOTERM-8. Solubility of Pu(IV)-Polymer in NaCl Media as a Function of pcH SOTERM-55

SOTERM-9. Calculations Performed by ALGEBRA for Each Replicate of 100 Realizations to Produce Effective Solubilities for Each Modeled Actinide. SOTERM-75

TABLES

SOTERM-1. Some Chemical Components of WIPP Brines SOTERM-4
SOTERM-2. Solubilities of the Oxidation State Analogs, in moles/liter, with MgO Backfill SOTERM-28
SOTERM-3. Oxidation States of the Actinides in the WIPP As Used in PA .. SOTERM-36
SOTERM-4. Organic Ligand Concentrations in Inundated Repository SOTERM-37
SOTERM-5. Apparent Stability Constants for Organic Ligands and Actinides in NaCl Media SOTERM-39
SOTERM-6. Apparent Stability Constants for Magnesium Complexation with Organic Ligands at High Ionic Strength SOTERM-39
SOTERM-7. Apparent Stability Constants for Organic Ligands with Metals (Martell and Smith 1982, 75, 284, 307, 328). SOTERM-40
SOTERM-8. Material and Parameter Names for Colloids SOTERM-46
SOTERM-9. Experimental Results for Mineral Fragment Colloids SOTERM-50
SOTERM-10. Plutonium Intrinsic Colloid Experiments SOTERM-57
SOTERM-11. Humic Substances Experimental Results SOTERM-60
SOTERM-12. Oxidation State Analogy Substitutions SOTERM-62
SOTERM-13. Microbe Experimental Results SOTERM-67
SOTERM-14. Colloid Concentration Factors SOTERM-69
SOTERM-15. Log Molar Total Maximum Mobilized Concentrations Using Median Parameter Values. SOTERM-79

ACRONYMS

BNL	Brookhaven National Laboratory
CFR	Code of Federal Regulations
DOE	U.S. Department of Energy
DRZ	disturbed rock zone
EDTA	ethylene diamine tetra-acetate
ERDA	U.S. Energy Research and Development Administration
HMW/FW	Harvie-Møller-Weare/Felmy and Weare
LANL	Los Alamos National Laboratory
LLNL	Lawrence Livermore National Laboratory
NIST	National Institute of Standards and Technology
SIT	Specific-ion Interaction Theory
SPC	Salado Primary Constituent
SWCF	Sandia National Laboratories WIPP Central File
TRU	transuranic
TWBIR	Transuranic Waste Baseline Inventory Report
WIPP	Waste Isolation Pilot Plant

1 **THIS PAGE INTENTIONALLY LEFT BLANK**

APPENDIX SOTERM

SOTERM.1 Introduction

The actinide source term at the Waste Isolation Pilot Plant (WIPP) represents the mobile concentration of select actinide elements in the WIPP repository. The source term is the sum of contributions from dissolved actinide species and mobile colloidal actinide species existing in the repository. The actinide source term establishes the mobile concentration of actinides that may move from the repository in brine. Release to the accessible environment in brine may follow a pathway up the sealed operational shafts, out through possible intrusion boreholes, and/or out laterally through Salado Formation interbeds. For a discussion of release scenarios and pathways, see Chapter 6.0 (Section 6.3). Quantification of the impact of these releases contributes directly to assessing compliance with Title 40 Code of Federal Regulations (CFR) Part 191. Direct release to the surface of actinides entrained as particulates with solid waste stemming from drilling, cuttings, and spallings, is not part of the actinide source term as described herein.

The actinide source term is limited to those radionuclides that may significantly impact the performance of the WIPP. Consequently, the actinide source term provides a quantification of mobile concentrations of thorium, uranium, neptunium, plutonium, americium, and curium. Other radionuclides, such as strontium, cesium, and radium, are not included in the actinide source term because of their relatively short half-lives or limited waste inventory (Appendix WCA, Sections WCA.3.2 and WCA.8.3).

Appendix SOTERM (SOurce TERM) focuses on the development of actinide source term parameter values and the implementation of those values in performance assessment calculations. In Section SOTERM.2, an overview of the repository system is presented, including a review of relevant geochemical and chemical constraints on the repository system, the conceptual framework on which the actinide source term is based, simplifications required to develop parameter values, and assumptions made. Sections SOTERM.3 and SOTERM.4 focus on the development of the dissolved actinide solubility parameters and oxidation state distribution, respectively. Section SOTERM.5 focuses on the impact of organic ligands on dissolved actinide concentration. The mobile colloidal actinide source term is described in Section SOTERM.6. In Section SOTERM.7 the performance assessment implementation of the dissolved actinide and colloidal actinide components of the actinide source term is described.

Appendix SOTERM is a supplement to information presented in Sections 6.4.3.4, 6.4.3.5, and 6.4.3.6 of this application.

SOTERM.2 Conceptual Framework of Chemical Conditions

In this section, an overview of the chemistry of the repository system is presented. The ambient geochemical conditions are described first. The effects of human intrusion and waste are then described. Emphasis is placed on how various components and processes within the repository will affect the dissolution and colloidal suspension of actinides. Excess MgO will be added to the repository for assurance purposes, so the effect of MgO is included in this discussion. Simplifications and assumptions used to model the components and processes are discussed in each section.

SOTERM.2.1 Ambient Geochemical Conditions

The Salado is predominantly halite (NaCl), but also contains accessory evaporite minerals such as anhydrite ($CaSO_4$), gypsum ($CaSO_4 \cdot 2H_2O$), polyhalite ($K_2MgCa_2(SO_4)_4 \cdot 2H_2O$), and magnesite ($MgCO_3$). Small quantities of intergranular and intragranular brines are associated with the salt at the repository horizon. These brines are highly concentrated solutions (up to 8 molar) of predominantly Na-Mg-K-Cl-SO_4 with smaller amounts of Ca, CO_3, and B. These brines have been in contact with the evaporite salts for geologic time and are saturated with respect to the evaporite minerals.

Underlying the Salado is the Castile, composed of bedded anhydrite. The Castile in the vicinity of the WIPP site is known to contain localized brine reservoirs under sufficient pressure to force brine to the land surface if penetrated by a borehole. Castile brines are predominantly saturated sodium chloride solutions containing calcium and sulfate, and small concentrations of other elements, and are about eight times more concentrated than sea water. Overlying the Salado in the vicinity of the WIPP site is the Culebra, a fractured dolomite ($CaMg(CO_3)_2$) layer. It is significant because it is expected to be the most transmissive geologic pathway to the accessible environment. Culebra brines are generally more dilute than the Salado and Castile brines, and are predominantly sodium chloride with potassium, magnesium, calcium, sulfate, and carbonate. See Chapter 2.0 (Section 2.4.2) of this application for information on the distribution of Culebra brine salinity.

SOTERM.2.2 Repository Chemical Conditions

Three aspects of the repository chemical environment can have a major impact on the dissolution and colloidal suspension of actinides. These are

- brine composition,
- the microbial degradation of organic waste, and
- corrosion of metallic waste.

For each of these, the effect, the range of possible behavior, and the simplifications used in modeling are discussed.

SOTERM.2.2.1 Brine

Brine required for mobilization of actinides and its composition will affect the quantity of actinide that may be dissolved or suspended. For example, high ionic strength brines have been shown to increase the solubility of actinides and also to increase the coagulation and settling rate of mineral fragment colloids.

In human intrusion scenarios, Salado and/or Castile brine will enter the repository, depending on whether the intrusion penetrates a brine reservoir in the Castile. However, in addition to Salado and Castile brines, brines from the Rustler and Dewey Lake can flow down the borehole to the repository, mix with the waste, and then be forced back up a borehole. Rustler and Dewey Lake brines are considerably less concentrated than Salado and Castile brines. As the Rustler and Dewey Lake brines flow into the repository, they would dissolve Salado halite until they attain compositions between that of Salado and Castile brines (see Section SOTERM.7.1.2). Under any intrusion scenario, therefore, the brine dissolving actinides would have the composition of Salado, Castile, or a mixture of Salado and Castile brines.

The Salado and Castile brine compositions bracket the range of possibilities within the repository, so experiments and modeling of repository chemistry were performed using the end member brines only. Modeling of brine mixing within the performance assessment was considered and rejected because it was not sufficiently accurate to reduce the uncertainty associated with brine mixing and related brine chemistry compared to bracketing this uncertainty with end-member brines. Brine mixing is addressed in Section SOTERM.7.1.2.

Several synthetic brines that simulate brines collected from the Salado, the Castile, and the Culebra were used in the experimental program. Brine A is a synthetic brine often used to simulate the upper range in Salado brine, magnesium concentration and ionic strength, as is SPC (Salado Primary Constituent) Brine, a version of Brine A with the trace elements removed. Synthetic ERDA-6 brine represents Castile brine. The primary chemical components of these brines are given in Table SOTERM-1 (from Brush 1990, pp. 20-22). As is evident in Table SOTERM-1, Salado brine contains high concentrations of magnesium chloride, whereas Castile brine is dominated by sodium chloride and contains bicarbonate.

In addition to using the end member brines, several other simplifying assumptions were made, including the following:

- Brine that may be in the repository is well-mixed with waste.
- Equilibrium with the more available minerals (halite, anhydrite, magnesite) is established. (Reduction-oxidation equilibrium with waste materials is not assumed.)
- For modeling purposes, brine composition is constant in time.

Table SOTERM-1. Some Chemical Components of WIPP Brines (from Brush 1990).

Ion or Chemical Property	Brine A	ERDA-6
Alkalinity (HCO_3^- equivalent, mM)	--	43
B^{3+} (mM)	20	63
Br^- (mM)	10	11
Ca^{2+} (mM)	20	12
Cl- (mM)	5,350	4,800
K^+ (mM)	770	97
Mg^{2+} (mM)	1,440	19
Na^+ (mM)	1,830	4,870
pH	6.5	6.17
SO_4^{2-} (mM)	40	170
TDS (mg/liter)	306,000	330,000

SOTERM.2.2.2 Microbial Degradation of Organic Materials

A large quantity of organic materials, including cellulosics, plastics, and rubber, will be emplaced in the WIPP, and will potentially be degraded by microbes.

There is considerable uncertainty whether significant microbial colonies will be viable in the WIPP for 10,000 years. As discussed in Appendix PAR, the U.S. Department of Energy (DOE) represents that uncertainty by assigning a 50 percent probability of significant microbial gas generation. It is further assumed that, in the event of significant microbial gas generation, there is a 50 percent chance that plastics and rubbers will be biodegraded (Wang and Brush 1996). Microbial degradation of organic carbon may influence actinide mobilization in four ways:

(1) fast reduction of oxidized actinide species, which in most cases are more soluble,

(2) consumption of solubilizing organic ligands,

(3) production of humic and microbial colloids, thereby increasing the amount of actinide sorbed on colloidal surfaces, and

(4) generation of CO_2, which in the absence of added MgO, would increase acidity and carbonate concentrations in the brine and thereby increase actinide solubility.

The first three of these are considered in the analyses that studied the oxidation state distributions (Section SOTERM.4), the effects of organic ligands (Section SOTERM.5), and the effects of colloids (Section SOTERM.6). The effect of CO_2 production is discussed further in this section. The simplifications used in the performance assessment calculations for all four of these effects are discussed at the end of this section.

The inventory of organic material, which includes cellulosics, plastics, and rubbers, is about 10^9 moles of carbon (DOE 1996, 3–13). At the maximum degradation rate of 0.3 mole carbon/kilogram of organic-materials/year in the inundated repository (Wang and Brush 1996), this inventory will be entirely biodegraded within about 200 years after closure. It is expected that the maximum time for complete degradation would be about 2000 years in cases where significant microbial action occurs.

The primary reaction for CO_2 production from organic carbon biodegradation is expected to be

$$C_6H_{10}O_5 + H_2O = 3CH_4 + 3CO_2 \quad (2\text{-}1)$$

Two other reactions can also contribute, although because of the limited amount of nitrate and sulfate relative to organic carbon in the waste (Wang and Brush 1996), the potential amount of CO_2 generated is much less:

$$C_6H_{10}O_5 + 4.8\,HNO_3 = 7.4\,H_2O + 6\,CO_2 + 2.4\,N_2 \quad (2\text{-}2)$$

$$C_6H_{10}O_5 + 3\,H_2SO_4 = 5\,H_2O + 6\,CO_2 + 3\,H_2S \quad (2\text{-}3)$$

The pmH ($-\log_{10}$ of the hydrogen ion molality) of the brine in the repository is a function of the amount of CO_2 dissolved in the brine (in high ionic strength solutions, the pmH is a better indication of acidity than pH, $-\log_{10}$ of the hydrogen ion activity). Figures SOTERM-1 and SOTERM-2 show the dependence of pmH on carbon dioxide fugacity [$f(CO_2)$] for Brine A (Salado brine) and ERDA-6 (Castile brine), respectively, calculated by Wang (1996a and 1996b) using the code EQ3/6 (Wolery 1992; Wolery and Daveler 1992). The range shown in these figures is the range expected only when significant CO_2 generation takes place, and when MgO is not added to the repository. As can be seen in these figures, the pmH may approach 4.5 as the CO_2 fugacity exceeds 50 atm. At these pmH and $f(CO_2)$ conditions, the solubilities of actinides are much higher than at neutral or slightly basic pmH and low $f(CO_2)$. Excess MgO, however, will be emplaced with the waste for assurance purposes, and will buffer the pmH and $f(CO_2)$ of the repository brine to values where the solubility of actinides is minimized. Figures SOTERM-3 and SOTERM-4 show the major minerals and pH obtained with titration of $Mg(OH)_2$ into each of the end member brines.

Hydrated MgO, $Mg(OH)_2$, will react with CO_2 by the reaction

$$Mg(OH)_2 + CO_2 = MgCO_3 + H_2O. \quad (2\text{-}4)$$

This reaction will buffer the CO_2 fugacity at approximately 10^{-7} atm. However, CO_2 can also react with $Ca(OH)_2$ present as cementitious material in the waste by the reaction

$$Ca(OH)_2 + CO_2 = CaCO_3 + H_2O. \quad (2\text{-}5)$$

If the reaction in Equation 2-5 buffered the hydrogen ion molality (pmH) of the repository, the pmH would be high. However, the effect of $Ca(OH)_2$ is minimal, because it will be quickly consumed by reactions 2.5 and 2.6 (reaction with $MgCl_2$ in Salado brine):

$$Ca(OH)_2 + MgCl_2 = CaCl_2 + Mg(OH)_2 \quad (2\text{-}6)$$

Figures SOTERM-5a and 5b show the amounts of generated CO_2, dissolved $Mg(OH)_2$ and $Ca(OH)_2$ that are expected within the repository and the corresponding buffers for each end member brine (Salado and Castile). It is estimated that $2x10^9$ moles of MgO will be added to the repository for assurance and $8x10^6$ moles of $Ca(OH)_2$ will be present as a cementious material in the waste (Storz 1996). Because the quantities of MgO and $Ca(OH)_2$ are fixed, the pH and $f(CO_2)$ will be a function only of the amount of CO_2 produced by microbial reaction, the volume of brine in the repository, and the type of brine. Figures 5a and 5b were constructed from the titration calculations with computer code EQ3/6 (Wolery 1992; Wolery and Daveler 1992). In the calculations, 0.004 moles $Ca(OH)_2$ were added for each mole of $Mg(OH)_2$. The figure indicates that, for Castile brine ERDA-6 (Figure SOTERM-5b), the transition from one buffer to another is very sharp whereas, for Salado brine Brine-A, a transition region (III) exists (Figure SOTERM-5a) (Wang 1996a, Figure 26). The existence of region (III) is due to the formation of Mg-oxychlorite. The transition region and region I have very similar pH values. Furthermore, the figure shows that the chemical conditions in the repository will be dominantly controlled by $Mg(OH_2)$ and carbonate minerals, because $Ca(OH)_2$ in the waste will be consumed easily by reaction with microbially-generated CO_2 or $MgCl_2$ in the Salado brine. (Note that even if there is no CO_2 generation, the Mg buffers will apply if more than 5000 cubic meters of Salado brine enter the repository. The amount of 5000 cubic meters is a small fraction of the repository pore volume.) The dashed line is included to show that the CO_2 produced from degradation of only 8 percent of the cellulosics is enough to react with all the $Ca(OH)_2$ in the waste.

Therefore, under all situations where repository performance may be affected, the brine pmH and $f(CO_2)$ will be controlled by the $Mg(OH)_2 + MgCO_3$ buffer.

Four effects of microbial degradation of organic materials are recognized in modeling system performance. A simplification has been made that the effects will be time independent after 100 years. The effects are

(1) Reduction-oxidation effects. After 100 years, the repository will have a reducing environment. Even though significant microbial action is only 50 percent likely, the corrosion of steel will also produce a reducing environment (Section SOTERM.2.2.3).

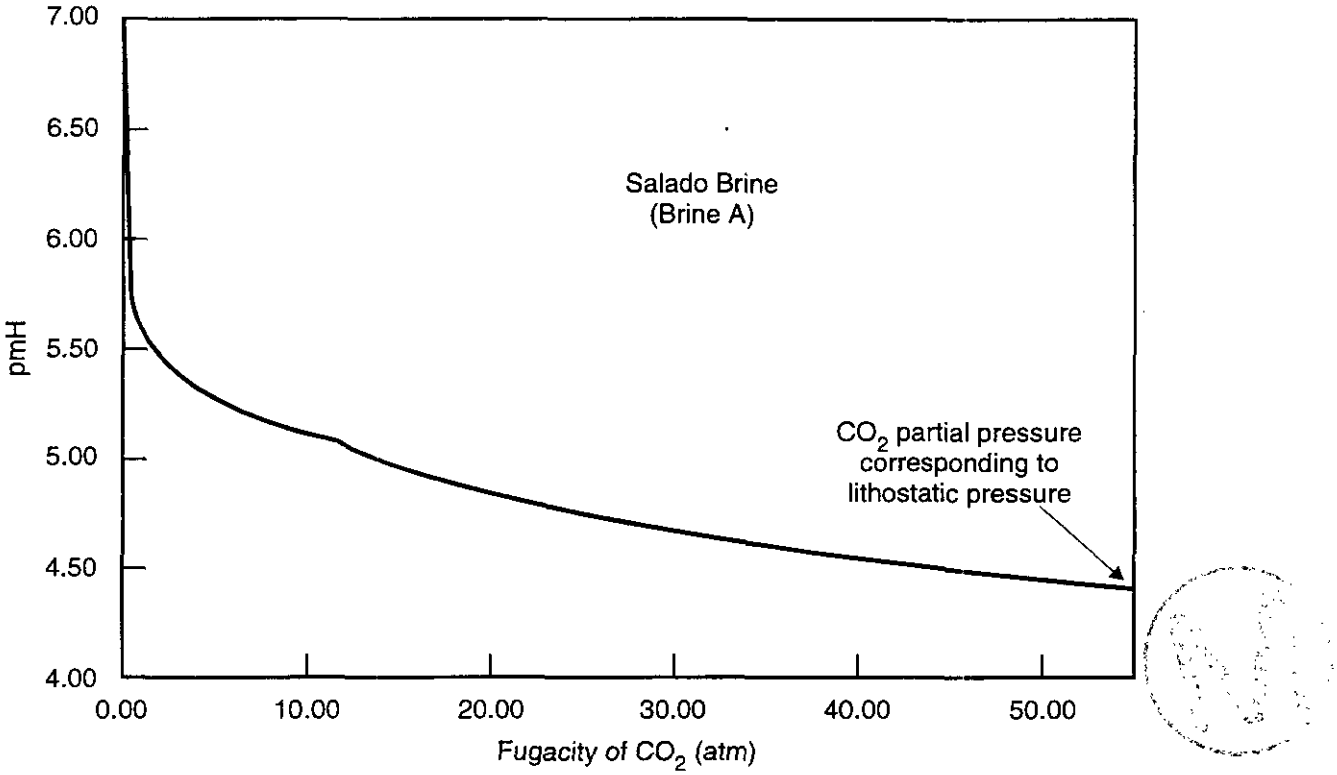

NOTE: It is assumed that CO_2 production by microbial reactions will be the dominant factor lowering brine pmH. Because of the difficulty in estimating the maximum CO_2 pressure in the repository, it is further assumed that the CO_2 pressure is limited by lithostatic pressure (approximately 150 atm), corresponding to approximately 55 atm CO_2 fugacity, according to a real-gas model developed by Duan et al. (1992) for a pure CO_2 system.

CCA-SOT002-0

Figure SOTERM-1. The pmH Changes of Salado Brine in the Absence of Added MgO as the Disposal Room is Pressurized with CO_2 Generated by Microbial Reactions

THIS PAGE INTENTIONALLY LEFT BLANK

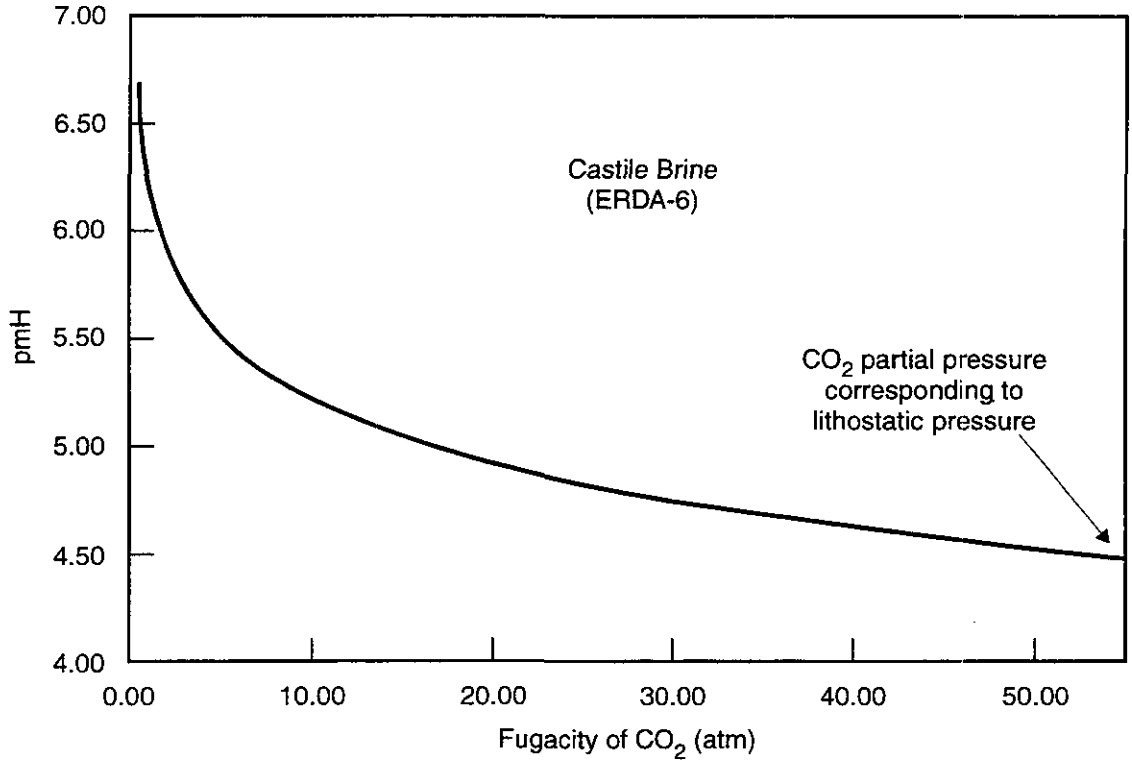

NOTE: It is assumed that CO_2 production by microbial reactions will be the dominant factor lowering brine pmH. Because of the difficulty in estimating the maximum CO_2 pressure in the repository, it is further assumed that the CO_2 pressure is limited by lithostatic pressure (approximately 150 atm), corresponding to approximately 55 atm CO_2 fugacity, according to a real-gas model developed by Duan et al. (1992) for a pure CO_2 system.

CCA-SOT003-0

Figure SOTERM-2. The pmH Changes of Castile Brine in the Absence of Added MgO as the Disposal Room is Pressurized with CO_2 Generated by Microbial Reactions

1 **THIS PAGE INTENTIONALLY LEFT BLANK**

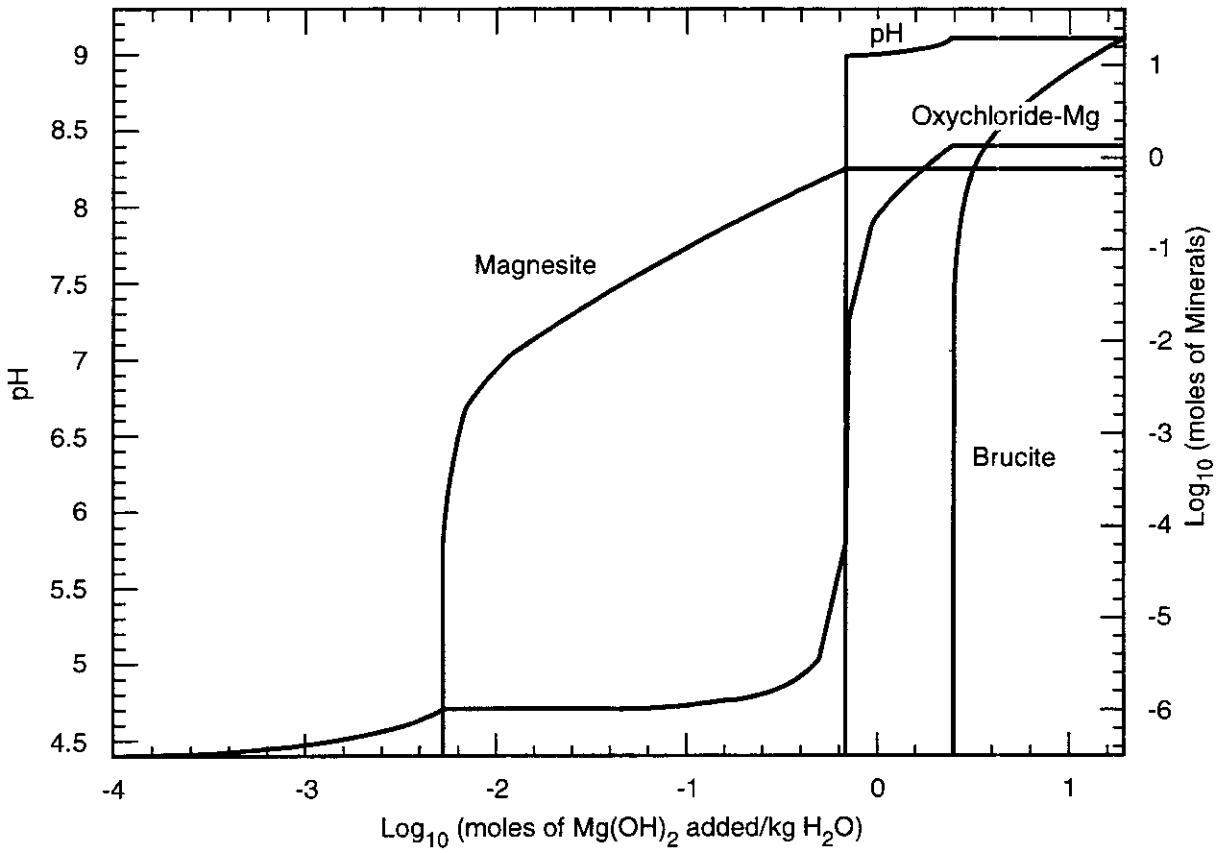

NOTE: The brine chemical composition used in the calculation is from Brush (1990, Table 2-2).

CCA-SOT004-0

Figure SOTERM-3. EQ3/6 Titration of Hydrated MgO into Salado Brine (Brine A)

1 THIS PAGE INTENTIONALLY LEFT BLANK

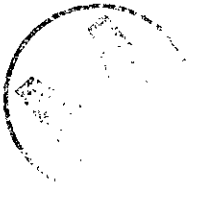

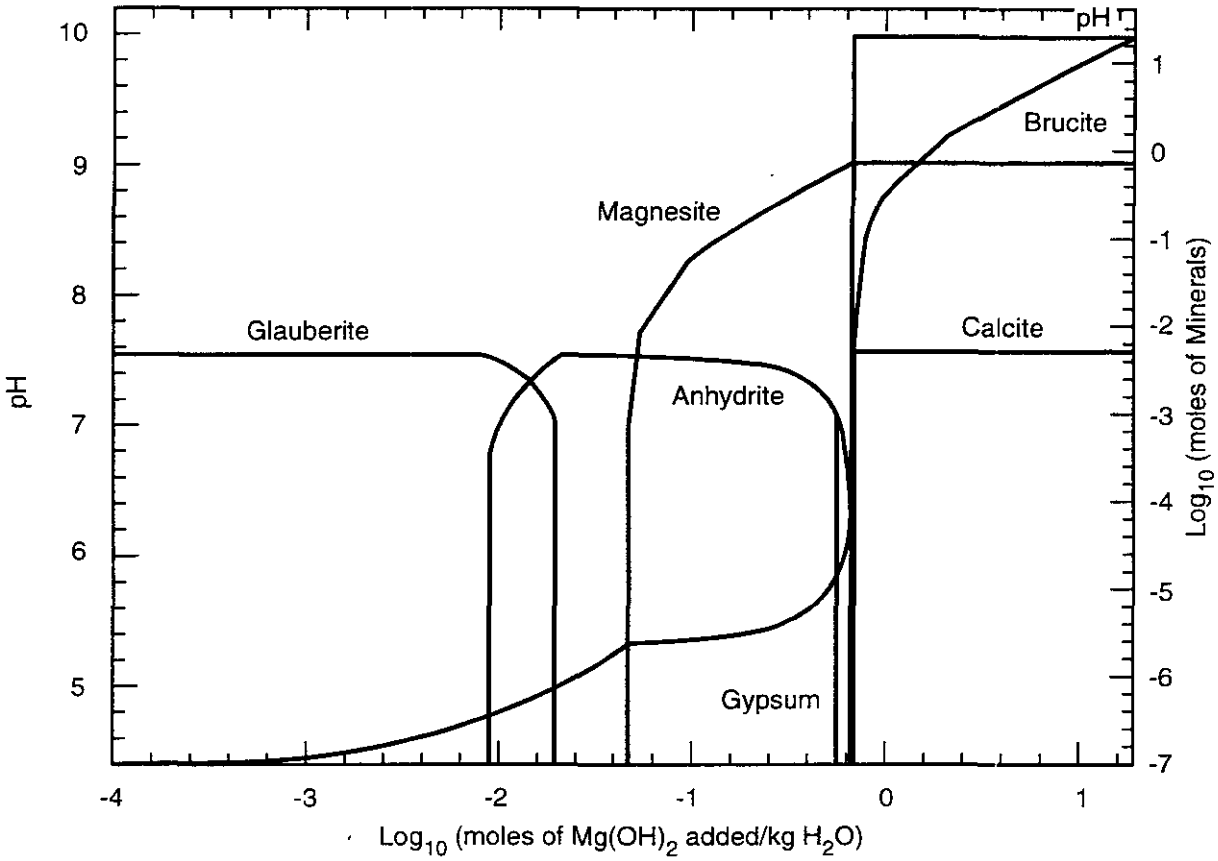

NOTE: The brine chemical composition used in the calculation is from Brush (1990, Table 2-3).

CCA-SOT005-0

Figure SOTERM-4. EQ3/6 Titration of Hydrated MgO into Castile Brine (ERDA-6)

1 **THIS PAGE INTENTIONALLY LEFT BLANK**

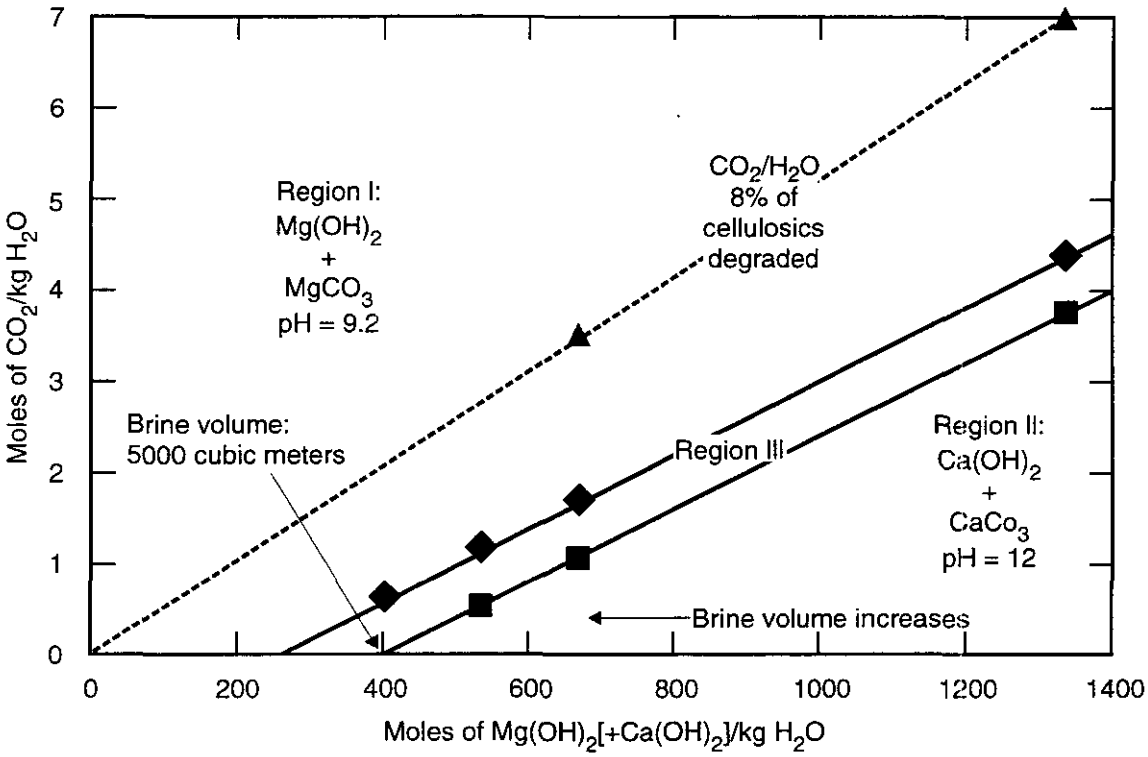

NOTE: Since MgO and $Ca(OH)_2$ are fixed, the ratio of $Mg(OH)_2/H_2O = 2 \times 10^9$ moles/kg of total water in the repository. The ratio of $Ca(OH)_2$/kg $H_2O = 0.004*Mg(OH)_2$/kg H_2O. The dashed line is the CO_2/H_2O ratio corresponding to 8% of cellulosics biodegraded. Region III can be combined into region I, because they have similar pH values.

CCA-SOT006-0

Figure SOTERM-5a. Chemical-Buffer Distribution for Salado Brine (Brine-A) as a Function of CO_2 Produced and $Mg(OH)_2$[+$Ca(OH)_2$] Added per Kilogram of Water

1 **THIS PAGE INTENTIONALLY LEFT BLANK**

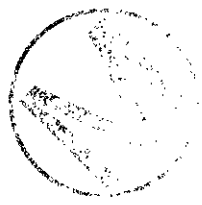

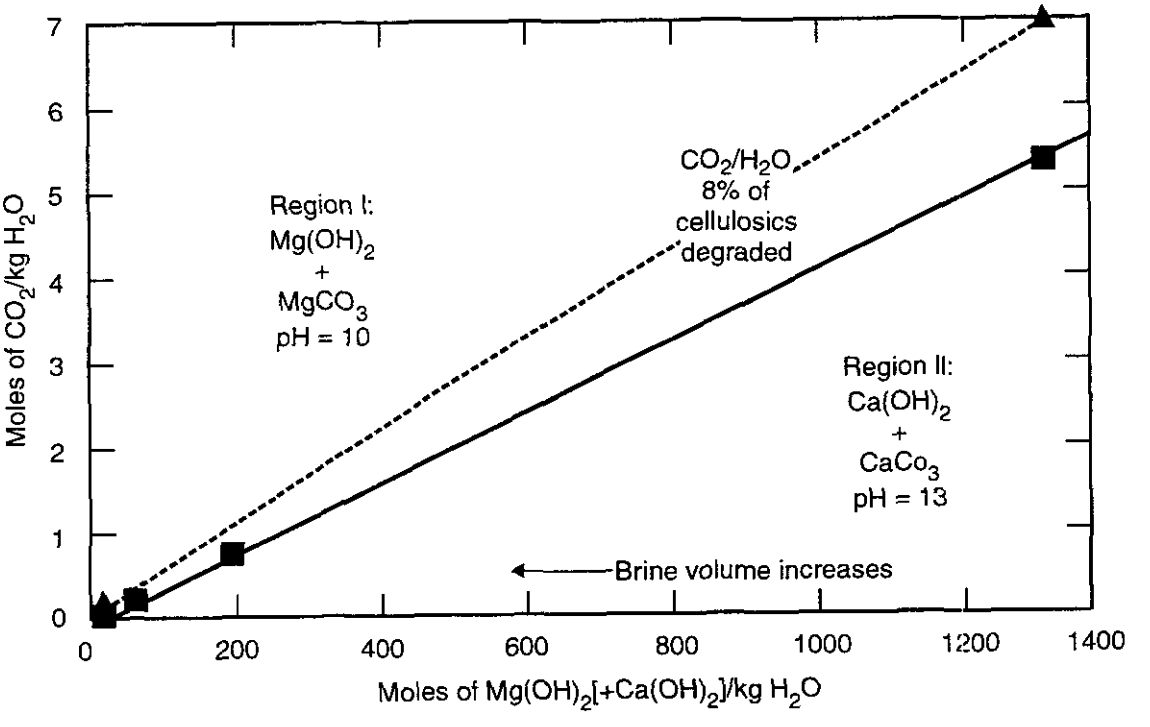

NOTE: Since MgO and $Ca(OH)_2$ are fixed, the ratio of $Mg(OH)_2/H_2O = 2 \times 10^9$ moles/kg of total water in the repository. The ratio of $Ca(OH)_2$/kg $H_2O = 0.004*Mg(OH)_2$/kg H_2O. The dashed line is the CO_2/H_2O ratio corresponding to 8% of cellulosics biodegraded.

CCA-SOT007-0

Figure SOTERM-5b. Chemical-Buffer Distribution for Salado Brine (ERDA-6) as a Function of CO_2 Produced and $Mg(OH)_2$[+$CA(OH)_2$] Added per Kilogram of Water

1 **THIS PAGE INTENTIONALLY LEFT BLANK**

(2) Consumption of organic ligands. While some microbes are known to consume some organic ligands, there is uncertainty as to the presence or viability of these particular microbes within the repository environment. Therefore, no credit has been taken for the microbial degradation of organic ligands. Other mechanisms for reducing the effect of organic ligands are discussed in Section SOTERM.5.

(3) Production of humic and microbe colloids. Even though microbes are modeled with only a 50 percent chance of significant growth, it is assumed that there are enough suspended microbes (viable or lysed) to increase the suspended actinide concentration. This is further discussed in Section SOTERM.6.

(4) CO_2 generation. With the addition of excess MgO backfill, the effects of CO_2 generation are minimized, and it is assumed that the system may be modeled using the $Mg(OH)_2 + MgCO_3$ buffer.

SOTERM.2.2.3 Corrosion of Steels and Other Metals

The corrosion of steels and other metals within the repository will have several effects on the dissolution and suspension of actinides. Corrosion is expected to

- reduce the oxidation states of some actinides, affecting their solubility and binding constants (Section SOTERM.4),
- release metal ions such as iron and nickel into solution. These metal ions can then bind organic ligands, thus reducing the ability of the ligands to increase actinide solubility (Section SOTERM.5),
- produce colloidal corrosion products on which actinides may sorb (Section SOTERM.6).

It is expected that the oxic corrosion of steels and aerobic biodegradation of organic materials will quickly consume the limited amount of O_2 trapped within the repository at emplacement. After the O_2 is consumed, anoxic corrosion of the metals will occur (Brush 1990, 30 et seq.). There will be about 2×10^9 moles of iron in the repository (DOE 1996, 2-5, 2-6) which is expected to corrode at a rate between 0.005 and 6.5 microns/year when inundated with brine but is immeasurably slow when in unsaturated conditions (Wang and Brush 1996). If the ferrous metals corroded at the maximum rate, they would be corroded within approximately 6,000 years after closure. In most cases, however, it is expected that there will be significant amounts of uncorroded metal in the repository throughout the 10,000-year regulatory period. In addition, WIPP specific experiments (Wang and Brush 1996) show that the steels will corrode by the following reaction:

$$Fe(O) + H_2O = Fe(OH)_2 + H_2 . \qquad (2\text{-}7)$$

Metal hydroxides such as $Fe(OH)_2$ are more soluble in the WIPP high ionic strength brines than in dilute waters, and significant amounts of Fe(II) may dissolve. Refait and Genin (1994) estimated Fe(II) solubilities between 10^{-4} and 10^{-6} M for pH between 8.5 and 10.5 at reduction-oxidation conditions expected for the repository. Sagoe-Crentsil and Glasser (1993) observed even higher solubilities at pH 13 with electrolytic dissolution of iron.

Corrosion of metals will produce reducing conditions within the repository, but the effective reduction-oxidation state of the system is unknown. The repository system is not described using Eh, because in low temperature systems reduction-oxidation equilibrium between the many reduction-oxidation couples may not necessarily be obtained and no unique Eh is defined. For this reason the reduction-oxidation states of the actinides have been determined experimentally as described in Section SOTERM.4.

SOTERM.2.2.4 Other Effects

High pressure in the repository after closure is expected to have an insignificant effect on actinide solubility and the association of actinides with colloids and therefore its effect is eliminated from performance assessment calculations. Temperature within the repository is not expected to change by more than a few degrees from ambient (α) (Sanchez and Trellue 1996; Wang and Brush 1996). Because the effect on solubility of a few degrees is insignificant compared to uncertainty of the measurements and modeling of solubility, temperature effects were also discounted (Section SOTERM.3.3).

Radiolysis of brine may change the effective reduction-oxidation state. When energy from radioactive decay is absorbed by water, the water is broken into energetic fragments that reassemble into oxidized and reduced species. Depending on the chemical reactivity of these species, the system may be effectively more oxidizing or more reducing as a result of the radiolysis. For example, radiolysis often occurs by the following reaction:

$$2\,H_2O + \text{radiation} = H_2(g) + H_2O_2 \quad (2\text{-}8)$$

Peroxide (H_2O_2) is more reactive than $H_2(g)$ at low temperature, and peroxide reduction-oxidation reactions will affect the system more than the slow H_2 reactions. If the system is initially very oxidized, the H_2O_2 will cause a reduction in the effective reduction-oxidation state, but if the system is initially very reduced, the peroxide will cause oxidation in the effective reduction-oxidation state. In the WIPP, it is expected that the repository will be quite reducing due to the large amount of iron metal and dissolved Fe(II) species. Any oxidized species such as peroxide generated from radiolysis are expected to quickly react with the iron metal and Fe(II) thus negating any oxidizing effect of radiolysis. Therefore, radiolysis is not expected to affect the reduction-oxidation state of the repository.

Other components of the waste may have a potential to influence the concentration of dissolved actinides within the repository. These include, for example, organic ligands (Section SOTERM.5); other salts such as $CaCl_2$, which may raise the ionic strength of the

brine; vermiculite, which may sorb actinides; and phosphate, which may precipitate insoluble actinide phosphates. The effects of most of these components are assumed beneficial and are unquantifiable, so they were not included in performance assessment modeling.

SOTERM.2.2.5 Summary

The chemical environment in the brine-inundated repository is a function of brine composition (Salado or Castile); microbial degradation of organic materials, which will produce various gases and colloidal particles; the MgO additive, which will control the pmH and the CO_2 fugacity; and corrosion of the large quantity of metals in the repository, which will cause reducing conditions and release ions that will bind with and sequester organic ligands.

SOTERM.3 Prediction of Dissolved Actinide Solubility

This section describes the basic approach to predicting dissolved actinide solubility for this application. Surveys of different possible conceptual and mathematical descriptions of the system are presented, followed by a more detailed discussion of the method selected.

The material in this section is intended to provide an overview of the modeling methods. More detailed descriptions of particular points or issues can be found in the indicated references.

SOTERM.3.1 Previous Approaches to Estimating Actinide Solubility in the WIPP

Brine flow through the repository was not considered early in the WIPP project history because none was expected (see Appendix Mass, Section MASS.2). As it was realized that brine may enter the waste disposal region from a variety of sources, scenarios involving brine flow were developed. These scenarios required investigation of potential mobilization of actinides, including actinide solubility in brine.

The solubility of actinides in the WIPP was initially estimated by an expert panel that reviewed the existing literature on actinide solubilities (Trauth et al. 1992). The range of solubilities obtained was about 14 orders of magnitude because the chemical conditions surveyed included extremes of acidity and other conditions. With the addition of MgO backfill and the demonstrated reducing conditions, these extremes will not occur in the WIPP. The expert panel also estimated the effect of high carbonate concentrations (which are known to increase actinide solubility significantly) on the actinide solubility despite the paucity of data for carbonate solutions. Median solubilities developed by the panel were Th, 10^{-10} M; U, 10^{-3} M; Np, 10^{-7} M; Pu, 10^{-9} M; and Am and Cm, 10^{-9} M (Trauth et al. 1992, p. 4-5; Hobart et al. 1996). Published studies of actinides under environmental conditions (that is, neutral or basic pH) have focused on actinides in surface waters and ground waters that are considerably more dilute than WIPP brines, which contributed to the wide range of concentration estimates because more pertinent data were unavailable.

Experimental investigations for other radioactive-waste projects (for example, Nitsche 1987) have approached the question of potential actinide solubility by measuring the solubility of the actinides in the waste directly. Although this is possible for well-characterized and homogeneous waste and ground waters, the waste intended for the WIPP is heterogeneous, and a relatively wide range of chemical conditions would be possible in the repository without the MgO backfill. Measuring solubility directly in experiments using transuranic (TRU) waste and ensuring that the measurements reflect steady-state WIPP conditions would entail an extremely large number of measurements and considerable uncertainty. This approach was determined to be neither practical nor feasible. The DOE therefore decided to estimate actinide solubilities by using an equilibrium thermodynamics model based on experimental parameterization.

SOTERM.3.2 Selection of the Pitzer Activity Coefficient Model

The thermodynamic activity of a dissolved species in solution is expressed as an activity coefficient multiplier of its analytical concentration. In dilute aqueous solutions, the activity coefficient is close to unity, but in high ionic strength brines such as encountered in the WIPP, the activity coefficient may be quite different than unity.

The calculation of activity coefficients is the central feature of thermodynamic models in concentrated electrolyte systems. Activity coefficients represent the deviation from the nearly ideal behavior that is observed or assumed in dilute electrolyte systems. Aqueous electrolyte activity coefficient models generally include the Debye-Hückel limiting law (see, for example, Pitzer 1991, 59 et seq.) to describe behavior in the dilute region (<0.1 molal), and often include one or more adjustable parameters to reproduce measured behavior in more concentrated solutions.

Numerous activity coefficient models for concentrated electrolytes have been proposed, including the Pitzer formalism (Pitzer 1991, Chapter 3), the Harned's Rule approach (Wood 1975), and the Specific-ion Interaction Theory (SIT) approach (Grenthe and Wanner 1992), given in order of approximately decreasing mathematical complexity. The Pitzer formalism contains parameters that explicitly represent the contributions to the excess free energy from every two-moiety and three-moiety interaction, where a moiety is a cationic, anionic, or neutral aqueous species. The Harned's Rule approach asserts that the "logarithm of the activity coefficient of one electrolyte in a mixture of constant total molality is directly proportional to the molality of the other component" (Robinson and Stokes 1959, 438), and thus by extension to multicomponent systems containing parameters for two-moiety interactions. The SIT formalism contains parameters for two-moiety cation-anion interactions.

A primary consideration for selecting an activity coefficient model for the WIPP actinide solubility data base was the demonstrated applicability of existing models and data bases to the brine and evaporite systems at the WIPP site. The Pitzer formalism, especially as parameterized by Harvie et al. (1980a), Harvie et al. (1984), and Felmy and Weare (1986),

includes an established data base describing solubility in the Na-K-Mg-Ca-H-Cl-SO_4-OH-HCO_3-CO_3-CO_2-B-H_2O system; this system includes the significant inorganic constituents of WIPP brines. The Harned's Rule approach has been parameterized for the NaCl-KCl-$MgCl_2$-$CaCl_2$ and NaCl-$MgSO_4$ systems (Wood 1975) but does not include the carbonate ion, which is one of the most important complexants for actinides in aqueous systems. The SIT formalism (Grenthe and Wanner 1992) is most commonly used for extrapolating apparent stability constants to zero ionic strength. No demonstrations that the SIT formalism has been applied to multicomponent concentrated electrolytes such as brine-evaporite systems have been identified in the literature.

The chemical behavior of the concentrated electrolytes that occur in evaporites like those at the WIPP site has been extensively studied and documented. The applications of the Harvie et al. (1980a), Harvie et al. (1984), and Felmy and Weare (1986) parameterization of the Pitzer formalism include: prediction of the mineral precipitation sequence accompanying sea water evaporation (Eugster et al. 1980; Harvie et al. 1980b); the formation of borate minerals in Searles Lake, CA (Felmy and Weare 1986); and an analysis of Permian sea water compositions based in part on fluid inclusion data from the Salado (Horita et al. 1991). Additional applications are given in Pitzer (1991, Chapters 6 and 7).

Brines in the WIPP system range from about 0.8 molal to 8 molal ionic strength. The Pitzer model is developed for and has been shown to work for electrolytes as concentrated as those in the WIPP system, and has been applied successfully to evaporite systems with concentrations greater than 10 molal (Felmy and Weare 1986). Rather than develop a new description of the chemical behavior of the nonactinide chemical constituents in WIPP brines, it was decided to use the Harvie et al. (1984)/Felmy and Weare (1986) (HMW/FW) parameterization of the Pitzer model as the reference activity coefficient formalism and thermodynamic data base for further WIPP application. The WIPP actinide solubility research focused on extending the data base to include the actinides of interest to the WIPP and the organic waste constituents that may impact actinide dissolved concentrations.

SOTERM.3.3 The FMT Computer Code

The FMT code (Novak 1995; WIPP Performance Assessment 1995) implements the Pitzer formalism, and is used to calculate the solubility of the actinide elements in equilibrium with the appropriate solubility-controlling solid(s) in WIPP brines through the minimization of the Gibbs free energy of the system. Where appropriate parameters already existed in the HMW/FW data base, they have been used in FMT calculations for the WIPP. Additional parameters, most notably those for the actinide ions, have been taken from the literature or determined from experimental data (see Section SOTERM.3.4) using the NONLIN code (Novak 1995; WIPP Performance Assessment 1996). NONLIN calculates the Pitzer parameters using a non-linear least squares fitting program.

The FMT calculations were done for three actinides: Am(III), Th(IV), and Np(V), that are chemical analogs for the actinide III, IV, and V oxidation states, respectively. Because

actinides in the same oxidation state exhibit similar chemical behavior, these FMT model calculations are applied to all actinides in that particular oxidation state; for example, the Am(III) FMT model applies to Pu(III) and Cm(III), and the Np(V) model applies to Pu(V).

The dissolved concentrations of the actinides Am, Cm, Np, Pu, Th, and U will be limited by solubility-controlling solids for each of the actinides in the brines. The important ions in WIPP brines are H^+, Na^+, K^+, Mg^{2+}, OH^-, Cl^-, CO_3^{2-} SO_4^{2-}, and Ca^{2+}. Other ions (for example, PO_4^{3-},F^-, Al^{3+}, and Fe^{2+}/Fe^{3+}, may be important at influencing dissolved actinide concentrations both by influencing solubility and by influencing reduction-oxidation reactions. Pitzer parameters for these other ions were not quantitatively included in the dissolved species source term model, but are qualitatively included in the understanding of the chemical environment. For example, phosphates are known to precipitate actinides (Cotton and Wilkinson 1988), but this effect has conservatively been ignored due to the uncertainty of the phosphate inventory in the WIPP and the lack of a complete set of Pitzer parameters for its inclusion. The existence of Fe(II) from the anoxic corrosion of iron is accounted for in the oxidation state distribution (see Section SOTERM.4), but is expected to have an insignificant effect on the solubility of an individual actinide oxidation state.

The expected temperature of the WIPP disposal rooms during the regulatory time frame is not expected to change by more than a few degrees from ambient (Sanchez and Trellue 1996; Wang and Brush 1996). The small differences in thermodynamic properties caused by these changes are well within acceptable uncertainty for the WIPP system. For these reasons, the small differences in properties over this temperature range are not significant for the WIPP, and all information was developed for 25°C. Literature information taken at approximately 20°C was deemed acceptable for model parameterization as well.

The development of the dissolved actinide concentration model was largely the development of a data base that includes the standard chemical potentials of the aqueous and solid chemical species containing actinides, and the specific ion interaction parameters required to describe the interactions between these species and other constituents of brines in WIPP scenarios. The following subsections describe briefly how these data bases were built and how the needed parameters were obtained. The development of the oxidation state distribution reflected in these sections is discussed in Section SOTERM.4.

Section SOTERM.3.4 provides a guide to the information that is needed for predicting dissolved actinide concentrations. The FMT data base used in this application is documented in Novak and Moore (1996). The user's manuals for the FMT and NONLIN codes are contained in Attachments 1 and 2 respectively to this appendix.

SOTERM.3.4 Overview of the Experimental Data

SOTERM.3.4.1 The III Actinides: Am(III), Pu(III), Cm (III) and the Lanthanide Analog Nd(III)

The III actinides of interest to the WIPP are Am(III), Pu(III), and Cm(III). The lanthanide analog Nd(III) has been shown to exhibit the same chemical properties as the III actinides. The An(III)* model has been demonstrated to describe the chemical behavior of both Am(III) and Pu(III) accurately, by a combination of comparisons with existing literature information and comparisons with additional experiments designed specifically to perform this demonstration. For the III system, working with Nd(III) provides a particular advantage because Nd is not radioactive, which simplifies the laboratory work, and is stable in the III state.

The dissolved concentration model was used to predict the behavior of the III actinides in the WIPP system, as is shown for the simple example of the solubility of Am(III) in a closed system of SPC brine as a function of pmH (Appendix E of Novak 1995).

Data for the III actinides and lanthanides are the most extensive of all the oxidation states of interest. The An(III) model was developed simultaneously from individual data for the Pu(III), Am(III), Nd(III), and Cm(III) systems. Cm(III) may be presumed to behave virtually identically with Am(III) (see, for example, Katz et al. 1986, 1498). The An(III) model has been parameterized in the Pitzer formalism for the Na, Cl, SO_4, CO_3, and PO_4 systems; Pu^{3+}-Na^+-Cl^- in Felmy et al. (1989); Am^{3+}-Na^+-HCO_3^--OH^--H_2O in Felmy et al. (1990); Am^{3+}-Na^+-SO_4^{2-} - PO_4^{3-} in Rai et al. (1995); and Nd^{3+}-Na^+ -CO_3^{2-}-HCO_3^--H_2O in Rao et al. (1996). Some of the aqueous species required are Am^{3+}, $AmCO_3^+$, $Am(CO_3)_2^-$, $Am(CO_3)_3^{3-}$, and the solid species $AmOHCO_3(s)$. These are represented by the following reactions, as written for Am(III):

$$Am^{3+} + CO_3^{2-} = AmCO_3^+$$

$$Am^{3+} + 2\,CO_3^{2-} = Am(CO_3)_2^-$$

$$Am^{3+} + 3\,CO_3^{2-} = Am(CO_3)_3^{3-}$$

$$Am^{3+} + OH^- = AmOH^{2+}$$

$$Am^{3+} + 2OH^- = Am(OH)_2^+$$

$$Am^{3+} + 3OH^- = Am(OH)_3(s)$$

$$Am^{3+} + OH^- + CO_3^{2-} = AmOH\,CO_3(s)$$

*The symbol An is used to designate any actinide element.

These reactions represent one set of orthogonal reactions for americium(III) species.

The An(III) data base has been extended to mixed Na^+-Cl^--CO_3^{2-} media, and has been shown to reproduce the independently measured solubility of $NaAm(CO_3)_2(s)$ in 5.6 M NaCl (Runde and Kim 1994) and Nd^{3+} solubility in WIPP brines.

SOTERM.3.4.2 The IV Actinides: Th (IV), U(IV), Pu(IV), Np(IV)

The IV actinides important to WIPP performance are Th (IV), U(IV), Pu(IV), and Np(IV). The variation in charge to radius ratio for the tetravalent actinides is greater than for actinides in other oxidation states (Cotton and Wilkinson 1988), and larger differences in the chemical behavior among the IV actinides is expected. The application of the Th(IV) model to the other IV species is more uncertain, yet still conservative because Th(IV) is the most soluble among these elements under WIPP conditions. The model was evaluated against data for Pu(IV) and Np(IV) solubility, and demonstrated to predict the chemical behavior of these actinides conservatively.

The Th(IV) dissolved concentration model is parameterized in the Pitzer formalism for interactions in the Na^+-K^+-Mg^{2+}-Cl^-- SO_4^{2-}-CO_3^{2-}-HCO_3^--OH^--H_2O system. This model requires the species Th^{4+}, $Th(OH)_2SO_4$ (s), $Th(SO_4)_3^{2-}$, $Th(SO_4)_2$ (aq), ThO_2, $Th(OH)_4$(aq), $Th(OH)_3CO_3^-$, and $Th(CO_3)_5^{6-}$ to describe the data pertinent to the WIPP (Felmy et al. 1991; Felmy and Rai 1992; Felmy et al. 1996). The principal reactions required are (as written for Th(IV)):

$$ThO_2\,(am) + 2H_2O = Th(OH)_4(aq)$$

$$Th^{4+} + 4OH^- = Th(OH)_4\,(aq)$$

$$Th^{4+} + 3OH^- + CO_3^{2-} = Th(OH)_3CO_3^-$$

$$Th^{4+} + 5CO_3^{2-} = Th(CO_3)_5^{6-}$$

$$Th^{4+} + 2SO_4^{2-} = Th(SO_4)_2\,(aq)$$

$$Th^{4+} + 3SO_4^{2-} = Th(SO_4)_3^{2-}$$

$$Th^{4+} + 2OH^- + SO_4^{2-} = Th(OH)_2SO_4\,(s)$$

These reactions represent one set of orthogonal reactions for actinide(IV) species.

The Th(IV) model has been extended to concentrated NaCl, $MgCl_2$, $NaHCO_3$ and Na_2CO_3 solutions. In addition, Th(IV) solubility has been measured in WIPP brines.

SOTERM.3.4.3 The V Actinides: Np(V)

The only V actinide of interest to the WIPP is Np(V), which exists as the neptunyl ion, NpO_2^+. The base model for Np(V) comes from Fanghänel et al. (1995), constructed for the German repository program. The Np(V) model was parameterized for the elements Na, Cl, CO_3, and ClO_4 (the last of which is not important for the WIPP but is invaluable for interpreting data in the literature). The model requires the aqueous species NpO_2^+, $NpO_2OH(aq)$, $NpO_2(OH)_2^-$, $NpO_2CO_3^-$, $NpO_2(CO_3)_2^{3-}$, and $NpO_2(CO_3)_3^{5-}$, and the solid species $NpO_2OH(am)$, $NpO_2OH(aged)$, $Na_3NpO_2(CO_3)_2$ (s), $KNpO_2CO_3 \cdot 2H_2O(s)$, $K_3NpO_2(CO_3)_2 \cdot 0.5H_2O(s)$ and $NaNpO_2CO_3\ 3.5H_2O(s)$ to explain the available data. These are represented by the reactions

$$NpO_2^+ + OH^- = NpO_2OH(aq)$$

$$NpO_2^+ + 2\ OH^- = NpO_2(OH)_2^-$$

$$NpO_2^+ + CO_3^{2-} = NpO_2CO_3^-$$

$$NpO_2^+ + 2CO_3^{2-} = NpO_2(CO_3)_2^{3-}$$

$$NpO_2^+ + 3CO_3^{2-} = NpO_2(CO_3)_3^{5-}$$

$$NpO_2OH(am) = NpO_2^+ + OH^-$$

$$NpO_2OH(s) = NpO_2^+ + OH^-$$

$$NaNpO_2CO_3 \cdot 3.5H_2O(s) = Na^+ + NpO_2^+ + CO_3^{2-} + 3.5H_2O$$

$$Na_3NpO_2(CO_3)_2\ (s) = 3Na^+ + NpO_2^+ + 2CO_3^{2-}$$

$$KNpO_2CO_3 \cdot 2H_2O(s) = K^+ + NpO_2^+ + CO_3^{2-} + 2H_2O$$

$$K_3NpO_2(CO_3)_2 \cdot 0.5H_2O(s) = 3K^+ + NpO_2^+ + 2CO_3^{2-} + 0.5H_2O$$

These represent a set of orthogonal reactions for neptunium(V) species. The Np(V) solubility model is being extended to potassium systems, including $K_3NpO_2\ (CO_3)_2(s)$.

SOTERM.3.4.4 The VI Actinides: U(VI)

The An(VI) FMT model has not been developed sufficiently for reliable use in predicting concentrations of this oxidation state in WIPP brines under various solution conditions. Although uranyl carbonate can be successfully modeled, the hydrolysis behavior of U(VI) is quite complicated and no satisfactory predictive models applicable to WIPP-like conditions are yet available. Because the implementation of an MgO backfill limits the pmH and fCO_2 to

discrete values, empirical measurement of the solubility of U(VI) in WIPP and/or WIPP like brines became practical. As documented in Hobart and Moore (1996), the solubility of U(VI) at pH 10, in the absence of carbonate, was determined to be 8.8×10^{-5} molal. The incorporation of U(VI) data into performance assessment is discussed in Section SOTERM.7.

SOTERM.3.5 Calculations of Actinide Solubility Using the FMT Computer Code

Details of the implementation of FMT and an early version of the CHEMDAT data base are given in Appendix D of Novak (1995), and in the FMT User's Manual. FMT calculated chemical equilibrium for user-specified total element amounts for aqueous or aqueous/mineral geochemical systems. The set of FMT calculations of actinide solubility in the WIPP system performed for the performance assessment included establishing equilibrium with halite, anhydrite, brucite, and magnesite (Novak et al. 1996), the minerals present in large quantities in the repository system. The effects of the MgO backfill are realized through the establishment of equilibrium of brine with brucite and magnesite.

SOTERM.3.6 Use of FMT Results in Performance Assessment

Table SOTERM-2 gives the solubilities for each actinide oxidation state analog as calculated with the thermodynamic model and FMT.

Table SOTERM-2. Solubilities of the Oxidation State Analogs, in moles/liter, with MgO Backfill

		Solubilities for PA Material Name and Oxidation State			
Brine	**PA Parameter Name**	**SOLMOD3 (III)**	**SOLMOD4 (IV)**	**SOLMOD5 (V)**	**SOLMOD6 (VI*)**
Salado	SOLSIM	5.82×10^{-7}	4.4×10^{-6}	2.3×10^{-6}	8.7×10^{-6}
Castile	SOLCIM	6.52×10^{-8}	6.0×10^{-9}	2.2×10^{-6}	8.8×10^{-6}

*Not calculated with the FMT model

Uncertainties in the solubility data and uncertainty in the NONLIN least squares refinement result in uncertainty in the model predictions. This is also evident when the data of Runde and Kim (1994) are compared with FMT model results. A measure of uncertainty was obtained by Bynum (1996) by examining the difference between the modeled solubilities for each oxidation state analog and comparing these to the experimental data used to generate the respective Pitzer parameters. The results of Bynum's analysis is given in Figure SOTERM-6. These results were combined as shown in Figure SOTERM-7 for entry into the parameter database as a cumulative distribution. This distribution was sampled in performance assessment as discussed in Section SOTERM.7.1.3. Note that the median of this distribution is -0.09 and not zero, indicating that slightly more experimental values were below the model

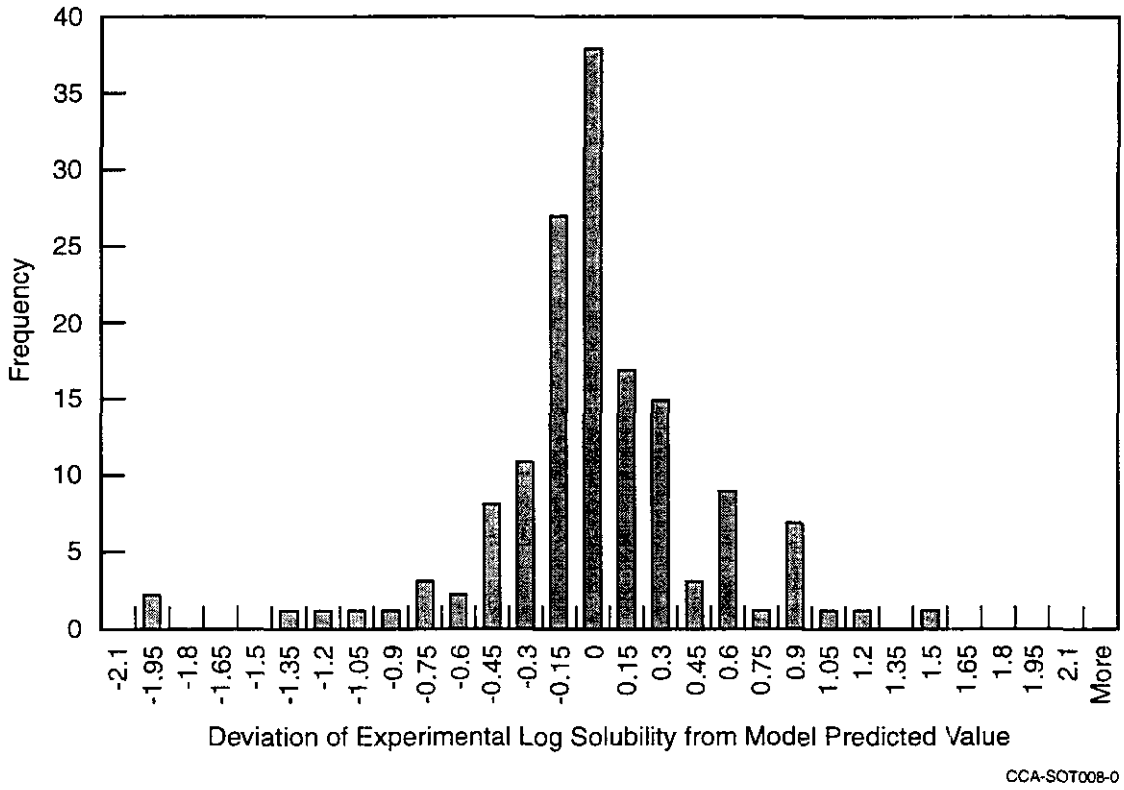

Figure SOTERM-6. Deviation of 150 Experimental Log Solubilities from the Model-Predicted Values

1 **THIS PAGE INTENTIONALLY LEFT BLANK**

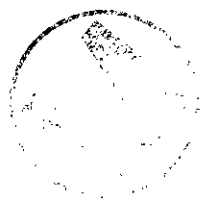

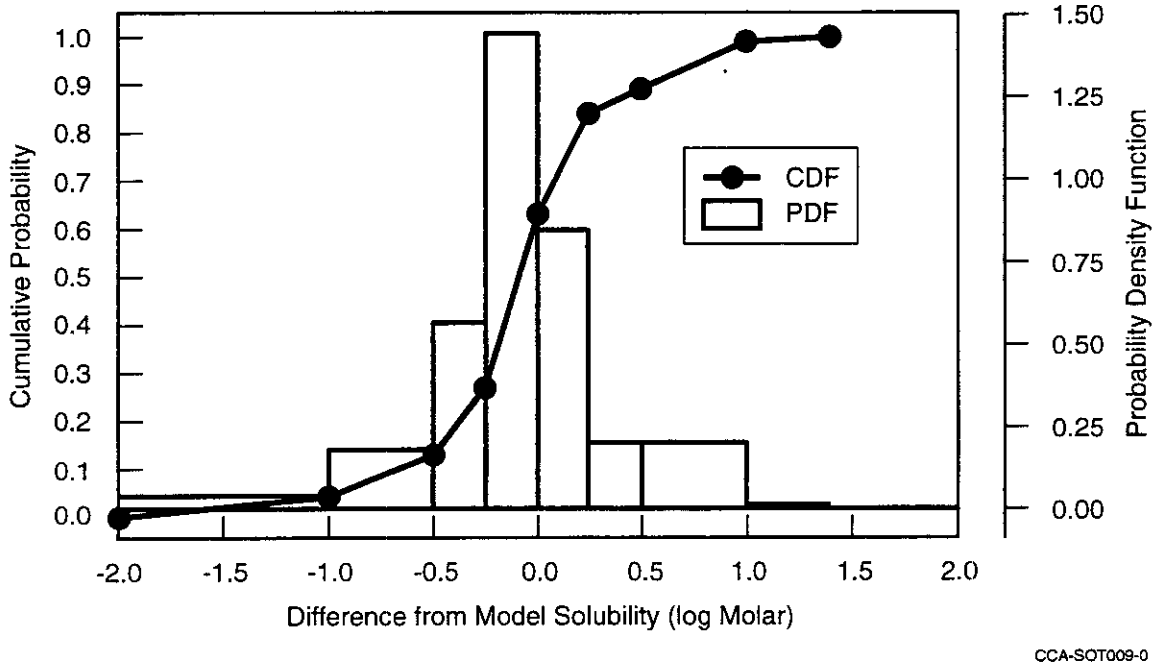

Figure SOTERM-7. Distribution of Actinide Solubility Uncertainty Utilized by Performance Assessments

1 **THIS PAGE INTENTIONALLY LEFT BLANK**

prediction than above. Table 6-11 in Chapter 6.0 of this application reports the median values, which are 10^{-9} (0.8128) times the model values shown in Table SOTERM-2, for those actinides assigned a distribution of solubilities rather than a constant value.

SOTERM.4 Oxidation State Distribution of the Actinides in Solution

This section describes the literature investigation and experimental program that resulted in identification of the oxidation states of the actinides that may be stable under expected repository conditions. The large quantities of iron in the repository, which will corrode to produce hydrogen and dissolved iron, provide a chemically reducing environment, thereby stabilizing reduced valence states. Microbial metabolism and the presence of organic material will add to this reducing environment.

SOTERM.4.1 Thorium

Thorium is known to exist only in the IV oxidation state in the natural environment (Hobart 1990; Katz et al. 1986, 1135, and following; 1486). The standard reduction potential for the Th(IV)/Th(III) couple is very low at -3.8 V. (with the standard hydrogen electrode potential = 0). Therefore, conditions in the inundated WIPP are not expected to produce any other valence state of thorium, nor has one been observed in any of the experiments done in connection with the WIPP Project. Thorium will be stable in the WIPP in oxidation state IV.

SOTERM.4.2 Uranium

Uranium can exist in aqueous solution in the III, IV, V, and VI oxidation states (Hobart 1990; Keller 1971; Clark et al. 1995). The dominant valence states for uranium in the natural environment are IV and VI. U(III) is metastable in aqueous solution but is easily oxidized (Katz et al. 1986, 1139, and following), and is difficult to isolate without traces of U(IV). In uranium, with open electronic shell structure $5f^3 6d 7s^2$, the shielding of the 5f electrons is not sufficiently effective for the trivalent state to dominate as it does in the transamericium actinides (Hobart 1990).

U(V) disproportionates rapidly in aqueous solution by the reaction

$$2U(V) = U(IV) + U(VI), \qquad (4\text{-}1)$$

and the reduction-oxidation potential for the U(VI)/U(V) couple is only +0.16 V. U(V) (UO_2^+) is most stable in the pH region 2-4 (Katz et al. 1986, 1144), which is considerably more acidic than anticipated WIPP conditions. U(VI) (UO_2^{2+}), on the other hand, is quite stable and difficult to reduce. However, in the highly reducing conditions expected in the WIPP, U(VI) may be reduced to U(IV). In experiments in simulated WIPP brines, Reed et al. (1996) have found that at pH 10 under anoxic conditions, U(VI) as a carbonate complex is quite stable. The stable oxidation states of uranium in the WIPP are IV and VI.

SOTERM.4.3 Neptunium

In the natural environment, neptunium may exist in oxidation states IV, V, and VI (Hobart 1990; Keller 1971; Clark et al. 1995). In the WIPP environment, Np(IV) is expected to be present (Rai and Strickert 1980; Rai et al. 1982; Kim et al. 1985; Pryke and Rees 1986). Np(V) appears to be the dominant oxidation state in natural groundwater (Hobart 1990). Nitsche and Edelstein (1985) have observed that Np(V) is the most stable state in Yucca Mountain well water. Studies of the solubility of NpO_2OH in 1 M and 5 M NaCl solutions at pH 6.5 suggest that Np(V) may be reduced to Np(IV) under these conditions (Kim et al. 1985; Neck et al. 1992). Np(VI) may be introduced into the WIPP or be produced by radiolysis, but its long-term stability is unlikely in the presence of the reducing agents that are expected to be present in the WIPP. The reduction-oxidation potential for the Np(VI)/Np(V) couple in basic solution is +0.6 V (Katz et al. 1986, 470); in neutral solution, +1.24V. (Martinot and Fuger 1985, 651 et seq.). Reed et al. (1996) have found spectroscopic evidence for reduction of Np(VI) to Np(V) in ERDA-6 (Castile) brine at pH 10, and have observed total reduction of Np(VI) to Np(V) in G-Seep (Salado) brine at pH 7. In the presence of oxalate, citrate, and ethylene diamine tetra-acetate (EDTA), Reed et al. (1996) have observed rapid and complete reduction of Np(VI) to Np(V). Neck et al. (1995) have shown Np(V) carbonate complexes to be stable in 5 M NaCl. The stable oxidation states of neptunium in the WIPP are IV and V.

SOTERM.4.4 Americium

The trivalent state of americium (AmIII) is the most stable aqueous oxidation state (Katz et al. 1986, 912), and it is quite difficult to oxidize in aqueous solution (Hobart et al. 1982). Am(IV) is unstable, but Am(V) and Am(VI) are accessible under highly oxidizing conditions. These higher oxidation states are not stable in natural waters and can be readily reduced by action of reductants naturally present in those waters. Reduction-oxidation potentials for americium couples (Martinot and Fuger 1985, 660 et seq.) are 2.62 V., 1.20 V. and 1.59 V. for the (IV)/(III), (V)/(IV), and (VI)/(V) couples, respectively.

As is evident from the relatively high values of the reduction-oxidation potentials, all of the americium oxidation states higher than III can oxidize water and are thermodynamically unstable. The report of Am(V) resulting from radiolytic oxidation of Am(III) in NaCl solution (Runde and Kim 1994) may occur in micro-environments within the WIPP disposal rooms, but would not be stable in the homogeneous mixture of waste and brine. Solubility studies carried out by Pryke and Rees (1986) and Felmy et al. (1990) indicate that Am(V) is unstable in brine above pH 9 and reduces to Am(III). These studies showed significant instability of Am(V) even at pH 7. The large quantities of iron in the repository, as well as the presence of microbes, will result in a highly reducing environment. The MgO backfill in the WIPP will keep the pH in brine that may be in the repository between 9 and 10 (Wang 1996a). The stable oxidation state of americium in brine that may be in the repository is III.

SOTERM.4.5 Curium

Curium is distinguished by the relatively great stability of the III oxidation state with respect to oxidation or reduction (Katz et al. 1986, 970). The stability of Cm(III) may be attributed to the half-filled f-shell electronic configuration ($5f^7$). The oxidation of Cm(III) is achieved only with the strongest oxidizing agents, and only one report claims evidence for an oxidation state higher than IV (Korpusov et al. 1975). The Cm(III) to Cm(IV) transition has not been successfully induced by ozone or electrochemically, and the Cm(IV) phosphotungstate produced by oxidizing with peroxysulfate is considerably less stable than the Am(IV) analog (Katz et al. 1986, 971). In the reducing environment of the WIPP repository, any Cm(IV) produced radiolytically would be unstable. The oxidation state of curium therefore expected to be stable in the repository brine is III.

SOTERM.4.6 Plutonium

Plutonium can exist in oxidation states III, IV, V, VI, and VII (Katz et al. 1986, 781). Pu(VII) is very unstable and exists only in extremely basic solutions (for example, 7 M NaOH). Thus, Pu(VII) will not be stable in the WIPP environment. Pu(VI) has been shown to form stable chloride complexes (albeit under oxic conditions) in high-ionic strength NaCl solutions (Clark and Tait 1996). However, Clark and Tait (1996) and Reed et al. (1996) have shown the complete reduction of Pu(VI) under expected WIPP repository conditions to Pu(IV), with a transient Pu(V) intermediate, by iron and other reductants.

Massive quantities of iron metal (approximately 10^9 moles), an effective reductant, will be placed within the repository. An estimate of the amount of iron with respect to the amount of plutonium, for example, can be made on the scale of an average drum; all repository solution chemistry is presumed to occur under average conditions and at equilibrium. Each drum contains on the average about 60 millimoles of Pu. Each drum contains about 170 moles of iron in the container alone—potentially about a 2800-fold excess of iron. The reaction rate of iron with the brine is very fast (Appendix PAR, Parameter 1). Therefore, as any brine moves into the repository it will react with the iron and establish a highly reducing environment, leading to the reduction of plutonium to one of the lower oxidation states.

As brine enters the repository, iron will undergo anoxic corrosion, producing Fe^{2+}. Both metallic iron (Fe^0) and Fe^{2+} have been shown to quantitatively reduce Pu(VI) in WIPP brines to either Pu(IV) or Pu(III). Clark and Tait (1996) and Felmy et al. (1996) have experimentally observed the reduction of Pu(VI) carbonates by either Fe^0 or Fe^{2+} to Pu(IV). In the absence of carbonates, a quantitative reduction of Pu(VI) is also observed but the determination of the oxidation state of the resulting species cannot be definitively determined due to its concentration being below the lower limit of detection of the oxidation state analytical process (about 10^{-9} molar). However, since the concentration should have been above the analytical detection limit if the plutonium had been in the V state, it is reasonably assumed that the plutonium must have been reduced to either the IV or III oxidation state. Neretnieks (1982)

has shown that when dissolved actinides in moving groundwater came in contact with Fe(II), the actinides were reduced to a much less soluble oxidation state and precipitated.

Pu(III) is not very stable under expected WIPP conditions, but Felmy et al. (1989) have observed Pu(III) in PBB1 and PBB3 brines at neutral and slightly basic conditions. Under highly basic conditions, the plutonium concentration is below the lower limit of detection, and it cannot be conclusively demonstrated that the plutonium remains in the III oxidation state.

The DOE has determined (Weiner 1996) that Pu(IV) will be the dominant oxidation state under WIPP conditions. Because the existence of Pu (III) cannot be conclusively excluded, it too has been included in the performance assessment.

SOTERM.4.7 Summary of Oxidation State Distribution

Table SOTERM-3 presents the oxidation states of the actinides as they are used in performance assessment of the WIPP.

Table SOTERM-3. Oxidation States of the Actinides in the WIPP As Used in PA

Actinide Element	Oxidation States			
thorium		IV		
uranium		IV		VI
neptunium		IV	V	
plutonium	III	IV		
americium	III			
curium	III			

SOTERM.5 The Role of Organic Ligands

Organic ligands may be a component of the wastes to be disposed of in the WIPP. Because organic ligands may complex with actinides and increase dissolved actinide concentrations, the effect of organic liquids was evaluated. Organic ligands also complex strongly with multivalent metal cations. The multivalent metal cations thereby compete with the actinides, and an assessment of this effect was performed. The analysis, summarized here, demonstrates that organic ligands will not be available to complex the actinides and thus will not impact dissolved actinide concentrations in the WIPP.

A number of organic compounds are capable of forming strong complexes with actinide ions, thereby stabilizing the actinide in solution. In general, the reactions that take place for one-to-one complexes are

$$An^{n+} + L^{m-} \rightarrow AnL^{(n+m)}, \quad (5\text{-}1)$$

where An is a general symbol for any actinide, with charge n, and L is a general symbol for an organic ligand with charge m. The apparent stability constant for this reaction is

$$\beta = [AnL^{(n+m)}]/[An^{n+}][L^{m-}]. \quad (5\text{-}2)$$

The square brackets indicate concentration. This constant is sometimes referred to as an association constant.

The TWBIR (DOE 1996, Appendix B4) initially identified about 60 organic compounds among the non-radioactive constituents of TRU waste to be emplaced in the WIPP (Drez 1991; Brush 1990). Ten of these compounds have the potential to increase radionuclide solubility (Choppin 1988). Screening studies of these compounds have been conducted by Florida State University. Deprotonation and complexation experiments have been performed with five of these: acetate, citrate, oxalate, lactate, and EDTA. Four of these (acetate, citrate, oxalate, and EDTA) were identified in the waste inventory of the WIPP (DOE 1996, 3–12) as the only water-soluble organic ligands present in significant quantities. Lactate was not included because none was identified in the initial inventory, and estimating its concentration resulting from both production and consumption by microbes is not possible. These organic ligands are capable of significantly enhancing dissolved actinide concentrations, are potentially present in the repository, and are generally representative of any organic ligand that could be present in the WIPP.

Ligand concentrations in the repository were estimated using inventory amounts of ligands and a brine volume of 29,841 m^3, the smallest quantity of brine required to be in the repository which will support transport away from the repository (Larson 1996). As per the TWBIR, Rev. 2, Page 3-1, a scaling factor of 2.05 was applied to all values. The results are listed in Table SOTERM-4.

Table SOTERM-4. Organic Ligand Concentrations in Inundated Repository

Organic Ligand	Inventory Amount (g)	Organic Concentration (molality)	Organic Concentration (scaled)
acetate	1.3×10^{6}	5.2×10^{-4}	1.1×10^{-3}
oxalate	1.6×10^{6}	2.3×10^{-4}	4.7×10^{-4}
citrate	1.4×10^{8}	3.6×10^{-3}	7.4×10^{-3}
EDTA	2.3×10^{4}	2.0×10^{-6}	4.2×10^{-6}

Apparent stability constants for organic ligand-actinide complexation and deprotonation constants for the organic acids were determined at Florida State University using

potentiometric titration and a solvent extraction technique. The results of these studies are summarized in Table SOTERM-5.

Complexation constants for each organic-actinide binding reaction were determined using the Pitzer formalism. The NONLIN computer code was used to calculate Pitzer interaction parameters and standard chemical potentials (Moore 1996). The parameters were added to the existing FMT data base for inorganic compounds and equilibrium calculations were performed. In FMT modeling calculations including organic ligands, all four of the water-soluble organic ligands identified in the WIPP inventory were included together at the expected concentrations so that competition among complexing sites could be examined (Novak et al. 1996). Calculations were done separately for Salado and Castile brines, using the brine formulations given by Brush (1990, 17-28). Complexation constants for magnesium with the organic ligands were measured at Florida State University and the results are listed in Table SOTERM-6. These results were included in the calculations so that magnesium (backfill component) competition with the actinides for ligand complexation could be evaluated. The FMT output is the calculated equilibrium solubility of the actinide as a function of the repository conditions.

As the iron and steel in the repository corrode, additional transition metal ions will dissolve. These ionic species include iron (Fe), nickel (Ni), chromium (Cr), vanadium (V), and manganese (Mn), because the steels used for the waste drums contain on average at least 0.001 weight percent of Ni, Cr, V, and Mn as minor constituents (National Institute of Standards and Technology 1995). Because at least 1.9×10^9 moles of steels will be disposed of in the WIPP, there should be at least 1×10^4 moles of Ni, Cr, V, and Mn in the repository. There are also expected to be $> 6 \times 10^7$ moles of Pb. Additionally, these and other metals will be present in some of the waste forms; however, these additional quantities in the waste were not considered in this evaluation because insufficient data were available.

The complexation constants for the various metals cited above with the four representative organic ligands are listed in Table SOTERM-7. To assess the ability of these metals to complex with the organic ligands, competition calculations with EDTA (selected because it is the most strongly complexing of the four organic ligands under consideration) in low ionic strength NaCl solution saturated with iron hydroxide, nickel hydroxide and magnesium oxide (backfill) were performed. The calculations showed that under these conditions 99.8 percent of the EDTA was complexed by Ni, thus effectively rendering the EDTA unavailable for complexation with the actinides and rendering complexation of actinides by organic ligands inconsequential. Although these results are approximate because complexation constants for low ionic strength media were used, the fact that a single metal cation could bind more than 99 percent of the EDTA strongly suggests that the full range of metals that will be present will readily overwhelm the complexation sites of the organic ligands. Additionally, at higher ionic strength, iron and nickel have much higher solubility than in dilute solutions. Variation in ionic strength is not expected to change the complexation constants sufficiently to reduce this effect on the organics.

Table SOTERM-5. Apparent Stability Constants for Organic Ligands and Actinides in NaCl Media

Organic Ligand	Actinide Ion	NaCl (molality)	$\log_{10}$ of Apparent Stability Constant (β)
Acetate	Am^{3+}	0.3 to 5	1.44 - 2.2
	Th^{4+}	0.3 to 5	3.68 - 4.18
	NpO_2^+	0.3 to 5	1.05 - 1.8
	UO_2^{2+}	0.3 to 4	2.23 - 3.09
Lactate	Am^{3+}	0.3 to 5	1.75 - 2.55
	Th^{4+}	0.3 to 5	3.83 - 4.28
	NpO_2^+	0.2 to 5	1.43- 1.95
	UO_2^{2+}	0.3 to 5	2.45 - 2.73
Oxalate	Am^{3+}	0.3 to 5	4.17 - 4.63
	Th^{4+}	0.3 to 5	7.04 - 7.47
	NpO_2^+	1.0 to 5.0	3.62 - 4.63
	UO_2^{2+}	0.3 to 5	5.82 - 6.7
Citrate	Am^{3+}	0.3 to 5	4.84 - 5.9
	Th^{4+}	0.1 to 5	9.31 - 10.18
	NpO_2^+	0.1 to 5	2.39 - 2.56
	UO_2^{2+}	0.3 to 5	7.07 - 7.32
EDTA	Am^{3+}	0.3 to 5	13.76 - 15.1
	Th^{4+}	0.3 to 5	15.56 - 16.94
	NpO_2^+	0.3 to 5	5.45 - 6.7
	UO_2^{2+}	0.3 to 4	10.75 - 12.16

Table SOTERM-6. Apparent Stability Constants for Magnesium Complexation with Organic Ligands at High Ionic Strength

Organic Ligand	NaCl (Molality)	$\log_{10}$ of Apparent Stability Constant
acetate	5	0.690
oxalate	5	2.20
citrate	3	2.02
EDTA	5	6.66

Table SOTERM-7. Apparent Stability Constants for Organic Ligands with Metals (Martell and Smith 1982, 75, 284, 307, 328).

Organic Ligand	Metal	Ionic Strength (molality)	$\log_{10}$ of Apparent Stability Constant
EDTA	Fe^{2+}	0.1	14.3
	Ni^{2+}	0.1	13.6
	Cr^{2+}	0.1	18.4
	Mn^{2+}	0.1	13.9
	V^{2+}	0.1	12.7
	Cu^{2+}	0.1	18.9
	Pb^{2+}	0.1	18
Citrate	Fe^{2+}	0.1	4.4
	Ni^{2+}	0.1	5.4
	Mn^{2+}	0.1	4.15
	Cu^{2+}	0.1	5.9
	Pb^{2+}	0.1	4.08
Oxalate	Fe^{2+}	1.0	3.05
	Ni^{2+}	0.0	5.16
	Cr^{2+}	0.1	3.85
	Cu^{2+}	0.1	4.84
	Pb^{2+}	0.16	4.00
Acetate	Fe^{2+}	0	1.4
	Ni^{2+}	0	1.43
	Cr^{2+}	0.3	1.25
	Mn^{2+}	0.16	0.8
	Cu^{2+}	0	2.22
	Pb^{2+}	0.1	2.15

In addition to the calculations using the HYDRAQL code, simple scoping type equilibrium calculations were performed including several of the expected transition metals. The following equations were solved simultaneously:

$$\beta_{Fe(II)} = [EDTA\text{-}Fe^{2-}] / [EDTA^{4-}] [Fe^{2+}]$$

$$\beta_{Ni(II)} = [EDTA\text{-}Ni^{2-}] / [EDTA^{4-}] [Ni^{2+}]$$

$$\beta_{Mg(II)} = [EDTA\text{-}Mg^{2-}] / [EDTA^{4-}] [Mg^{2+}]$$

$$\beta_{Th(IV)} = [EDTA\text{-}Th] / [EDTA^{4-}] [Th^{4+}]$$

along with mass balance equations for each metal. The nickel concentration of 3.65×10^{-4} used in the calculations was determined by taking the minimum number of moles of nickel expected in the repository, dividing by the available repository volume reported by Weiner (1996) and converting the value to molality. An approximation of 1×10^{-4} molal was chosen for the iron concentration. All other values for component concentrations and apparent

stability constants are reported above. To approximate the effect of ionic strength on the apparent stability constants for nickel and iron the values used were an order of magnitude lower than those reported in Table WCA-10. These calculations do not include all possible metal ions expected under repository conditions, for example calcium and chromium are not included. Therefore, these results are considered conservative. The results indicate more than 97 percent of the total EDTA is complexed by the transition metals. Thus the excess of nonradioactive metals present in the repository will overwhelm the complexation sites of the organic ligands and complexation of the organic ligands with actinides will be negligible.

SOTERM.6 Mobile Colloidal Actinide Source Term

Colloidal particles will be generated in the repository environment as a result of microbial degradation of cellulosics, corrosion of steel waste containers and waste constituents, by the hydrodynamic entrainment of colloidal-sized mineral fragments, and several other mechanisms. Those colloidal particles may sorb dissolved actinides or the dissolved actinides themselves may form colloidal-sized particles. In an intrusion scenario, actinide-bearing colloidal particles, together with dissolved actinides, may be transported to the Culebra by Castile or Salado brines that are present in the repository. Additional colloidal particles may be present in natural Culebra groundwater and could form additional actinide-bearing colloidal particles. After introduction to the Culebra, the dissolved actinides and actinide-bearing colloidal particles are transported by Culebra ground waters. Colloidal actinides may also be transported through the fractured anhydrite interbeds of the Salado.

The actinide source term at the WIPP is defined as the sum of contributions from dissolved actinide species and mobile colloidal actinide species. Colloidal actinides that are not suspended in the aqueous phase (that is, not mobile) are not included in the colloidal actinide source term. Sorption of colloidal actinides onto fixed substrates will also reduce the mobile colloidal actinide source term, but no credit is currently being taken for reduction by that means.

In this section, the quantification of the mobile actinide-bearing colloid component of the actinide source term is described. The quantification of colloid-facilitated transport of actinides in the overlying Culebra, in the event of an intrusion into the repository, is described in Chapter 6.0 (Section 6.4.6.2.2) and Appendix MASS (Section MASS.15.3).

SOTERM.6.1 Introduction

Colloidal particles are generally defined as particles with at least one dimension between 1 nm and 1 μm, suspended in a liquid, and maintained in suspension for very long periods of time by Brownian (random thermal) motion (Hiemenz 1986; Buddemeier and Hunt 1988; Stumm 1992, 1993). Those size boundaries are approximately defined on the basis of physical phenomena. Particles larger than about 1 μm are too large for Brownian motion to overcome gravitational forces, and the particles will rather quickly settle by gravity. An exception is the case of microbes, which are considered to be colloidal, but may exceed 1 μm. The specific

gravities of microbes are typically quite close to that of the dispersant, and so they may not settle by gravitational forces. Generally, particles smaller than approximately 1 nm behave in transport like dissolved ionic species.

SOTERM.6.1.1 Formation and Behavior of Colloidal Particles

Inorganic colloidal particles have been reported to form by a variety of processes. Colloidal particles may form by condensation or homogenous nucleation from dissolved species when a mineral phase is supersaturated or as hydrolyzed precipitates of mixed metal ions (Kim 1992). Colloidal particles may also form by release of particles from bulk material due to disruption of fragile aggregates by changes in ionic strength or hydrodynamic forces, dissolution of a more soluble surrounding matrix (Buddemeier and Hunt 1988; Kim 1994), mechanical grinding of mineral surfaces, or mechanical disruption of secondary minerals present at mineral surfaces (McCarthy and Zachara 1989).

Organic colloidal particles may form from microbial degradation of materials, condensation reactions of organic molecules to form humic substances, or microbe activity. A variety of naturally occurring organic materials, such as viruses, microbes, and pollen, are colloidal-sized particles (McCarthy and Zachara 1989; Stumm 1992, 243).

Colloidal particles may interact with actinides to form radiocolloids in two ways (see, for example, Lieser et al. 1986a,b, 1990; Kim et al. 1984a,b; Buddemeier and Hunt 1988; Kim 1992, 1994). First, radiocolloids may form as a result of chemical reactions involving dissolved polyvalent actinide ions. Hydrolysis and condensation reactions have been shown to form actinide macromolecules in which the actinide ions are bridged with hydroxyl ions to form polymers. Those radiocolloids are termed "actinide intrinsic colloids," "true colloids," "real colloids," "Eigenkolloide," or "type I colloids."

A second means to form radiocolloids is by sorption of actinides by ordinarily non-radioactive colloidal particles. In the actinide environmental geochemistry literature, the non-radioactive colloidal particle has been called a "ground-water colloid." Once actinide sorption has occurred, the resulting radiocolloids may be called "pseudo-colloids," "carrier colloids," "Fremdkolloide," or "type II colloids." The colloidal substrate for sorption may be a mineral fragment, a microbial cell, or a humic substance. Bates et al. (1992) recently described radiocolloids, which they called "primary colloids," forming in situ at the surfaces of vitrified radioactive waste as it reacts chemically with water. Considering that coprecipitation is a continuum with adsorption (see, for example, Comans and Middleburg 1987; Stumm 1992, 253 et seq.), the "primary colloid" can be included in the carrier colloid category, and more specifically, a mineral fragment type colloidal particle. A similar sort of colloid would form by isomorphous lattice substitution of actinide ions during mineral precipitation (that is, coprecipitation) or precipitation of actinide minerals.

In the traditional colloid chemistry literature, two types of colloidal particles are defined on the basis of how they interact with the dispersant (see, for example, Alexander and Johnson

1949, 114; Vold and Vold 1983; Hirtzel and Rajagopalan 1985; Hiemenz 1986; Ross and Morrison 1988; Hunter 1991-1992). Hydrophobic colloids are stabilized by electrostatic forces, whereas hydrophilic colloids are stabilized by solvation forces. In light of increased knowledge of aqueous surface chemistry gained over the past two decades, the terms hydrophilic and hydrophobic must be used cautiously, because even hydrophobic surfaces have hydrophilic surface functional groups. It is important, however, to make the distinction between how those two types of colloidal particles behave, because they exhibit different kinetic stability behaviors in electrolytes.

Kinetic stability differs from thermodynamic stability. Thermodynamic stability refers to the chemical equilibrium between the colloidal particles and the dispersant, whereas kinetic stability refers to the rate at which colloidal particles in a colloidal dispersion are removed from suspension due to agglomeration followed by gravitational settling. Thermodynamic stability may be most important for actinide intrinsic colloids, because that type of colloid forms directly from solution by chemical reactions. Kinetic stability is inversely related to the rate of particle aggregation, which is dependent on the frequency and efficiency (the fraction resulting in permanent joining) of collisions between colloidal particles. The behavior of colloidal particle types as a function of ionic strength is probably the single most important phenomenon affecting the importance of colloid-facilitated actinide transport at the WIPP.

Hydrophobic colloidal particles are kinetically stabilized and destabilized by electrostatic forces. In an aqueous dispersant, hydrophobic colloidal particles are attracted to one another by van der Waals forces. That electrostatic attraction is countered by repulsive forces generated by a cloud of counterions surrounding each particle (Lyklema 1978; Hiemenz 1986). In a kinetically-stable colloidal dispersion, colloidal particles are usually repelled from one another before they get close enough to become agglomerated. However, as the ionic strength of the dispersion is increased, the thickness of the cloud of counterions is compressed, allowing closer particle-particle interaction. The net effect is that as colloidal particles come into proximity with one another in the dispersion, a greater chance for sticking exists, and so the rate of agglomeration increases. That phenomenon is very effective at removing colloidal particles from suspension even at fairly low ionic strengths over periods of hours to days. Mineral fragments, which are a hydrophobic colloid type, are affected by ionic strength in this way.

Hydrophilic colloidal particles are stabilized by solvation forces, which are largely independent of the ionic strength of the dispersant (Alexander and Johnson 1949). This type of colloidal particle is essentially a dissolved macromolecule. Humic materials are an example of the traditional hydrophilic colloid type. Two major categories of hydrophilic colloidal particles are recognized. Micelles are aggregates of dissolved monomers, that are in thermodynamic equilibrium with those monomers. Polyelectrolytes are charged polymers that are not in thermodynamic equilibrium with a monomeric species (examples of polyelectrolytes include gum arabic, gelatin, pectin, and proteins). An important distinction, therefore, is that micelles require a minimum threshold concentration of monomers (the critical micellization concentration, or c.m.c.) to form. In contrast, the formation of

polyelectrolytes is not dependent on monomer concentration. Polyelectrolytes may act as an association colloid by adsorbing on hydrophobic colloidal particles. The resulting dispersions may be extremely kinetically stable (Hiemenz 1986, 659).

The kinetic stability of hydrophobic colloidal particles may be modified by coatings of steric stabilizing compounds, which themselves are essentially hydrophilic materials (also referred to as protective or association colloids) which modify the surface behavior to inhibit close interaction of particles. Such colloidal systems are rendered kinetically stable. Particles stabilized by organic compounds in seawater are an example of a sterically stabilized colloidal system. Microbes can be considered as stabilized in a similar manner, except that the stability is imparted by molecules (for example, polysaccharides), attached to the surface of the microbe, which have hydrophilic parts extending into the dispersant.

Colloidal particles may have rigid or flexible structures, which may affect the way in which they interact with the host rock during transport. "Hard-sphere" colloidal particles, such as mineral fragments, have discrete well-defined boundaries at the particle-water interface, and are rigid. "Soft-sphere" colloidal particles, such as humic substances, have less distinct boundaries at the particle-water interface, are flexible and may undergo conformational changes in response to environmental variations. "Soft-sphere" colloids are essentially dissolved macromolecules and are closest in form and behavior to particles referred to as hydrophilic colloids in the traditional colloid chemistry literature (Lyklema 1978; Hiemenz 1986).

SOTERM.6.1.2 Definition of Colloidal Particle Types

On the basis of the phenomena described in the previous section, several classification schemes have been proposed by various workers, and a large number of descriptive terms have evolved and been propagated in the literature. For actinide environmental geochemistry, most of the classification schemes are based on how the colloidal particle interacts with radionuclides. Colloidal particles are classified into the following four types for evaluation of the impact of colloidal particles at the WIPP site:

(1) Mineral fragments are hydrophobic, hard-sphere particles, that are kinetically stabilized or destabilized by electrostatic forces, and may consist of crystalline or amorphous solids. Mineral fragments may be made kinetically stable by coatings with steric stabilizers that prevent close contact. Mineral fragments may act as substrates for sorption of actinides or they may consist of precipitated or coprecipitated actinide solids.

(2) Actinide intrinsic colloids are macromolecules of actinides that, at least in some cases, may mature into a mineral fragment type colloidal particle. When immature, they are hydrophilic; when mature, they become hydrophobic.

(3) Humic substances are hydrophilic, soft-sphere particles, that are stabilized by solvation forces. They are often powerful substrates for uptake of metal cations and are relatively small (less than 100,000 atomic mass units).

(4) Microbes are relatively large colloidal particles that are stabilized by hydrophilic coatings on their surfaces, which behave as steric stabilizing compounds. They may act as substrates for extracellular actinide sorption or they may actively bioaccumulate actinides intracellularly.

SOTERM.6.2 Performance Assessment Implementation

Results of the colloidal actinide investigation were used in performance assessment in three types of parameter values: (1) constant concentration values; (2) concentration values proportional to the dissolved actinide concentration; and (3) maximum concentration values. The parameter types are summarized below and are described in parameter record packages (Papenguth 1996a,b,c,d).

For actinide intrinsic colloids and mineral fragment colloids, actinide concentrations associated with them were described as constant values. Table SOTERM-8 summarizes the material and parameter names and descriptions. As discussed in Appendix PAR (Section PAR.3), IDMTRL is the material name in the INGRES data base, and IDPRAM is the parameter name.

Experiments conducted to quantify actinide concentrations associated with humic substances and microbes provided the basis for a more sophisticated representation, in which colloidal actinide concentations were related to the dissolved actinide concentration by proportionality constants. For microbes, the proportionality relationship was made by element. For humic actinides, however, the relationship was made by oxidation state rather than by element. For microbes and humic substances, the experiments also provided a basis to define upper limits for the concentration of actinide that could be associated with each of those colloid types. For both humic and microbial actinides, the upper limit parameter was defined by element rather than oxidation state, and is in units of molarity. The use of the two upper limit parameters is slightly different, and is described in the sections below discussing humic substances and microbes.

SOTERM.6.3 Development of Parameter Values

In this section, the experimental basis for the parameter values is described. For each of the four colloidal particle types, the characteristics of the colloidal particle type are described, the experimental program is outlined, methods of interpretation are described, and results are summarized.

Table SOTERM-8. Material and Parameter Names for Colloids

IDMTRL	IDPRAM	Brief Description of Parameter
Th, U, Np, Pu, Am	CONCMIN	concentration of actinide associated with mobile mineral fragment colloids
Th, U, Np, Pu, Am	CONCINT	concentration of actinide associated with mobile actinide intrinsic colloids
Th, U, Np, Pu, Am	PROPMIC	proportionality constant for concentration of actinides associated with mobile microbes.
PHUMOX3* PHUMOX4 PHUMOX5 PHUMOX6	PHUMCIM	proportionality constant for concentration of actinides associated with mobile humic colloids, in Castile brine, actinide solubilities are inorganic only (complexes with man-made organic ligands are not important), solubilities were calculated assuming equilibrium with Mg-bearing minerals (brucite and magnesite);
PHUMOX3* PHUMOX4 PHUMOX5 PHUMOX6	PHUMSIM	proportionality constant for concentration of actinides associated with mobile humic colloids, in Salado brine, actinide solubilities are inorganic only (complexes with man-made organic ligands are not important), solubilities were calculated assuming equilibrium with Mg-bearing minerals (brucite and magnesite).
Th, U, Np, Pu , Am	CAPMIC	maximum (cap) concentration of actinide associated with mobile microbes;
Th, U, Np, Pu, Am	CAPHUM	maximum (cap) concentration of actinide associated with mobile humic colloids.

* Proportionality constant for concentration of actinides associated with mobile humic substances, for PHUMOX3, for actinide elements with oxidation state 3 [that is, Pu(III) and Am(III)]; PHUMOX4, oxidation state 4 [that is, Th(IV), U(IV), Np(IV), and Pu(IV)]; PHUMOX5, oxidation state 5 [that is, Np(V)]; and PHUMOX6, oxidation state 6 [that is, U(VI)].

SOTERM.6.3.1 Mineral Fragment Colloids

Mineral fragment type colloidal particles may be present in naturally occurring groundwaters, and they may be released from the host rock due to disruption of fragile aggregates by changes in ionic strength or hydrodynamic forces, dissolution of a more soluble surrounding matrix, mechanical grinding of mineral surfaces, or mechanical disruption of secondary minerals present at mineral surfaces. Under certain conditions, such as extreme changes in ionic strength of the groundwater or by physical disruption due to natural or human-induced events, mineral fragment type colloidal particles could also be produced within the Culebra. In an intrusion scenario at the WIPP, mixing of repository brines with Culebra brines may result in mineral precipitation that may include coprecipitation of actinide-bearing mineral fragment type colloidal particles. Within the repository, mineral fragment type colloidal particles may form from corrosion of iron-bearing waste and the steel packaging materials. In addition,

Portland cement based matrixes will be attacked and will produce mineral fragment type colloidal particles. Bentonite, which may be a constituent of drilling mud is itself a potential source of mineral fragment type colloidal material that should be considered for actinide transport.

In terms of colloidal actinide transport, mineral fragment type colloids act as carriers, in that actinide ions sorb onto the surfaces of the colloids. Because each mineral substrate has a different affinity for actinides, quantification of actinide concentrations associated with the wide range of mineralogies likely to be present at the WIPP is insurmountable. Instead, a bounding approach was used based on residual concentrations of colloidal particles in WIPP-relevant brines coupled with estimates of reasonable maximum concentrations of actinides that could be sorbed onto the colloid surfaces. That approach requires three pieces of information: (1) the number of mineral fragment type colloidal particles in the aqueous phase; (2) the geometric surface area of individual colloidal particles; and (3) the site-binding capacity of the mineral surface. In the remainder of this section, descriptions of the determination of items (1) through (3), the interpretation of that information, and the development of parameter values are provided.

SOTERM.6.3.1.1 Description of Experiments

Hydrophobic colloidal particles, such as mineral fragments, are kinetically stabilized and destabilized by electrostatic forces (refer to detailed discussion in Papenguth and Behl 1996, Sections 2.5.1 and 2.6). In an aqueous dispersant, hydrophobic colloidal particles are attracted to one another by van der Waals forces. That electrostatic attraction is countered by repulsive forces generated by a cloud of counterions surrounding each particle. In a kinetically stable colloidal dispersion, colloidal particles are usually repelled from one another before they get close enough to become agglomerated. However, as the ionic strength of the dispersion is increased, the thickness of the cloud of counterions is compressed, allowing closer particle-particle interaction. The net effect is that as colloidal particles come into proximity with one another in the dispersion, a greater chance for sticking exists, and so the rate of agglomeration increases. That phenomenon is very effective at removing colloidal particles from suspension even at fairly low ionic strengths over periods of hours to days.

The kinetic stability of the mineral-fragment-type colloids in WIPP-relevant brines was evaluated in coagulation series experiments. Colloidal dispersions of mineral fragments were prepared by mechanical disaggregation of representative mineral, rock samples, and other materials or by chemical precipitation from laboratory reagents. Brine simulants were prepared that covered the ranges of ionic strengths observed in WIPP brines. The brines were sequentially diluted with deionized water by factors of 10 and adjusted to acidic, neutral, and basic pH conditions to evaluate the effects of ionic strength and pH on kinetic stability. At the ionic strength referred to as the critical coagulation concentration (c.c.c.), colloidal particles will rapidly coagulate, forming agglomerates large enough to settle by gravitational forces. The number population of colloidal particles remaining in suspension in the various

dispersions was measured over time to assess their stability as a function of solution ionic strength and time.

Colloidal dispersions were prepared for the following minerals or materials: bentonite, kaolinite, montmorillonite, vermiculite, illite, anhydrite, calcium carbonate, magnesite, hematite (mechanically disaggregated), hematite (chemical precipitate), limonite, goethite, magnetite, quartz, siderite, brucite, strontianite, diatomaceous earth, pyrite, and cellulosic materials (Masslinn paper towels and Scott paper towels). The brine solutions used included a Salado-like brine simulant (SPC brine) and a Culebra brine simulant (H-17). For c.c.c. experiments, sequential dilutions of those brines were made that spanned approximately five orders-of-magnitude. Brine simulants consisting of 0.5 M NaCl or $CaCl_2$ were also used. For the residual concentration measurements which were used as the basis for the performance assessment deliverables described herein, the one order-of-magnitude dilution (that is, 10 percent of original strength) of the Salado-like brine and the Culebra brine simulants were used. That reduction in ionic strength provides a degree of conservatism in the results.

The c.c.c. experiments for the various concentrations of WIPP brine simulants were conducted under acidic (observed pH generally ranging from 3 to 4), neutral (pH 6 to 8), and basic (pH 9 to 12) conditions. Following the introduction of an aliquot of dispersed colloidal particles to a series of test tubes containing the sequentially diluted brine, colloidal particle concentrations remaining near the top of the fluid columns (residual concentration) were measured as a function of time. The degree of coagulation and settling was quantified using an inductively coupled argon-plasma atomic emission spectrophotometer, nephelometry, and direct particle counting.

Most of the experiments conducted relating to the kinetic stability of mineral fragment colloidal particles were qualitative to semi-quantitative, and were focused on evaluating whether a c.c.c. existed. For the final experiments, however, a state-of-the-art particle spectrometer was used with significantly greater sensitivity. That device was designed for semiconductor fabrication plants, which require extremely pure processing water, and use a similar instrument to ascertain purity. The final experiments were conducted over an extended period of time using the more sensitive analytical technique to determine the number and size of colloids in the brine suspensions. Those experiments were conducted in a similar fashion to previous experiments for bentonite (supplied by the Aldrich Chemical Co.), goethite, and hematite (mechanically disaggregated), but in a relatively dilute (and therefore conservative) brine simulant consisting of 0.1 M NaCl. Residual particle concentrations made with the particle spectrometer compared favorably with measurements made with spectroscopic techniques made at similar experiment times. Generally after the first day of the c.c.c. experiments, the majority (greater than 99 percent) of the colloidal particles had already settled out of suspension. With the more sensitive particle spectrometer, however, residual concentrations of colloidal particles were observed to continue to decrease. For experiments analyzed by spectroscopic or light-scattering techniques, final residual colloid number populations remaining suspended in the test vessels were determined by multiplying the initial colloid number populations determined at the start of the experiments by the fraction of

suspended colloids remaining at the final reading. Using the particle spectrometer, final number populations were measured directly.

SOTERM.6.3.1.2 Interpretation and Discussion

Parameter values (CONCMIN) describing the amount of actinide element bound by mineral fragment type colloidal particles were determined from the information described above, combined with estimates of adsorption site densities.

Actinides sorbed to the surfaces of colloidal particles can be estimated using ranges of values for adsorption site densities taken from published surface complexation modeling research. The actinide concentration contained by a single mineral fragment type colloidal particle is calculated by considering the geometrical surface area of a spherical particle:

$$[An]_p = \frac{\pi D^2 N_s}{N_A} \quad , \qquad (6\text{-}1)$$

where:

$[An]_p$	=	concentration of an adsorbed actinide element (moles/particle)
D	=	spherical colloidal particle diameter (nm)
N_S	=	adsorption site density (sites/nm^2)
N_A	=	Avogadro constant

An adsorption site density of 1 site/nm^2 was used for N_S in the above equation, a value which is realistic, but probably conservative. With that site density, 1 nm and 1 μm diameter particles could have a maximum of about 10^{-24} and 10^{-18} moles actinide per particle, respectively. To obtain an estimate of the maximum actinide concentrations that could be associated with the colloids, the estimates of residual colloid number populations (particles per liter of dispersion) were multiplied by the estimated maximum actinide transport capacity described by Equation 6-1. The use of a uniform adsorption site density is a conservative approach, because the actual sorption on mineral surfaces should be described by some kind of isotherm which will result in less than 100 percent coverage. Further, if multivalent adsorbates are present [for example, U(VI)], multiple adsorption sites may be required for one adsorbate ion, reducing the net adsorption capacity of the surface.

Final residual colloid number populations quantified by spectrophotometry or nephelometry showed that mineral fragment type colloidal particles are kinetically destabilized by brines similar in composition to those present at the WIPP site. Colloid number population values were, with a few exceptions, reduced to less than 5 percent of the initial values within 1 day. Conservative estimates of maximum actinide concentrations associated with those residual colloid populations are on the order of 10^{-7} to 10^{-9} moles actinide per liter of dispersion.

The final experiments, which utilized the particle spectrometer to measure the quantity of colloids remaining in suspension offered the most sensitive estimates. Moreover, those experiments were conducted for substantially longer periods of time than the semi-quantitative c.c.c. experiments. Those experimental results are shown in Table SOTERM-9.

Table SOTERM-9. Experimental Results for Mineral Fragment Colloids

Mineral	Time of Final Reading (days)	Estimated Actinide Concentration (moles/liter dispersion)
hematite	12.8	1.6×10^{-8}
goethite	12.9	9.5×10^{-10}
bentonite	12.8	1.6×10^{-10}
geometric mean		1.3×10^{-9}

The DOE believes that the experimental results using the particle spectrometer with the three distinct colloids (hematite, goethite, and bentonite), are representative of other mineral fragment type colloidal particles in terms of their behavior in brine solutions. The geometric mean was assumed to be a more representative average of the final colloid concentrations than the arithmetic mean because of the very small final colloid concentrations (which, for this particular case, is also conservative).

Mineral fragment type colloidal particles are unique among the four colloidal particle types addressed for the WIPP, because their concentrations are not generally linked to solubility, as are actinide intrinsic colloids and humic substances, or to a maximum supportable population in the case of microbes. Consequently, in an intrusion scenario at the WIPP, as dissolved actinide elements are introduced to the Culebra, it is possible that those dissolved actinides could sorb onto a separate population of indigenous mineral fragments, producing a supplemental source term. To account for that possibility, the geometric mean value listed above was multiplied by a factor of two, producing a final "most-likely value" of 2.6×10^{-9} moles actinide per liter of dispersion.

To capture uncertainty, mainly stemming from knowledge of the adsorption site density value, a triangular distribution with "minimum values" and "maximum values" spanning one order of magnitude about the geometric mean was provided for performance assessment calculations. Additional conservatism is incorporated into the mineral fragment parameter values in that the total concentration of actinides carried by mineral fragment colloidal particles have essentially been multiplied by a factor of five, because a separate population of colloidal particles has been assumed for each actinide element. No consideration of competition for sorption sites is incorporated into the calculation approach. The value used for adsorption site density is conservative, but reasonable. For the performance assessment calculations, however, the triangular distribution was not sampled. Instead, the maximum parameter values were used as constant values, which essentially results in a site density of 10

sites/nm^2. Parameter values for CONCMIN are summarized in Section SOTERM.6.3.5. Section SOTERM.7 discusses details on performance assessement implementation.

SOTERM.6.3.2 Actinide Intrinsic Colloids

Actinide intrinsic colloids (also known as true colloids, real colloids, type I colloids, and Eigenkolloide) form by condensation reactions of hydrolyzed actinide ions and consist solely of actinide cations linked by anions. There are several stages in the development of actinide intrinsic colloids at which they have significantly different behaviors. When immature, actinide intrinsic colloids display physiochemical properties that are similar to ionized humic substances. With age, they become more similar to mineral-fragment type colloidal particles.

The experimental approach used was strongly influenced by reviews of published literature on actinide intrinsic colloids. Pertinent literature is discussed below (see also Papenguth and Behl 1996).

SOTERM.6.3.2.1 Intrinsic Colloids of Plutonium

The most well-known and well-studied actinide intrinsic colloid is the Pu(IV) intrinsic colloid, which has been used as a basis of comparison for investigating intrinsic colloids of other actinides. Most of the knowledge about the Pu(IV) intrinsic colloid comes from research at high Pu concentrations in highly acidic solutions, which was conducted to help improve the efficiency of processing techniques. The Pu(IV) intrinsic colloid is notorious in its propensity to polymerize to form a gel-like material, which can even plug process lines.

A conclusive demonstration of the mechanisms of formation of the Pu(IV) intrinsic colloid has not yet been made, but there is a preponderance of evidence that suggests that polymerization is strongly linked to hydrolysis, and that the initial polymerization, or condensation, produces a macromolecule that becomes progressively more crystalline with time. The final mature colloid has a composition between $Pu(OH)_4$ (am) and PuO_2 (c), although the latter compound may be only partly crystalline and both may include interstitial water molecules.

The most convincing and consistent explanation for the chemistry of the Pu(IV) intrinsic colloid is presented by Johnson and Toth (1978). Those authors developed a conceptual model to explain the solution chemistry of a variety of metal cations and a variety of oxidation states. The conceptual model involves processes referred to as "olation" and "oxolation" in which metal cations become bridged with hydroxyl groups, which in turn undergo irreversible elimination of water and concurrent formation of oxygen bridges. Johnson and Toth demonstrate that the model is consistent with the observed behavior of the Pu(IV) intrinsic colloid.

Hydrolysis reactions for metal cations such as plutonium may be written as follows:

first: $Pu^{4+} + H_2O \ddot{O} PuOH^{3+} + H^+$ (6-2)

second: $PuOH^{3+} + H_2O \ddot{O} Pu(OH)_2^{2+} + H^+$ (6-3)

third: $Pu(OH)_2^{2+} + H_2O \ddot{O} Pu(OH)_3^{+} + H^+$ (6-4)

fourth: $Pu(OH)_3^{+} + H_2O \ddot{O} Pu(OH)_4\,(aq) + H^+$ (6-5)

Johnson and Toth (1978) point out, however, that in interpreting the formation of the Pu(IV) intrinsic colloid, it makes better sense to include the implied waters of hydration that surround metal cations in solution. Hydrolysis Equations 6-2 through 6-5 can be rewritten as follows, where n equals 4:

first: $[Pu(H_2O)_m]^{n+} \ddot{O} [Pu(OH)(H_2O)_{m-1}]^{n-1} + H^+$ (6-6)

second: $[Pu(H_2O)_{m-1}]^{n-1} \ddot{O} [Pu(OH)(H_2O)_{m-2}]^{n-2} + H^+$ (6-7)

third: $[Pu(H_2O)_{m-2}]^{n-2} \ddot{O} [Pu(OH)(H_2O)_{m-3}]^{n-3} + H^+$ (6-8)

fourth: $[Pu(H_2O)_{m-3}]^{n-3} \ddot{O} [Pu(OH)(H_2O)_{m-4}]^{n-4} + H^+$ (6-9)

From the literature, it is clear that polymerization occurs nearly immediately after the first hydrolysis (Equation 6-6) occurs. Johnson and Toth (1978) suggest the following reaction involving polymerization of two hydrolyzed species by loss of water (oxolation):

$$2\{[(H_2O)_{d-2}Pu(OH)(H_2O)]^{+(y-1)}\} \ddot{O} [(H_2O)_{d-2}Pu(OH)(OH)Pu(H_2O)_{d-2}]^{+2(y-1)} + 2H_2O \quad (6\text{-}10)$$

Aging or maturation of polymer then occurs by loss of water (olation) as follows:

$$[Pu(OH)(OH)Pu(OH)(OH)Pu(OH)(OH)...] \ddot{O} [Pu(O)Pu(O)Pu(O)...]_n + 3nH_2 \quad (6\text{-}11)$$

Maiti et al. (1989) and Laul et al. (1985) describe similar reactions, but it appears that they believe that the third hydrolysis reaction occurs, because they use the $Pu(OH)_3^+$ ion in their proposed polymerization reaction. Use of that ion does not appear to be consistent with observations by many workers that polymerization occurs immediately after the first hydrolysis reaction.

As the actinide polyelectrolytes mature through the olation process to become closer in composition to an actinide-oxide mineral, they will be kinetically destabilized by the high ionic strengths of the WIPP brines and will not be mobile. Further, the solubilities of the mature solid phase cannot be exceeded. In fairly long-term experiments, Nitsche et al. (1992, 1994) showed that the concentration of Pu(IV) intrinsic colloid stabilized at about 10^{-8} M. It is not known whether the form was Pu(IV) polyelectrolyte or Pu(IV) mineral fragment type colloid.

SOTERM.6.3.2.2 Intrinsic Colloids of other Actinides

Reference is made to a variety of intrinsic colloids of other actinides, but no systematic investigations of their formation and behaviors appear to have been made. Plutonium is

apparently unique in its propensity to form an intrinsic colloid. No mention is made in the literature of maturation of polyelectrolytes of other actinides to form mineral fragment type colloidal particles as plutonium does.

In general, the tendency of actinides to hydrolyze and to polymerize to form intrinsic colloids follows the order:

$$An^{4+} >> An(VI)O_2^{2+} > An^{3+} > An(V)O_2^{+} \qquad (6\text{-}12)$$

(Cleveland 1979a,b; Choppin 1983; Kim 1992; Lieser et al. 1991, 119). The order of oxidation states in the equation above results from the ionic charge to ionic radius ratios. The tendency for hydrolysis of $An(VI)O_2^{2+}$ is greater than for An^{3+} because the effective charge on the central cation on the linear $[O\text{-}An\text{-}O]^{2+}$ ion is 3.3±0.1, slightly greater than 3. This trend generally holds true for the actinide elements in general, because of the very small changes in ionic radii among the actinide elements (this is the oxidation state analogy; refer to Novak 1996). There are differences in the behaviors of the actinides from element to element that stem from very subtle changes in the charge to radius ratio and the nature of the configuration of the f molecular orbital.

Considering Pu as an example, hydrolysis becomes significant for Pu^{4+}, $Pu(VI)O_2^{2+}$, Pu^{3+}, and $Pu(V)O_2^{+}$ at pH values of <1, 4-5, 6-8, and 9-10, respectively (Choppin 1983). On the basis of the hydrolysis trend, it is not likely that An(III) and An(V) actinides will form actinide intrinsic colloids. There are suggestions in the literature, however, that Am^{3+} may form an intrinsic colloid, which is surprising because it does not undergo hydrolysis until relatively high pH. Thorium does not follow the trend described by Equation 6-12 because its large size makes it resistant to hydrolysis (Cotton and Wilkinson 1988). Nevertheless, thermodynamic data suggest that in almost all environments (near neutral or higher pH) thorium exists as $Th(OH)_4$ (aq). Moreover, thorium has been reported to form a polymer (Kraus 1956; Johnson and Toth 1978), although as discussed below, this species should be referred to as an oligomer.

Examples can be found in the literature of polymeric species of many of the actinides of importance to the WIPP (see, for example, Baes and Mesmer 1976; Kim 1992). It is important, however, to note the sizes of polymers described in the literature. It is well known that as polyvalent metals, the actinides can form polynuclear species, but they are largely lower polymers (that is, oligomers) such as dimers, trimers, tetramers, and hexamers (see, for example, Choppin 1983, 46). However, in terms of physical transport behavior, lower polymers will behave no differently than dissolved monomeric species. In contrast, the higher polymers, such as the Pu(IV)-polymer, may reach colloidal sizes (1 nm to 1 μm) and will have different hydrodynamic properties than the sub-colloidal-sized dissolved species. Johnson and Toth (1978) reported a molecular weight of 4000 for a Th polymer. Assuming that it consisted of $Th(OH)_4$, that polymer would consist of about 13 thorium metal ions (that is, the degree of polymerization number, N). That observation is consistent with Kraus (1956), in which he quotes an N value of about 9 for Th polyelectrolyte.

Empirical evidence published in the literature does not always support the suggestion that Am, as a trivalent cation, will form an intrinsic colloidal particle. Avogadro and de Marsily (1984) suggested that, like Pu, Am is a likely candidate to form an insoluble hydroxide. Buckau et al. (1986) reported the formation of Am(III) intrinsic colloids at near neutral pH conditions, with a particle size greater than 1 nm. In their study of the hydrolysis of Am(III) over a pH range from 3 to 13.5, however, Kim et al. (1984a) found only monomers of Am. Regardless of whether Am(III) intrinsic colloids will form under highly idealized laboratory environments, it would be highly unlikely that they would form in a geologic system, because of the tremendously strong sorption properties of the Am(III) ion.

SOTERM.6.3.2.3 Experimental

The focus of experiments, conducted at Lawrence Livermore National Laboratory (LLNL), were to test phenomena described in the published literature, under WIPP-relevant conditions:

- critical coagulation concentration for mature Pu(IV) mineral fragment type colloid (refer to description of experiment AIC-1 in Papenguth and Behl [1996]),
- formation of Pu(IV) colloid, from oversaturation and undersaturation in the absence of carbon dioxide (AIC-8 and AIC-9, respectively),
- inhibition of Pu(IV) polymerization due to organic complexants (AIC-2),
- depolymerization of Pu-colloid due to organic complexants (AIC-2b),
- polyelectrolyte chain termination by non-actinide metal cations (AIC-4), and
- sorption effects of WIPP repository substrates on Pu(IV) colloid (AIC-5).

The last four experiments listed above provide evidence that, under some conditions at the WIPP, the Pu(IV)-colloid is less likely to form or is sorbed. To parameterize the WIPP performance assessment calculations, however, the first two experiments listed above were used. Both sets of experiments (AIC-1, AIC-8/9) can essentially be viewed as solubility experiments. The critical coagulation experiments are solubility experiments conducted from undersaturation conditions, in which the in-growth of free Pu(IV) is observed (and are therefore equivalent to AIC-9). In both sets of experiments (AIC-1, AIC-8/9), the Pu solution concentration is measured as a function of time for as long as five weeks, as steady-state concentration is being reached. The two sets of experiments were anticipated to provide information to resolve the question of kinetic versus thermodynamic stability control on the formation and development of the Pu(IV) colloid. That question was not resolved, but the data still provide the necessary information for parameterizing the WIPP performance assessment calculations. The values for the parameters submitted for calculations were derived from the experiments listed in Table SOTERM-10.

The data from those experiments are plotted in Figure SOTERM-8 along with regression lines for data collected by Rai et al. (1980) for $Pu(OH)_4$ (am) and PuO_2 and Rai and Swanson (1981) for Pu(IV)-polymer under acidic pH conditions. With MgO backfill, the pcH of the

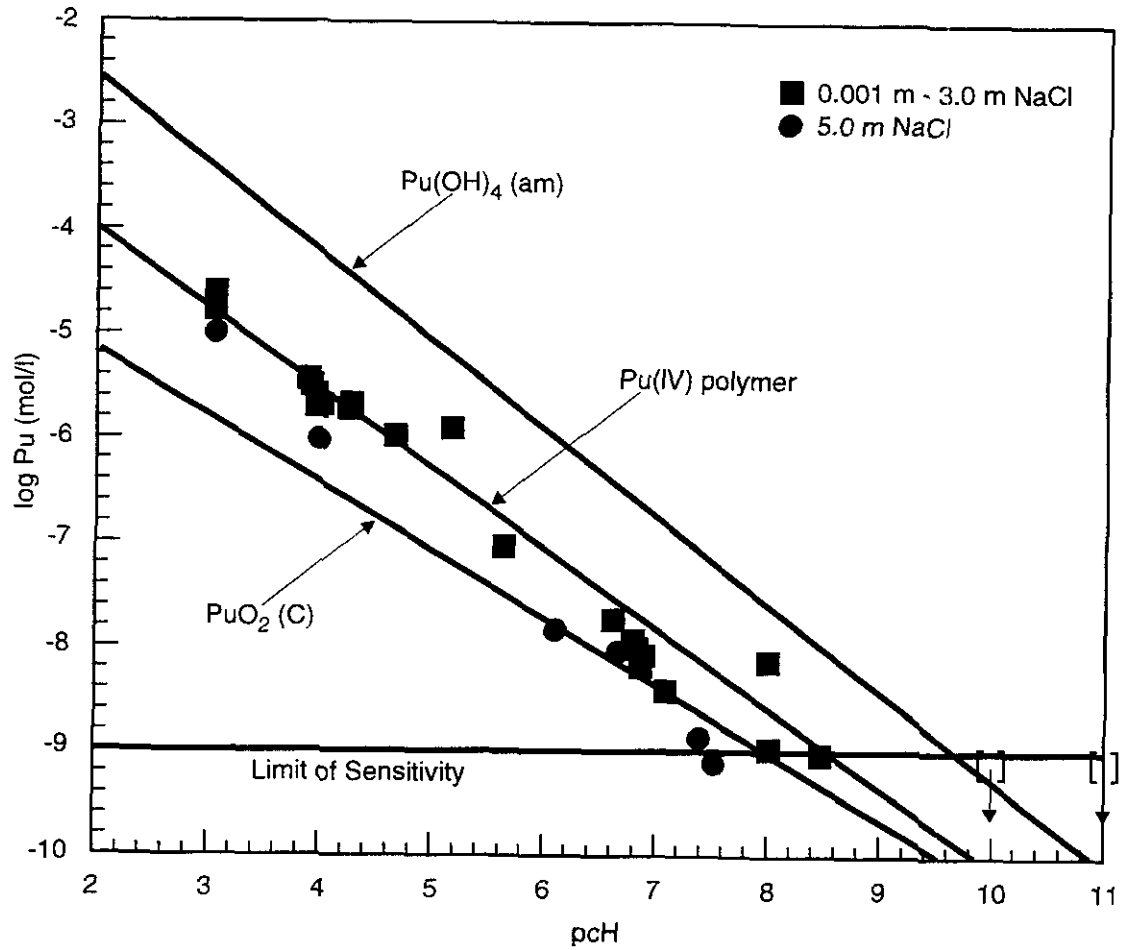

NOTE 1: Open brackets with arrows pointing down indicate Pu concentration is below the minimum analytical detection limit. Solubility lines for $Pu(OH)_{4amorphous}$ and $PuO_{2crystalline}$ are extrapolated from Rai et al. (1980). The solubility line for Pu(IV)-polymer is extrapolated from Rai and Swanson (1981). Plotted values were collected at LLNL as part of the WIPP colloid research program.

NOTE 2: Note that under basic pH conditions fixed by MgO, the solubility of the Pu(IV)-polymer is below the minimum analytical detection limit of 10^{-9} M.

CCA-SOT010-0

Figure SOTERM-8. Solubility of Pu(IV)-Polymer in NaCl Media as a Function of pcH

1 THIS PAGE INTENTIONALLY LEFT BLANK

Table SOTERM-10. Plutonium Intrinsic Colloid Experiments

Number	Experiment	Starting Material	pcH approx.	NaCl (molality)	Duration
AIC-1	c.c.c. (equivalent to undersaturation experiment AIC-9)	Pu(IV) colloid: aged 1 month: about 2×10^{-4} M	4 7 10	0.001 0.01 0.1 0.8 3.0 5.0	3 to 5 weeks
AIC-8	oversaturation	Pu(IV) aquo ion: about 1×10^{-4} M	3 7 10	0.05 0.5 1.0 5.0	4 weeks

repository brine is expected to be about 9.3 (refer to Wang 1996a; also see Novak and Moore 1996; Siegel 1996). As shown in Figure SOTERM-8, the regression line calculated from the LLNL data suggests that at a pcH of 9.3 the solubility of Pu(IV)-polymer is approximately 5×10^{-10} M. Because the extrapolated solubility is less than the minimum analytical detection limit of 1×10^{-9} M, the minimum analytical detection limit value was selected for use in WIPP performance assessment calculations. The LLNL results are consistent with the extrapolated relationships based on published results of Rai et al. (1980) and Rai and Swanson (1981).

SOTERM.6.3.2.4 *Interpretation and Discussion*

Parameter values (CONCINT) describing the amount of actinide element bound by actinide intrinsic colloidal particles were determined from the information described above. For the Pu(IV)-polymer, the minimum analytical detection limit was selected. In the absence of conclusive evidence that intrinsic colloids of other actinides form, or form polymers rather than oligomers, the concentration of Th-, U-, Np-, and Am-intrinsic colloids was set to zero.

Geochemical conditions in the Culebra are not conducive to the formation of a new supplementary population of actinide intrinsic colloids. In particular, the concentration of actinide ions is reduced. Therefore, the source term for actinide intrinsic colloids reflects what would form in the WIPP repository, under most favorable conditions for the formation of the Pu(IV)-polymer.

Parameter values for CONCINT are summarized in Section SOTERM.6.3.5.

SOTERM.6.3.3 Humic Substances

Humic substances are defined as high-molecular-weight organic compounds generally present as anions in natural waters. Humic substances may consist of humic acids, which may be aliphatic or aromatic, or fulvic acids. The difference between humic acids and fulvic acids is largely an operational distinction; humic acids can be precipitated at pH values below about 2, whereas fulvic acids are soluble over the entire pH range. Fulvic acids generally have lower molecular weights than humic acids. The dominant functional group that may react with dissolved actinides are carboxyl groups, but phenolic hydroxyl and alcoholic hydroxyl groups also contribute to complexation. At the WIPP, humic substances may be introduced to the repository as a constituent of soil-bearing waste or may be a constituent of the organic carbon component of Castile, Salado, or Culebra groundwaters. Probably more importantly, humic substances may form from condensation reactions between microbial metabolites (for example, carboxylic acids), cellulosic degradation products, and the extracellular polymers associated with microbes. Because of the general lack of knowledge in the scientific community regarding the formation of humic substances, as well as very slow kinetics of formation, a direct attempt has not been made to quantify the amounts of humic substances that would form in situ. Instead, the contribution of humic-bound actinides was bounded through quantification of humic-actinide complexation behavior coupled with quantification of solubilities of humic substances in WIPP-relevant brines. Regardless of the source of humic substances, the total concentration of humic substance available to mobilize actinides is limited by the solubility of humic substances in WIPP brines. The chemical nature of humic substances generated in situ cannot be predicted either, but can be bounded by the three types of humic substances.

To determine the concentration of actinides associated with humic substances, four pieces of information are required: (1) the concentration of reactive humic substance in the aqueous phase (humic solubility); (2) the binding capacity of the humic substance; (3) actinide uptake (that is, actinide complexation constants); and (4) concentrations of actinide ions in the aqueous phase (that is, actinide solubility). The quantification of actinide solubilities (4) is described in Novak and Moore (1996) and results are summarized in Siegel (1996). In the remainder of this document, the focus is on the determination of items (1) through (3), the interpretation of that information, and the development of parameter values suitable for performance assessment calculations.

SOTERM.6.3.3.1 Experimental

In general, humic substances encompass a broad variety of high-molecular-weight organic compounds. The range of their chemical behaviors, however, is covered by consideration of three types: aliphatic humic acid (generally terrestrial); aromatic humic acid (generally marine); and fulvic acid. The following humic substances were used:

FA-Suw:	fulvic acid isolated from the Suwannee River acquired from the International Humic Substances Society, Golden, Colorado;

HAal-LBr: aliphatic humic acid isolated from sediments collected from Lake Bradford, Florida, prepared by Florida State University;

HAal-Ald: aliphatic humic acid purchased from Aldrich Chemical Co., purified by Florida State University;

HAar-Gor: aromatic humic acid isolated from groundwaters near Gorleben, Germany, obtained from Professor J.-I. Kim, Institut für Radiochemie, München; and

HAar-Suw: aromatic humic acid isolated from the Suwannee River acquired from the International Humic Substances Society, Golden, Colorado.

Solubilities were measured in experiments that were conducted over periods of several weeks. The solubilities of humic substances remaining in the fluid column were determined using a scanning fluorometer, carbon coulometer, and UV/Visible light spectrophotometer, in WIPP-relevant brine simulants with FA-Suw, HAal-LBr, HAal-Ald, and HAar-Suw. In addition to spectroscopic data, visible inspection proved valuable. In oversaturation experiments, humic substances were dissolved in deionized water under basic pH conditions to enhance dissolution and then added as a spike to a brine solution. In undersaturation experiments, humic substances were added directly to brine solutions and allowed to dissolve until an equilibrium was reached. In either case, an equilibrium was reached between dissolved (that is, ionic) and precipitated humic substances. The precipitated humic substances coagulated and settled by gravity. The kinetics of precipitation were sufficiently slow that several weeks were required for equilibrium to be reached. Brine solutions consisted of a NaCl matrix with various concentrations of Ca^{2+} and Mg^{2+}. The concentration of Na^{+} in the brine had little effect on solubility except at very high concentrations, but the concentration of the divalent cations had a significant impact on humic substance solubilities. Consequently, experiments were conducted with a NaCl background electrolyte concentration with concentrations of Ca and Mg ranging from 10 mM each (representative of natural WIPP brines) to 500 mM each (representative of a MgO backfill scenario). At Sandia National Laboratories, solubilities between approximately 1.5 mg/L and 2.0 mg/L were observed in systems containing 10 mM or greater Ca^{2+} and Mg^{2+}. For the calculations described below, the higher solubility value of 2.0 mg/L was used.

Site-binding capacity values were determined by titration at Florida State University for two humic substances (HAal-LBr and HAal-Ald). Those values were supplemented with values for a variety of humic substances compiled from published literature. In general, site-binding capacities for humic substances are between 3 and 6 meq OH^{-}/g, but in isolated cases are as low as about 1.5 and as high as about 9.5 meq OH^{-}/g. For the calculations described below, values of 4.65, 5.38, and 5.56 meq OH^{-}/g were used for aliphatic humic acid, aromatic humic acid, and fulvic acid, respectively. The aliphatic humic acid value was determined from HAal-LBr at Florida State University. The aromatic humic acid value was from Gorleben

(Gohy-573). The fulvic acid value represents the mean of 11 published values for fulvic acids collected in Europe (Ephraim et al. 1995).

Actinide complexation factors for Am(III) and U(VI) binding on three humic substances (FA-Suw, HAal-LBr, and HAar-Gor) were measured at Florida State University. Complexation measurements were made at measured pH_{obs} values of approximately 4.8 and 6, conditions at which the humic substances are highly deprotonated, and actinides U and Am have not undergone extensive hydrolysis reactions. Those conditions were chosen to maximize complexation between the humic substances and those actinide elements. Measurements were made in NaCl media with ionic strengths of approximately 3 and 6 molal. These experiments were completed prior to the DOE establishing the position that MgO backfill would be emplaced to sequester CO_2 and fix pcH at about 9.3. The experiments conducted at Florida State University represent conservative conditions designed to provide high-end estimates of actinide uptake by humic substances. Actinide complexation by humic substances generally decreases at basic pH values because of the reduction in actinide-complex charges due to hydrolysis reactions. In addition, the high concentrations of Mg^{2+} in solution due to the presence of MgO backfill will compete with actinides for binding sites on humic substances and reduce the actinide uptake. Florida State University reported the first and second stability constants defined as follows (square brackets represent concentration):

$$An + HS \leftrightarrow AnHS;\ \beta_{1:An} = [AnHS]/[An][HS] \qquad (6\text{-}13)$$

$$An + 2(HS) \leftrightarrow An(HS)_2;\beta_{2:An} = [An(HS)_2]/[An][HS]^2 \qquad (6\text{-}14)$$

where:

HS	=	humic substance (eq OH-/L, that is, site-binding capacity incorporated)
An	=	actinide element
$\beta_{1:An}$	=	first stability constant, for 1:1 An:humic binding
$\beta_{2:An}$	=	second stability constant, for 1:2 An:humic binding

For the calculations described below, complexation constants were selected from the most relevant experimental conditions, which were pH_{obs} 6 and 6 molal NaCl. The following stability constants reported by Florida State University were used (reported as log values), as shown in Table SOTERM-11.

Table SOTERM-11. Humic Substances Experimental Results

Humic Substance	Am^{3+} : β_1	Am^{3+} : β_2	$U(VI)O_2^{2+}$: β_1	$U(VI)O_2^{2+}$: β_2
HAal-LBr	6.09 +/- 0.05	10.46 +/- 0.12	5.91 +/- 0.16	10 43 +/- 0.19
HAal-Gor	6.02 +/- 0.04	10.40 +/- 0.10	5.35+/- 0.15	8.98 +/- 0.26
FA-Suw	4.6 +/-0.3	8.95 +/- 0.45	not measured	not measured

The Florida State University results show that there is little difference in Am(III) and $U(VI)O_2^{2+}$ uptake by aliphatic and aromatic humic acids, but that uptake by fulvic acid is significantly less. The Florida State University results also show that an increase of NaCl ionic strength from 3 to 6 has little effect on actinide uptake. Those observations aid in justifying the use of published stability constants for other actinide elements experimentally determined at lower ionic strengths and for other humic substances. On the basis of the similarities in stability constants for Am(III) and $U(VI)O_2^{2+}$ for the humic acids, Sandia National Laboratories has used the Am(III) stability constant for FA-Suw for $U(VI)O_2^{2+}$ on FA-Suw.

Stability constants for Th(IV) with several humic and fulvic acids were reported by Nash and Choppin (1980). In NaCl media at pH values between 3.95 and 5.03, those authors reported log stability constants between 9.7 and 13.2. Under basic conditions expected in the WIPP repository, it is likely that complexation of Th(IV) will be markedly less, because the dominant Th(IV)-bearing aqueous species will be $Th(OH)_4$ (aq) (Novak and Moore 1996). No reports of direct investigations of Th-complex binding on humic substances were found. For the calculations described herein, the published results from Baskaran et al. (1992) describing the distribution of Th(IV) in sea water were used. From that work, a ratio of dissolved versus colloidal Th(IV) of 6.349 was calculated, assuming that the solubility of colloidal organic material in sea water is equivalent to our measured value of humic substances in WIPP-relevant brines (that is, 2.0 mg/liter). The nature of the humic substances is likely to be dominated by aromatic humic acid, but may also contain fulvic acid.

For the calculations described herein, a log stability constant for $Np(V)O_2^+$ of 3.67 measured at pH 9 for a Gorleben humic acid (Gohy-573; Kim and Sekine 1991) was used. Results presented in Rao and Choppin (1995) for Lake Bradford humic acid and a Gorleben humic acid (Gohy-573) show little effect of pH on Np(V) stability constants, presumably because of the lack of hydrolysis of reactions for Np(V) over the pH range those authors studied. The Gorleben humic acid is aromatic in nature.

No published stability constants were found for plutonium. For the calculations described herein, an oxidation state analogy was used for the plutonium oxidation species, an approach that is conservative. Allard et al. (1980) have shown that at pH 9, Pu(IV) undergoes hydrolysis reactions to a greater extent than Th(IV), which should result in reduced complexation of Pu(IV).

An oxidation state analogy was used to develop parameter values for elements expected to have multiple oxidation states in the WIPP repository. Oxidation speciation of the actinide elements was evaluated as part of the dissolved actinide source term program. Weiner (1996) has concluded that in the WIPP repository, the following species will be present: Th(IV); U(IV) and U(VI); Np(IV) and Np(V); Pu(III) and Pu(IV); and Am(III). The relative concentrations of oxidation species of a particular element are designated by their respective solubility values. The substitutions made following the oxidation state analogy are summarized in Table SOTERM-12.

Table SOTERM-12. Oxidation State Analogy Substitutions

Required Binding Constant	Substitute	Source of Data
Th(IV)	none required	Baskaran et al. (1992)
U(IV)	Th(IV)	Baskaran et al. (1992)
U(VI)	none required	WIPP-specific data, Florida State University
Np(IV)	Th(IV)	Baskaran et al. (1992)
Np(V)	none required	Kim and Sekine (1991)
Pu(III)	Am(III)	WIPP-specific data, Florida State University
Pu(IV)	Th(IV)	Baskaran et al. (1992)
Am(III)	none required	WIPP-specific data, Florida State University

To compensate for the effects of competition for actinide complexation by the high concentrations of calcium and magnesium in repository brines in the presence of MgO backfill, stability constants for Ca^{2+} and Mg^{2+} were used in simultaneously solved equations (described below). Stability constants for Ca^{2+} and Mg^{2+} at basic pH values are not available, but several published reports provide values in the acidic range. Choppin and Shanbhag (1981) reported log stability constants of 2.25 to 3.32 for Ca^{2+} in 0.1 M NaClO4 at pH 3.9 and 5.0 for an aliphatic humic acid (Aldrich humic acid). Schnitzer and Skinner (1967) reported log binding constants ranging from 2.2 to 3.72 for Ca^{2+} in low ionic strength solutions over a pH range of 3.5 to 5.0 for fulvic acid. For Mg^{2+}, Schnitzer and Skinner (1967) reported log stability constants ranging from 1.23 to approximately 2.0 under the same experimental conditions. For the calculations, a log stability constant of 2.0 for the sum of Ca^{2+} and Mg^{2+} concentrations was used, which is a conservative value.

Binding of Ca^{2+} and Mg^{2+} to humic substances is described in the same way as Equation 6-13 above:

$$(Ca+Mg) + HS \leftrightarrow (CaMg)HS; \quad \beta_{1;Ca,Mg} = [(CaMg)HS]/[Ca+Mg][HS] \qquad (6\text{-}15)$$

where:

$\beta_{1;CaMg}$ = first stability constant, for 1:1 (Ca+Mg):humic binding (note that no second stability constants exist for divalent cation binding)

SOTERM.6.3.3.2 *Interpretation and Discussion*

Proportionality constants (PHUMCIM and PHUMSIM) describing the amount of actinide element bound to humic substances were determined from the data listed above, coupled with dissolved actinide concentrations. In addition, maximum theoretical concentrations of actinides that could be associated with humic substances (CAPHUM) were calculated from the data above.

The concentration of an actinide element of a given oxidation state was calculated by simultaneous solution of Equations 6-13 and 6-15, combined with a mass-balance expression:

$$[HS_{tot}] = [AnHS] + [(CaMg)HS] + [HS] \quad (6\text{-}16)$$

where:

- $[HS_{tot}]$ = total concentration of humic substance
- $[HS]$ = concentration of uncomplexed humic substance
- $[AnHS]$ = concentration of humic complexed with an actinide element
- $[(CaMg)HS]$ = concentration of humic complexed with divalent cations

Equation 6-13 describing the effect of two humic substances binding with one actinide ion was disregarded for these calculations, because its contribution to the total humic-bound actinide concentrations was negligible.

Rearranging Equations 6-13 and 6-15 provides:

$$[AnHS] = \beta_{1:An}\,[An]\,[HS]\,, \quad (6\text{-}17)$$

$$[(CaMg)HS] = \beta_{1:CaMg}\,[Ca+Mg]\,[HS]\,. \quad (6\text{-}18)$$

Substituting Equations 6-17 and 6-18 into Equation 6-16 results in:

$$[HS_{tot}] = \beta_{1:An}\,[An]\,[HS] + \beta_{1:\,CaMg}\,[Ca+Mg]\,[HS] + [HS]\,. \quad (6\text{-}19)$$

Rearranging Equation 6-19 provides:

$$[HS] = \frac{[HS_{tot}]}{\beta_{1:An}[An] + \beta_{1:CaMg}[Ca+Mg] + 1}\,. \quad (6\text{-}20)$$

Equations 6-17, 6-18, and 6-20 were used to calculate humic-bound actinide concentrations ([AnHS]). The resulting AnHS concentration values were then summed for actinide elements with multiple oxidation states, and then divided by the dissolved concentration of the respective actinide element. The final forms of the parameter values PHUMCIM and PHUMSIM are proportionality constants in units of "moles humic-bound colloidal actinide per mole of dissolved actinide." The proportionality values may be multiplied by the dissolved actinide concentration expressed in molarity or molality, depending on the desired final unit.

Depending on the intrusion scenario, the WIPP repository may be dominated by Castile brine or by intergranular Salado brine, resulting in different actinide solubilities, but also different

solubilities of Ca^{2+} and Mg^{2+}. Under MgO backfill conditions, solubility parameters calculated for a system buffered by brucite and magnesite were used (Siegel 1996).

Equations 6-17, 6-18, and 6-20 were used to determine humic-bound actinide concentrations ([AnHS]) for one or more humic substance types for Am(III), Th(IV), Np(V), and U(VI). The oxidation state analogy is most heavily utilized for plutonium, because stability constants for Pu(III) or Pu(IV) are not available. Concentrations of Ca^{2+} and Mg^{2+} in the Salado and Castile brines with MgO backfill were obtained from Novak and Moore (1996). In the performance assessment calculations, the humic-bound actinide concentration in the III oxidation state in Castile brine was sampled. All other humic-bound actinide concentrations were held constant.

The PHUMCIM and PHUMSIM parameters, used in conjunction with materials (idmtrls) PHUMOX3, PHUMOX4, PHUMOX5, or PHUMOX6, provide the means to calculate actinide-humic concentrations by actinide oxidation state and for intrusion scenarios involving different brines. For example, in an E1 scenario under "more reducing" conditions in the WIPP repository, PHUMCIM would be used with the following materials (idmtrls) to determine actinide-humic concentrations: thorium = PHUMOX4; uranium = PHUMOX4; neptunium = PHUMOX4; plutonium = PHUMOX3; and americium = PHUMOX3. For an E2 scenario under less reducing conditions in the WIPP repository, PHUMSIM would be used with the following idmtrls to determine actinide-humic concentrations: thorium = PHUMOX4; uranium = PHUMOX6; neptunium = PHUMOX5; plutonium = PHUMOX4; and americium = PHUMOX3.

Uncertainties due to analytical precision are small compared to uncertainties in knowledge of the dominant humic substance type, site binding densities, and actinide solubilities. The proportionality factor approach coupled with the actinide solubility model uncertainty results in an adequate representation of the uncertainty in the concentration of actinides bound by mobile humic substances.

The CAPHUM parameter simply represents the theoretical maximum concentration of actinides that can be bound by a humic substance. Based on a solubility limit concentration of humic substances of 2.0 mg/liter, and the highest site-binding capacity (for fulvic acids) of 5.56 meq OH^-/g, the theoretical maximum is 1.1×10^{-5} eq/liter. Assuming the conservative case in which actinide species are monovalent, the maximum theoretical concentration of actinides that can be bound by humic substances is 1.1×10^{-5} molar. That number is conservative, because it assumes a pool of humic substances is available for each actinide element, when in reality, actinide elements will compete for the same pool of humic substances. CAPHUM is used in an expression such as the following:

$$[\text{AnHS}] = \text{MIN}(\text{AnHS value calculated with proportionality constant}, 1.1 \times 10^{-5}) \quad (6\text{-}21)$$

in which the calculated concentration of a particular actinide is compared to the upper limit value. Parameter values for PHUMCIM, PHUMSIM, and CAPHUM are found in Appendix PAR (Table PAR-39) and Appendix SOTERM (Section SOTERM.6.3.5).

SOTERM.6.3.4 Microbes

Potentially important colloidal-sized microorganisms include bacteria, fungi, yeast, and protozoa. For the WIPP site, the focus is on the halophilic and halotolerant microbes that have been identified at the site (Brush 1990; Francis and Gillow 1994). Microbes are important to consider in performance assessments of the WIPP because they may significantly affect the characteristics of the waste stored at the WIPP, and also participate in transport of actinides. Microbes are known to actively bioaccumulate actinides intracellularly as well as act as substrates for passive extracellular sorption.

At the WIPP site, concentrations of naturally occurring microbes are on the order of 10^4 to 10^7 cells per milliliter (Francis and Gillow 1994, Table 1). In the presence of nutrients provided by WIPP waste constituents, including nitrates, sulfates, and cellulosic materials such as protective clothing and wood, the population of microbes is likely to increase. Lysis, a natural phenomenon whereby cells die and release their cell constituents to the solution, also provides a source of nutrients to microbes.

When introduced to nutrient, microbes typically follow a predictable growth curve (defined by the population number of microbes plotted as a function of time), consisting of an initial period of inactivity (very early log phase) ranging up to several days, followed by a sharp increase in growth (early log phase). That level of growth is sustained for one or more days (log phase) during which time microbial metabolites, including carboxylic acids, enzymes, and exocellular polymers, are generated. The growth rate eventually begins to decline (late log phase) due to the effects of those metabolites, limitations in nutrients or substrates, or population dynamics, and reaches a steady-state population (stationary phase). Viable microbes may aggregate to form clusters.

SOTERM.6.3.4.1 Description of Experiments

Several types of experiments were conducted to evaluate the impact of microbes in support of the WIPP colloid research program (refer to descriptions in Papenguth and Behl 1996): (1) evaluation of indigenous concentrations of microbes; (2) quantification of mobile concentrations under nutrient- and substrate-rich conditions; (3) quantification and characterization of actinide bioaccumulation by microbes; and (4) evaluation of toxicity effects of actinide elements on microbe growth.

Experiments were conducted at Brookhaven National Laboratory (BNL) and as a collaborative effort between BNL and Los Alamos National Laboratory (LANL). Evaluation of indigenous concentrations was a collaborative effort between BNL and LANL. Quantification of mobile concentrations was conducted at BNL. The bioaccumulation and

toxicity work was conducted at BNL or LANL depending on actinide element. Thorium and uranium were investigated at BNL. The other actinide elements of interest, neptunium, plutonium, and americium, were investigated at LANL under the guidance of BNL personnel.

Experiments to determine the mobile concentrations of microbes remaining suspended in the fluid column were conducted similarly to experiments previously conducted in support of the WIPP gas generation program (Brush 1990; Francis and Gillow 1994). Bacterial cultures were introduced to a solution containing nutrient and substrate, and sealed. Bacteria population was monitored over periods of several weeks or more using measurements of optical density or by direct counting of aliquots of fixed cells. An important change in protocol from previous experiments, however, is that instead of filtering the entire contents of the vessels, only the mobile cells remaining suspended in the fluid column were counted. Results of the experiments showed that the mobile concentration of microbes was a couple orders-of-magnitude less than the total concentration of microbes. The existence of indigenous microbes in Salado groundwaters has been demonstrated in previous work (Francis and Gillow 1994). As part of the WIPP colloid research program, samples of Culebra groundwater were carefully collected from the H-19 hydropad, processed, and characterized for indigenous microbes. Concentrations of naturally occurring microbes were on the order of 10^5 cells per milliliter, determined using direct counting methods.

The evaluation of indigenous concentrations of microbes and quantification of mobile concentrations provided important supporting evidence for quantifying the microbial actinide source term and for evaluating microbe-facilitated transport of actinides in the Culebra. However, the basis for developing the actual parameter values to be used in performance assessment calculations was established with bioaccumulation and toxicity experiments, referred to herein as filtration experiments. Those experiments were conducted by combining microbe cultures with various concentrations and complexes of ^{232}Th, ^{238}U, ^{237}Np, ^{239}Pu, or ^{243}Am. The actinide reagents used were thorium nitrate, thorium EDTA, uranyl(VI) nitrate, uranyl(VI) citrate, neptunyl(V) EDTA, plutonyl(V) perchlorate, plutonyl(V) EDTA, and americium EDTA. For those experiments, a pure bacterial culture (WIPP-1A) and a mixed bacterial culture (BAB) were used. Most of the experiments were conducted with the WIPP-1A culture, because of the fast growth of that pure culture. The WIPP-1A mixed culture typically reaches steady-state concentration within several days, whereas the BAB mixed culture requires several weeks. Because of the rapid response of the WIPP-1A culture, most of the experiments were conducted with that culture to expedite the research program. A complementary set of experiments were repeated with the BAB mixed culture, to evaluate the representativeness of the pure culture. Experiments were conducted over periods of 11 to 15 days for the WIPP-1A microbe culture, and up to 21 days for the BAB culture. Each experiment consisted of a subset of two or three replicate test vessels, that were sampled during the overall test interval, to provide time sequence data. In addition, replicate test vessels that were not innoculated with microbes were included in each experiment to provide a control. Sequential filtration with 0.03 μm, 0.4 μm, and 10 μm filter pore sizes was conducted on each vessel. The following size fractions were obtained as shown in Table SOTERM-13.

Table SOTERM-13. Microbe Experimental Results

Fluid Column Sample	Particle Size	Actinide Association with
not filtered	all	all forms listed below
0.22 m syringe filter, filtrate	< 0.22 μm	dissolved; lysed microbes
10 m filter, filter retentate	> 10 μm	clumped microbes
10 m filter, filtrate	< 10 μm	dissolved; dispersed microbes; lysed microbes
0.4 m filter, filter retentate	= 0.4 to 10 μm	dispersed microbes
0.4 m filter, filtrate	<0.4 μm	dissolved; lysed microbes
0.03 m filter, filter retentate	= 0.03 to 0.4 μm	lysed microbes
0.03 m filter, filtrate	< 0.03 μm	dissolved; lysed microbes

In addition to the potential actinide associations listed above, there was some evidence of the formation of inorganic precipitates in some of the experiments. The nutrient used in many experiments was phosphate (1 g PO_4^{3-} /liter), which is known to coprecipitate actinide cations. The inoculated control samples provided the means to evaluate the extent of that experimental artifact. The control samples also provided the means to assess the extent of sorption of actinides onto test vessels, sampling, and filtration equipment. All sequential filters were composed of the same material, which simplifies assessment of sorption on the filtration equipment.

The toxicity experiments were conducted as a component of the filtration experiments described above, by varying the actinide concentration, and comparing growth curves measured by optical density and/or by direct cell counting. To increase the total concentration of actinides in solution, EDTA was added in some experiments in a one-to-one molar ratio with the actinide element. That approach was taken for some Pu experiments, and all of the Th, Np, and Am experiments.

SOTERM.6.3.4.2 Interpretation and Discussion

Proportionality constants (PROPMIC) describing the amount of actinide element bound to mobile microbes were determined from the data listed above. In addition, maximum concentrations of actinides that could be associated with microbes (CAPMIC) were determined from the experimental data. Those two parameters are suitable for use in performance assessment calculations, when coupled with dissolved actinide solubility values (refer to Section SOTERM.7.2 for details).

The 0.4 μm filter retentate and 0.03 μm filtrate (acquired from the inoculated vessels, not the uninoculated control vessels) were selected to represent the microbial actinide and dissolved

actinide concentrations, respectively. The ratio between the microbial actinide and dissolved actinide, both expressed in molarity, represents the proportionality constant value used for the PROPMIC parameter. The 0.4 μm filter retentate was selected to represent the microbial fraction because nearly all of the bacteria biomass was associated with that filter. A small concentration of actinides was associated with suspected biomass trapped on the 10 μm filter, as clumped microbes, and on the 0.03 μm filter, as lysed microbes. The contribution of actinides-associated biomass consisting of clumped and lysed microbes was typically at least one order-of-magnitude less than the actinide concentration associated with the dispersed microbes collected on the 0.4 μm filter. The concentration of dissolved actinides measured from the 0.03 μm filter filtrate was used in the ratio because it provides the best indication of final dissolved actinide concentration. Representative values for PROPMIC were developed on an element-by-element basis. Results of experiments using the BAB culture were disregarded, because of their lower uptake of actinides (especially plutonium), and because of the limited number of experiments conducted with that culture. For the WIPP-1A culture, the first sampling period (2 to 4 days, but generally 3 days) was disregarded in determining proportionality constants because steady state population had not yet been reached. The remaining values were averaged arithmetically.

The filtration experiments discussed above also provided the basis for determining CAPMIC values. Final cell population numbers in the test vessels were estimated using measurements of optical density at a wavelength of 600 nm or by direct counting with epifluorescent microscopy. The magnitude of the toxicity effects was estimated by comparing final cell numbers obtained from a series of test vessels with varying actinide concentration. The direct counting technique provided the most dependable measure of cell number and was used where available. The CAPMIC value is defined as the actinide concentration in molarity at which no growth was observed. For cases where growth clearly diminished as actinide concentration increased, but the actinide concentration was not great enough to stop growth, CAPMIC values were determined by linear extrapolation of population numbers, and then adding an order-of-magnitude to account for uncertainty. On the basis of WIPP experimental results (Papenguth 1996b), it appears that the toxicity effects are due to chemical toxicity rather than radiotoxicity. Because of the high radiation levels of americium and safety considerations in the laboratory facility used, the molar concentration could not be increased to the point at which toxicity effects could be observed. Consequently no CAPMIC value is currently available for americium. CAPMIC values are used similarly to the CAPHUM values (see Equation 6-21), except that the upper limit for microbe concentration is due to toxicity rather than geometric limitations imposed by the colloid itself. Consequently, for microbes, the total concentration of mobile actinides in a performance assessment realization is used in the comparison, rather than the amount of actinides associated with the microbes.

The experiments conducted do not provide sufficient information to enable us to formulate a distribution of values for PROPMIC and CAPMIC. Therefore, single values for PROPMIC and CAPMIC are used in the performance assessment. Uncertainties due to analytical precision are small compared to uncertainties in knowledge of the microbe culture that might predominate in the WIPP repository or in the Culebra in an intrusion scenario. The

proportionality factor approach coupled with the actinide solubility model uncertainty results in an adequate description of the uncertainty in the concentration of actinides bound by mobile microbes.

Parameter values for PROPMIC and CAPMIC are summarized in Section SOTERM.6.3.5.

SOTERM.6.3.5 Summary of Parameter Values

Parameter values for CONCMIN, CONCINT, PROPMIC, CAPMIC, PHUMSIM, PHUMCIM, and CAPHUM are summarized in Table SOTERM-14.

Table SOTERM-14. Colloid Concentration Factors

	CONCMIN Concentration on Mineral Fragments[a]	CONCINT Concentration as Intrinsic Colloid[a]	PROPMIC Proportion Sorbed on Microbes[b]	CAPMIC Maximum Sorbed on Microbes[c]	Proportion Sorbed on Humics[b]		CAPHUM Maximum Sorbed on Humics[a]
					PHUMSIM Salado	PHUMCIM Castile	
Th(IV)	2.6×10^{-8}	0.0	3.1	0.0019	6.3	6 3	1.1×10^{-5}
U(IV)	2.6×10^{-8}	0.0	0.0021	0.0021	6.3	6 3	1.1×10^{-5}
U(VI)	2.6×10^{-8}	0.0	0.0021	0.0023	0.12	0.51	1.1×10^{-5}
Np(IV)	2.6×10^{-8}	0.0	12.0	0.0027	6.3	6.3	1.1×10^{-5}
Np(V)	2.6×10^{-8}	0.0	12.0	0.0027	9.1×10^{-4}	7.4×10^{-3}	1.1×10^{-5}
Pu(III)	2.6×10^{-8}	0.0	0.3	6.8×10^{-5}	0.19	1.37[d]	1.1×10^{-5}
Pu(IV)	2.6×10^{-8}	1.0×10^{-9}	0.3	6.8×10^{-5}	6.3	6.3	1.1×10^{-5}
Am(III)	2.6×10^{-8}	0.0	3.6	NA	0.19	1.37[d]	1.1×10^{-5}

[a]In units of moles colloidal actinide per liter
[b]In units of moles colloidal actinide per mole dissolved actinide
[c]In units of moles total mobile actinide per liter
[d]A cumulative distribution from 0.065 to 1.60 with a mean value of 1.1 was used
NOTE: The colloidal source term is added to the dissolved source term to arrive at a total source term. Mineral fragments were provided with distributions, but the maximum was used as described in SOTERM.7.1.3. Humic proportionality constants for III, IV, and V were provided with distributions, but only the Castile Am(III) and Pu(III) were sampled.

SOTERM.6.4 Summary

Results of the colloidal actinide investigation are used in performance assessment in three types of parameter values: (1) constant concentration values for actinides associated with mineral fragment and actinide intrinsic colloids; (2) concentration values proportional to the dissolved actinide concentration for actinides associated with microbes and humic substances;

and (3) maximum concentration values providing an upper limit for actinide concentrations associated with microbes and humic substances. The parameter values are summarized in Table SOTERM-14. Given the actinide solubilities calculated for Salado and Castile brines in the presence of MgO backfill material, the largest contributors to the mobile colloidal actinide source term are actinides associated with humic substances and microbes. The contribution from mineral fragment and actinide intrinsic colloids is comparatively small. More details can be found in the SWCF parameter record packages describing the determination of the mobile colloidal actinide source term (Papenguth 1996a,b,c,d).

SOTERM.7 Use of the Actinide Source Term in Performance Assessment

As described in the preceding sections, the actinide source term program provided the parameters that were needed to construct maximum dissolved and suspended colloidal actinide concentrations for use in modeling the mobilization and transport of actinides in the disposal system, as modeled by NUTS and PANEL. Prior to these transport calculations, however, some simplifications and manipulations (using ALGEBRA) were required as discussed in the following sections.

SOTERM.7.1 Simplifications

The DOE has concentrated on those processes that are most likely to have a significant impact on system performance. Therefore, several simplifications were used in the modeling of radionuclide mobilization in performance assessment calculations. These include

(1) using constant solubility and colloid parameters throughout the repository and regulatory period for a given realization as described in Section SOTERM.2.2,

(2) limiting the number of isotopes modeled to the ones most important to compliance (see Appendix WCA, Section WCA.3),

(3) using the chemistries of Castile and Salado brines—the end member brines—to bracket the behavior of mixed brines within the repository,

(4) sampling only the uncertain parameters having the most significant effect on repository performance

(5) combining dissolved and colloidal species for transport within the disposal system, as modeled by NUTS and PANEL.

SOTERM.7.1.1 Elements and Isotopes Modeled

Selection of isotopes for modeling transport in the disposal system with NUTS and PANEL is described in Appendix WCA, Section WCA.3. PANEL model runs included nearly all isotopes of the 6 actinides studied in the AST program: Am, Cm, Np, Pu, Th, and U. NUTS

model runs included 5 isotopes: ^{238}Pu, ^{239}Pu, ^{241}Am, ^{234}U, and ^{230}Th. The rationale for use of these isotopes is also reported by Garner (1996).

SOTERM.7.1.2 Use of Brine End Members

Brine from three sources may enter the repository, depending on the nature of future human intrusion. The general scenarios described in Chapter 6.0 (Section 6.3), and considered in the source term calculations may be categorized into three groups: (1) undisturbed performance (UP), (2) intrusion through the repository and into the Castile intersecting a pressurized brine reservoir (E1 and E1E2); and (3) intrusion through the repository but not into a pressurized brine reservoir (E2).

Under all scenarios, brine may flow from the surrounding Salado through the disturbed rock zone (DRZ), and into the repository in response to the hydraulic head difference between the repository and the surrounding formation. In scenarios where a borehole is drilled into the repository, brine may flow down the borehole from the Rustler and Dewey Lake. In scenarios where a pressurized Castile brine reservoir is intercepted, brine from the Castile may flow up the borehole into the repository. As mentioned in Section SOTERM.2.2.1, the brines in these three formations have considerably different compositions and the solubility of actinides are significantly different in each of these end member compositions. The composition of the more dilute brines of the Rustler and Dewey Lake, however, are expected to change rapidly upon entering the repository due to fast dissolution of host Salado minerals (about 93.2 percent halite and about 1.7 percent each of polyhalite, gypsum, anhydrite, and magnesite; Brush 1990) from the walls and floor of the repository. EQ3/6 calculations titrating Salado rock into dilute brines show that gypsum, anhydrite and magnesite saturate before halite. When halite saturates, the brine composition is very similar to that of Castile brine. One hundred times as much polyhalite must be added to the system before the resulting brine has a composition similar to Salado brines. These calculations indicate that if dilute brines dissolve away only the surfaces of the repository, they will obtain Castile-like compositions, but if they circulate through the Salado after saturating with halite, they may obtain compositions similar to Salado brine. Similarly, if Castile brine circulates through enough host rock, it may also approach Salado brine composition. In either case, the actual brine within the repository may be described as a mixture of the two concentrated brine end members—Salado and Castile. This mixture, however, is very hard to quantify, because it is both temporally and spatially variable. Only in the undisturbed scenario is the mixture well defined as 100 percent Salado brine over the 10,000-year regulatory period.

For a panel intersected by a borehole, the BRAGFLO calculations show that in the 10 percent of the repository represented by the BRAGFLO panel computational cells, the ratio of brine inflow that enters by the borehole versus inflow from the repository walls varies through time and depends on the sampled parameter values and scenario being considered. This ratio was the only measure of brine mixing available to the source term ALGEBRA runs in the performance assessment calculations. This ratio was quite crude because it (1) did not account for brine composition changes that occur when water was consumed by corrosion

reactions, (2) did not resolve the details of flow, diffusion and brine interaction with internal pillars and the disturbed rock zone (DRZ), and (3) was an average over one tenth of the repository. It is expected that the fraction of Salado brine will be quite high in areas of the repository distant from the borehole and the fraction will be much lower near the borehole. Because radionuclide travel up the borehole is required for significant release, it is the solubility of radionuclides near the borehole that is most important. Given these uncertainties, the DOE decided to calculate radionuclide solubilities using the Castile end member composition for scenarios in which a borehole penetrates a brine reservoir and Salado end member composition for scenarios where it does not.

SOTERM.7.1.3 Sample Uncertain Parameters

Distributions of parameter values for up to 30 source-term parameters are available, but many of these are expected to have very limited impact on disposal system performance. The most important parameters are expected to be the oxidation state parameter and the solubilities of Pu(III), Pu(IV), and Am(III) in the two brine end members.

A single distribution (Figures SOTERM-6 and SOTERM-7) was provided for modeling the solubility of all oxidation states of all actinides in both brines. However, the amount of correlation between the solubilities of the actinides was uncertain. Some factors that cause uncertainty in the solubility affect all oxidation states of all actinides similarly and some factors will affect only some actinides or some oxidation states. For example, uncertainties in the sulfate concentrations will have more effect in the uncertainty of the solubility of the actinides in the IV oxidation state, while uncertainties in the ionic strength has a more generalized effect of increasing the uncertainty in the stability of any highly charged species. In nature, solubilities show correlation due to reduction-oxidation effects as well as compositional effects. It is therefore expected that solubilities within the WIPP should show some correlation, but not 100 percent correlation.

The use of the end member brines in the calculations results in a correlation of solubilities due to ionic strength and major ion effects, and the use of the oxidation state parameter results in a correlation due to reduction-oxidation effects. The DOE assumes these effects (that is, ionic strength, major ions, and reduction-oxidation state) encompass the major correlations and therefore impose no further correlations. A better estimate of this correlation would be necessary for more detailed chemical modeling, but for use in performance assessment, this decision is not very important. With nine possible element-oxidation state combinations (Am(III), Cm(III), Np(IV), Np(V), Pu(III), Pu(IV), Th(IV), U(IV), and U(VI)), and two brines, a 0 percent correlation implies 18 independent samples of the distribution.

The parameters to be sampled were selected based on expectations of their significance of effect on disposal system performance.

- A 100 percent correlation was made between Am and Cm dissolved solubilities. Only the parameters for Am were sampled, and these were copied for Cm.

- Np solubilities were not sampled because Np does not have a very large EPA unit during the 10,000-year regulatory period (see Appendix WCA, Section WCA.3, for discussion of EPA unit and the relative importance of Np).
- The solubilities of U(IV) and Th(IV) in Castile brine were not sampled because (1) the EPA units of U and Th are only a little larger than the EPA unit of Np during the regulatory period (Garner 1996), and (2) the solubility of the IV oxidation state in Castile brine is low enough that it cannot adversely affect system performance.
- The actinide concentration on mineral fragment parameters was not sampled because the concentrations of actinides that may be mobilized on mineral fragments were in most cases much lower that the possible concentrations of dissolved actinides.
- Of the humic acid proportionality constants, only the one for the III oxidation state in Castile brine was sampled because it was high and it applied to significant elements (Pu and Am).

Parameters not sampled were fixed at a maximum reasonable value during the calculations.

Twelve parameters were sampled in the performance assessment for the source term (see Appendix PAR):

Material Name	Parameter Name
SOLAM3	SOLSIM, SOLCIM
SOLPU3	SOLSIM, SOLCIM
SOLPU4	SOLSIM, SOLCIM
SOLU4	SOLSIM
SOLU6	SOLSIM, SOLCIM
SOLTH4	SOLSIM
GLOBAL	OXSTAT
PHUMOX3	PHUMCIM

where
SOLAM3 = distribution parameter for SOLubility of AM(III),
SOLSIM = SOLubility in Salado brine, Inorganic only, $Mg(OH)_2/MgCO_3$ buffer,
SOLCIM = SOLubility in Castile brine, Inorganic only, $Mg(OH)_2/MgCO_3$ buffer,
OXSTAT = OXidation STATe parameter,
PHUMOX3 = the Proportionality constant for HUMic colloids and actinides in the +3 OXidation state,
PHUMCIM = the Proportionality constant for HUMic colloids in Castile brine, Inorganic only, $Mg(OH)_2/MgCO_3$ buffer.

SOTERM.7.1.4 Combining the Transport of Dissolved and Colloidal Species in the Salado Formation

Dissolved and colloidal species may transport differently because of different diffusion rates, sorption onto stationary materials, and size exclusion effects (filtration and hydrodynamic

chromatography). With maximum molecular diffusion coefficients of about 4 x 10^{-10} meters squared per second, actinides are estimated to diffuse about 10 meters in 10,000 years, a negligible distance. Sorption and filtration have beneficial but unquantifiable effects on performance. Hydrodynamic chromatography may increase colloid transport over dissolved transport by at most a factor of 2 for theoretically perfect colloid transport conditions. In real situations, the increase is much less. Given the small or beneficial nature of these effects, the DOE did not model them in the performance assessment calculations of radionuclide transport.

Because there was no modeled mechanism to differentiate dissolved from colloidal species, the DOE combined them for transport within the Salado. In the modeling of transport within the Culebra, however, these simplifications were not appropriate. While transport within the repository is through at most hundreds of meters of poorly defined waste that is undergoing decomposition, transport through the Culebra is over kilometers in a relatively homogeneous (as compared to waste) fractured dolomite. Diffusion of radionuclides into, and sorption on, a dolomite matrix have been shown by sensitivity analysis (WIPP Performance Assessment Department 1992) to be processes important in performance assessment. Therefore, the mobilized actinide delivered to the Culebra by Salado transport codes was separated into its five species (dissolved, humic, microbe, mineral fragment, intrinsic colloid).

SOTERM.7.2 Construction of Source Term

The parameters required for constructing the source term were (1) modeled solubilities for four oxidation states in each brine end member, (2) a distribution to be used around the modeled solubility values, (3) a scheme for assigning sampled dominant oxidation states, (4) colloidal concentrations or proportionality constants for the 5 actinides or the 4 oxidation states for each of four colloid types, and (5) caps on the actinide concentrations that may be carried on two colloid types. Use of these parameters in the performance assessment calculations required combining these into a single effective solubility or maximum concentration for each modeled actinide. The term effective solubility is used for the maximum combined mobilized actinide concentration due to dissolved and colloidal species, because the NUTS and PANEL codes use these numbers for each actinide as if they were solubilities. The maximum is not the maximum of the distribution, but is called the maximum because the concentration may be lower due to inventory limits. Both NUTS and PANEL assume that the actinides instantly mobilize up to this effective solubility limit as long as sufficient inventory is available in the computational cell for this to occur. When the inventory is not sufficient, the actual mobilized concentration will be lower and is said to be inventory limited. The calculation of the effective solubilities was performed prior to NUTS and PANEL using ALGEBRA, for each of 100 sampled realizations, as shown in Figure SOTERM-9.

All the source term parameter values and their distributions were entered into the performance assessment parameter database. For the sampled parameters, the LHS code read the distribution information from the performance assessment parameter database and created 100

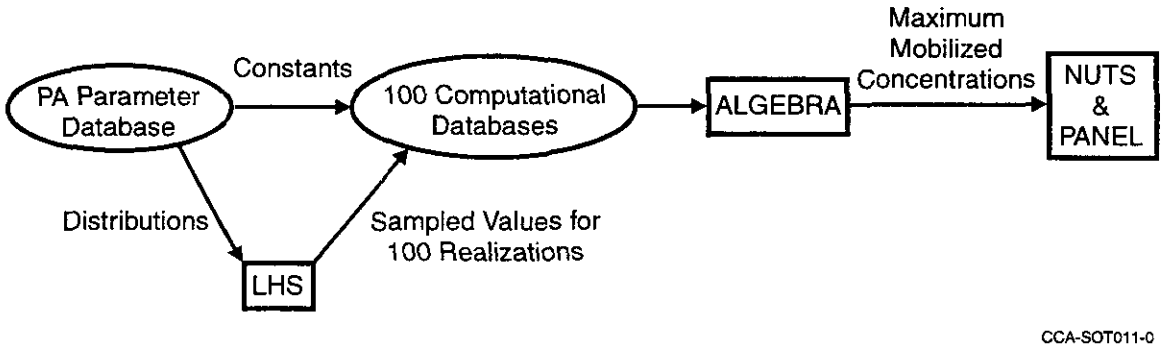

Figure SOTERM-9. Calculations Performed by ALGEBRA for Each Replicate of 100 Realizations to Produce Effective Solubilities for Each Modeled Actinide

1 **THIS PAGE INTENTIONALLY LEFT BLANK**

sampled values for each. These values were combined with the constant value parameters and stored in computational databases for each of the 100 realizations, which comprised one replicate. For each realization, ALGEBRA read both the constant and sampled values for all the source term parameters, and constructed effective solubilities for NUTS and PANEL, as shown below. This process was repeated for scenarios using Salado end-member effective solubilities and for scenarios using Castile end-member effective solubilities. (Parameters that are sampled and values derived from them are indicated by italics. Parameters read by ALGEBRA are in bold.)

Dissolved = **Model Solubility** * 10 ***Sampled from Solubility Distribution***

Humic = *Dissolved* * ***Proportionality Constant***
if *Dissolved* * ***Prop. Const.*** < **Humic Cap**, otherwise
Humic = **Humic Cap**

Microbe = *Dissolved* * **Proportionality Constant**
if the *Total Mobile* < **Microbe Cap**, otherwise
Microbe = **Microbe Cap**

Mineral = **Database Concentration**

Intrinsic = **Database Concentration**

Total Mobile = *Dissolved* + *Humic* + *Microbe* + Mineral + Intrinsic

For actinides with more than one oxidation state, the above procedure is performed for each oxidation state, and the final total mobile concentration is set based on the oxidation state parameter:

Total Mobile = Total Mobile (lower oxidation state) if OXSTAT ≤ 0.5
= Total Mobile (higher oxidation state) if OXSTAT > 0.5

where OXSTAT is the oxidation state parameter that is sampled uniformly from 0 to 1.

For example, for one realization, in Salado brine, the sampled value for OXSTAT was 0.9 so Pu would be present in the IV state. The sample of the solubility distribution was 0.8 for the modeled solubility for the IV state, which has a model solubility of 4.4×10^{-6}. The humic proportionality constant for the IV oxidation state in Salado brine is 6.3, the microbe proportionality constant for Pu is 0.3, the humic cap is 1.1×10^{-5} M, the microbe cap for Pu is 2.1×10^{-3}, the actinide on mineral fragment concentration is 2.6×10^{-8}, and the Pu intrinsic colloid concentration is 1×10^{-9}.

For this realization, the maximum concentration of dissolved plutonium used by performance assessment would be:

Maximum concentration of dissolved Pu: $C_{Pu} = (4.4 \times 10^{-6})(10^{0.8}) = 2.8 \times 10^{-5}$ mole/liter

(This example has been rounded to two significant figures, although performance assessment would not round at this intermediate point.) C_{Pu} is the maximum concentration of all combined isotopes of Pu.

The maximum humic complexed plutonium would be:

$$(2.8 \times 10^{-5} \text{ mole/liter})(6.3 \text{ moles adsorbed per mole}) = 1.8 \times 10^{-4} \text{ moles/liter}$$

This value, however, exceeds the cap for humic-mobilized plutonium, 1.1×10^{-5} mole/liter. Therefore, in this case, the cap would be used for the maximum humic mobilized actinide concentration.

The maximum microbial mobilized plutonium would be:

$$(2.8 \times 10^{-5} \text{ mole/liter})(0.3 \text{ moles bioaccumulated per mole}) = 8.3 \times 10^{-6} \text{ moles/liter}$$

which is less than the cap.

The total maximum plutonium concentration or effective solubility for this realization would then be the sum of the dissolved and colloidal actinides:

Dissolved + *Humic* + *Microbe* + Mineral + Intrinsic

$$2.8 \times 10^{-5} + 1.1 \times 10^{-5} + 8.3 \times 10^{-6} + 2.6 \times 10^{-8} + 1.0 \times 10^{-9} = 4.7 \times 10^{-5} \text{ moles/liter}$$

ALGEBRA also calculates the fraction of each actinide that is mobilized by the 5 different mechanisms as follows:

Fraction dissolved = Dissolved/Total Mobile
Fraction on humics = Humic/Total Mobile
Fraction in/on microbes = Microbe/Total Mobile
Fraction on mineral fragments = Mineral/Total Mobile
Fraction as intrinsic colloid = Intrinsic/Total Mobile

The total mobile concentration and mobile fractions are then copied from Am to Cm. In addition, the ALGEBRA run also combines isotopes (Section WCA.3.2; Garner 1996) for the NUTS and SECOTP2D transport codes. For example, the curies of ^{233}U are added to the curies of ^{234}U and the uranium solubility is decreased by a factor of 100 to account for the shared solubility with the low activity ^{238}U, which is not modeled, enabling NUTS to properly model the effect of the uranium isotopes on compliance using the single "lumped" isotope ^{234}U.

The output of the ALGEBRA calculations are computational databases that contain the effective solubilities and effective inventories. NUTS and PANEL both assume instantaneous dissolution and colloidal mobilization up to the effective solubility limit when sufficient inventory is present, as discussed in Chapter 6.0 (Section 6.4.13). Table SOTERM-15 shows the total effective solubilities obtained when median parameter values are used.

Table SOTERM-15. Log Molar Total Maximum Mobilized Concentrations Using Median Parameter Values

Brine	Am(III)	Pu(III)	Pu(IV)	U(IV)	U(VI)	Th(IV)	Np(IV)	NP(V)
Salado	-5.64	-6.14	-4.80	-4.84	-5.10	-4.59	-4.17	-4.52
Castile	-6.47	-6.77	-7.19	-7.16	-4.96	-7.05	-6.85	-4.54

REFERENCES

Alexander, A.E., and P. Johnson. 1949. *Colloid Science.* New York, NY: Oxford University Press. Vol. 1.

Allard, B., H. Kipatsi, and J. O. Liljenzin. 1980. "Expected Species of Uranium, Neptunium and Plutonium in Neutral Aqueous Solutions," *Journal of Inorganic Nuclear Chemistry.* Vol. 42, no. 7, 1015-1027.

Avogadro, A., and G. de Marsily. 1984. "The Role of Colloids in Nuclear Waste Disposal," *Scientific Basis for Nuclear Waste Management VII, Materials Research Society Symposia Proceedings, Boston, MA, November 14-17, 1983.* Ed. G.L. McVay. New York, NY: North-Holland. Vol. 26, 495-505.

Baes, C.F., Jr., and R.E. Mesmer. 1976. *The Hydrolysis of Cations.* New York, NY: Wiley Interscience.

Baskaran, M., P. H. Santschi, G. Benoit, and B. D. Honeyman. 1992. "Scavenging of Thorium Isotopes by Colloids in Seawater of the Gulf of Mexico," *Geochimica et Cosmochimica Acta.* Vol. 56, no. 9, 3375-3388.

Bates, J.K., J.P. Bradley, A. Teetsov, C.R. Bradley, and M. Buchholtz. 1992. "Colloid Formation During Waste Form Reaction: Implications for Nuclear Waste Disposal," *Science.* Vol. 256, no. 5057, 649-561.

Brush, L.H. 1990. *Test Plan for Laboratory and Modeling Studies of Repository and Radionuclide Chemistry for the Waste Isolation Pilot Plant.* SAND90-0266. Albuquerque, NM: Sandia National Laboratories. WPO 26015.

Buckau, G., R. Stumpe, and J.I. Kim. 1986. "Americium Colloid Generation in Groundwaters and Its Speciation by Laser-Induced Photoacoustic Spectroscopy," *Journal of the Less-Common Metals.* Vol. 122, 555-562.

Buddemeier, R.W., and J.R. Hunt. 1988. "Transport of Colloidal Contaminants in Groundwater: Radionuclide Migration at the Nevada Test Site," *Applied Geochemistry.* Vol. 3, no. 5, 535-548.

Bynum, R. V. May 23, 1996. Memo to M. S. Tierney and C. Stockman. "Update of Uncertainty Range and Distribution for Actinide Solubilities to be Used in CCA NUTS Calculation." WPO 35835.

Choppin, G.R. 1983. "Solution Chemistry of the Actinides," *Radiochimica Acta.* Vol. 32, no. 1-3, 43-53.

Choppin, G. R. 1988. Unpublished Letter to L. H. Brush, December 29, 1988, Tallahassee, FL. (Copy on file at Sandia WIPP Central Files.)

Choppin, G. R., and P. M. Shanbhag. 1981. "Binding of Calcium by Humic Acid," *Journal of Inorganic and Nuclear Chemistry.* Vol. 43, no. 5, 921–922.

Clark, D. L. and Tait, C. D. 1996. Monthly Reports Under SNL Contract AP2274, Sandia WIPP Central File A:WBS 1.1.10.1.1. These data are qualified under LANL QAPjP CST-OSD-QAP1-001/0. WPO 31106.

Clark, D.L., D.E. Hobart, and M.P. Neu. 1995. "Actinide Carbonate Complexes and Their Importance in Actinide Environmental Chemistry," *Chemical Reviews.* Vol. 95, no. 1, 25-48.

Cleveland, J.M. 1979a. *The Chemistry of Plutonium.* La Grange Park, IL: American Nuclear Society.

Cleveland, J.M. 1979b. "Critical Review of Plutonium Equilibria of Environmental Concern," *Chemical Modeling in Aqueous Systems: Speciation, Sorption, Solubility, and Kinetics, 176th Meeting of the American Chemical Society, Miami Beach, FL, September 11-13, 1978.* Ed. E.A. Jenne. Washington, DC: American Chemical Society. 321-338.

Comans, R.N.J., and J.J. Middelburg. 1987. "Sorption of Trace Metals on Calcite: Applicability of the Surface Precipitation Model," *Geochimica et Cosmochimica Acta.* Vol. 51, no. 9, 2587-2591.

Cotton, F.A., and G. Wilkinson. 1988. *Advanced Inorganic Chemistry.* 5th ed. New York, NY: John Wiley & Sons.

DOE (U.S. Department of Energy). 1996. *Transuranic Waste Baseline Inventory Report (Revision 3).* DOE/CAO-95-1121. Carlsbad, NM: U.S. Department of Energy.

Drez, P.E. 1991. "Preliminary Nonradionuclide Inventory of CH-TRU Waste,"*Preliminary Comparison with 40 CFR Part 191, Subpart B for the Waste Isolation Pilot Plant, December 1991. Volume 3: Reference Data.* WIPP Performance Assessment Division Eds. R.P. Rechard, A.C. Peterson, J.D. Schreiber, H.J. Iuzzolino, M.S. Tierney, and J.S. Sandha. SAND91-0893/3. Albuquerque, NM: Sandia National Laboratories, A-43 through A-53.

Duan, Z., N. Møller, J. Greenberg, and J.H. Weare. 1992. "The Prediction of Methane Solubility in Natural Waters to High Ionic Strengths from 0 to 250°C and from 0 to 1600 bar," *Geochimica et Cosmochimica Acta.* Vol. 56, no. 4, 1451-1460.

Ephraim, J. H., C. Petersson, M. Norden, and B. Allard. 1995. "Potentiometric Titrations of Humic Substances: Do Ionic Strength Effects Depend on the Molecular Weight?" *Environmental Science and Technology*. Vol. 29, no. 3, 622-628.

Eugster, H.P., C.E. Harvie, and J.H. Weare. 1980. "Mineral Equilibria in the Six-component Seawater System, Na-K-Mg-Ca-SO_4-Cl-H_2O, at 25°C," *Geochimica et Cosmochimica Acta.* Vol. 44, no. 9, 1335-1347. WPO 30424.

Fanghänel, Th., V. Neck, and J.I. Kim. 1995. "Thermodynamics of Neptunium(V) in Concentrated Salt Solutions: II. Ion Interaction (Pitzer) Parameters for Np(V) Hydrolysis Species and Carbonate Complexes," *Radiochimica Acta.* Vol. 69, no. 3, 169-176. WPO 40233.

Felmy, A.R., and J.H. Weare. 1986. "The Prediction of Borate Mineral Equilibria in Natural Waters, Application to Searles Lake, California," *Geochimica et Cosmochimica Acta.* Vol. 50, no. 12, 2771-2783. WPO 30421.

Felmy, A.R., and D. Rai. 1992. "An Aqueous Thermodynamic Model for a High Valence 4:2 Electrolyte Th^{4+}-SO in the System Na^+-K^+-Li^+-NH-SO-HSO-H_2O to High Concentration," *Journal of Solution Chemistry.* Vol. 21, no. 5, 407-423. WPO 40224.

Felmy, A. R., D. Rai, J. A. Schramke, and J. L. Ryan. 1989. "The Solubility of Plutonium Hydroxide in Dilute Solution and in High-Ionic-Strength Chloride Brines," *Radiochimica Acta.* Vol. 48, no. 112, 29-35.

Felmy, A. R., D. Rai, and R. W. Fulton. 1990. "The Solubility of $AmOHCO_3$(c) and the Aqueous Thermodynamics of the System Na^+-H CO_3--$(CO_3)^{2-}$-OH-H_2O," *Radiochimica Acta.* Vol. 50, no. 4, 193-204.

Felmy, A.R., D. Rai, and M.J. Mason. 1991. "The Solubility of Hydrous Thorium(IV) Oxide in Chloride Media: Development of an Aqueous Ion-Interaction Model," *Radiochimica Acta.* Vol. 55, no. 4, 177-185. WPO 40225.

Felmy, A.R., D. Rai, S.M. Sterner, M.J. Mason, N.J. Hess, and S.D. Conradson. 1996. "Thermodynamic Models for Highly Charged Aqueous Species: The Solubility of Th(IV) Hydrous Oxide in Concentrated $NaHCO_3$ and Na_2CO_3 Solutions." In preparation. (Copy on file in the Sandia WIPP Central Files. A:1.1.10.1.1: TO: QA: Inorganic (IV) Actinide Thermodynamic Data, WPO 40226, 8/14/96).

Francis, A.J., and J.B. Gillow. 1994. *Effects of Microbial Processes on Gas Generation Under Expected Waste Isolation Pilot Plant Repository Conditions. Progress Report through 1992.* SAND93-7036. Albuquerque, NM: Sandia National Laboratories. WPO 26555.

Garner, J. March 15, 1996. "Radioisotopes to Be Used in the 1996 CCA Calculations." Memorandum to Christine Stockman. WPO 35202.

Grenthe, I., and H. Wanner. 1992. *Guidelines for the Extrapolation to Zero Ionic Strength.* NEA-TBD-2, Revision 2, Gif-sur-Yvette, France: OECD Nuclear Energy Agency, Data Bank. WPO 21109.

Harvie, C.E., N. Møller, and J.H. Weare. 1980a. "The Prediction of Mineral Solubilities in Natural Waters, The Na-K-Mg-Ca-Cl-SO_4-H_2O System from Zero to High Concentration at 25°C," *Geochimica et Cosmochimica Acta.* Vol. 44, no. 7, 981-997. WPO 30423.

Harvie, C.E., J.H. Weare, L.A. Hardie, and H.P. Eugster. 1980b. "Evaporation of Seawater: Calculated Mineral Sequences," *Science.* Vol. 208, no. 4443, 498-500.

Harvie, C.E., N. Møller, and J.H. Weare. 1984. "The Prediction of Mineral Solubilities in Natural Waters, The Na-K-Mg-Ca-H-Cl-SO_4-OH-HCO_3-CO_2-H_2O System to High Ionic Strengths at 25°C," *Geochimica et Cosmochimica Acta.* Vol. 48, no. 4, 723-751. WPO 30422.

Hiemenz, P.C. 1986. *Principles of Colloid and Surface Chemistry.* 2nd ed. New York, NY: Marcel Dekker, Inc.

Hirtzel, C.S., and R. Rajagopalan. 1985. *Colloidal Phenomena. Advanced Topics.* Park Ridge, NJ: Noyes Publications.

Hobart, D.E. 1990. "Actinides in the Environment," *Proceedings of the Robert A. Welch Foundation Conference on Chemical Research, No., XXXIV: 50 Years With Transuranium Elements, Houston, TX, October 22-23, 1990.* Vol. 34, 378-436.

Hobart, D.E., and R. Moore. 1996. "Analysis of Uranium (VI) Solubility Data for WIPP Performance Assessment: Implementation of Analysis Plan AP-028." Copy on file in Sandia WIPP Central File. WPO 39856 (5/28/96).

Hobart, D. E., K. Samhoun, and J. R. Peterson. 1982. "Spectroelectrochemical Studies of the Actinides: Stabilization of Americium (IV) in Aqueous Carbonate Solution," *Radiochimica Acta.* Vol. 31, no. 3/4, 139-145.

Hobart, D.E., C.J. Bruton, F.J. Millero, I-Ming Chou, K.M. Trauth, and D.R. Anderson. 1996. *Estimates of the Solubilities of Waste Element Radionuclides in Waste Isolation Pilot Plant Brines: A Report by the Expert Panel on the Source Term.* SAND96-0098. Albuquerque, NM: Sandia National Laboratories.

Horita, J., T. J. Friedman, B. Lazar, and H.D. Holland. 1991. "The Composition of Permian Seawater," *Geochimica et Cosmochimica Acta.* Vol. 55, no. 2, 417-432.

Hunter, R.J. 1991-1992. *Foundations of Colloid Science.* Reprinted. New York, NY: Oxford University Press. Vols. I-II.

Johnson, G.L., and L.M. Toth. 1978. *Plutonium(IV) and Thorium(IV) Hydrous Polymer Chemistry.* ORNL/TM-6365. Oak Ridge, TN: Oak Ridge National Laboratory, Chemistry Division.

Katz, J.J., G.T. Seaborg, and L.R. Morss, eds. 1986. *The Chemistry of the Actinide Elements.* 2nd ed. New York, NY: Chapman and Hall. Vols. 1-2.

Keller, C. 1971. *The Chemistry of the Transuranium Elements.* Weinheim, Germany: Verlag Chemie, GmbH.

Kim, J.I. 1992. "Actinide Colloid Generation in Groundwater," *Radiochimica Acta.* Vol. 52/53, pt. 1, 71-81.

Kim, J.I. 1994. "Actinide Colloids in Natural Aquifer Systems," *MRS Bulletin, A Publication of the Materials Research Society.* Vol. 19, no. 12, 47-53.

Kim, J.-I., and T. Sekine. 1991. "Complexation of Neptunium(V) with Humic Acid," *Radiochimica Acta.* Vol. 55, no. 4, 187-192.

Kim, J.I., M. Bernkopf, Ch. Lierse, and F. Koppold. 1984a. "Hydrolysis Reactions of Am(III) and Pu(VI) Ions in Near-Neutral Solutions," *Geochemical Behavior of Disposed Radioactive Waste.* Eds. G.S. Barney, J.D. Navratil, and W.W. Schulz. ACS Symposium Series 246. Washington, DC: American Chemical Society. 115-134.

Kim, J.I., G. Buckau, F. Baumgärtner, H.C. Moon, and D. Lux. 1984b. "Colloid Generation and the Actinide Migration in Gorleben Groundwaters," *Scientific Basis for Nuclear Waste Management VII, Materials Research Society Symposia Proceedings, Boston, MA, November 14-17, 1983.* Ed. G.L. McVay. New York, NY: North-Holland. Vol. 26, 31-40.

Kim, J.I., Ch. Apostolidis, G. Buckau, K. Bueppelmann, B. Kanellakopulos, Ch. Lierse, S. Magirius, R. Stumpe, I. Hedler, Ch. Rahner, and W. Stoewer. 1985. *Chemisches Verhalten von Np, Pu und Am in verschiedenen knozentrierten Salzloesunger = Chemical Behaviour of Np, Pu, and Am in Various Brine Solutions.* RCM 01085. Munich, Germany: Institut für Radiochemie der Technische Universitaet Muenchen. (Available from National Technical Information Service, 555 Port Royal Road, Springfield, VA 22161, 703/487-4650 as DE857 2334.)

Korpusov, G.V., E.N. Patrusheva, and M.S. Dolidze. 1975. "The Study of Extraction Systems and the Method of Separation of Trivalent Transuranium Elements Cm, Bk, and Cf," *Soviet Radiochemistry.* Vol 17, no. 1-6, 230-236.

Kraus, K.A. 1956. "Hydrolytic Behavior of the Heavy Elements," *Proceedings of the International Conference on the Peaceful Uses of Atomic Energy, Geneva, August 8-20, 1955.* New York, NY: United Nations. Vol. 7, 245-257.

Larson, K.L., March 13, 1996. "Brine Waste Contact Volumes for Scoping Analysis of Organic Ligand Concentration." Memorandum to R. V. Bynum. WPO 30644.

Laul, J.C., M.R. Smith, and N. Hubbard. 1985. "Behavior of Natural Uranium, Thorium and Radium Isotopes in the Wolfcamp Brine Aquifers, Palo Duro Basin, Texas," *Scientific Basis for Nuclear Waste Management, Materials Research Society Symposia Proceedings, Boston, MA, November 26-29, 1984.* Eds. C.M. Jantzen, J.A. Stone, and R.C. Ewing. Pittsburgh, PA: Materials Research Society. Vol. 44, 475-482.

Lieser, K., B. Gleitsmann, S. Peschke, and T. Steinkopff. 1986a. "Colloid Formation and Sorption of Radionuclides in Natural Systems," *Radiochimica Acta.* Vol. 40, no. 1, 39-47.

Lieser, K., B. Gleitsmann, and T. Steinkopff. 1986b. "Sorption of Trace Elements or Radionculides in Natural Systems Containing Groundwater and Sediments," *Radiochimica Acta.* Vol. 40, no. 1, 33-37.

Lieser, K.H., A. Ament, R. Hill, R.N. Singh, U. Stingl, and B. Thybusch. 1990. "Colloids in Groundwater and Their Influence on Migration of Trace Elements and Radionuclides," *Radiochimica Acta.* Vol. 49, no. 2, 83-100.

Lieser, K.H., R. Hill, U. Mühlenweg, R.N. Singh, T. Shu-De, and Th. Steinkopff. 1991. "Actinides in the Environment," *Journal of Radioanalytical and Nuclear Chemistry, Articles.* Vol. 147, no. 1, 117-131.

Lyklema, J. 1978. "Surface Chemistry of Colloids in Connection with Stability," T*he Scientific Basis of Flocculation.* Ed. K.J. Ives. NATO Advanced Study Institute Series, Series E, Volume E27. Alphen aan den Rijn: Sijthoff & Noordhoff. 3-36.

Maiti, T.C., M.R. Smith, and J.C. Laul. 1989. "Colloid Formation Study of U, Th, Ra, Pb, Po, Sr, Rb, and Cs in Briny (High Ionic Strength) Groundwaters: Analog Study for Waste Disposal," *Nuclear Technology.* Vol. 84, no. 1, 82-87.

Martell, A.E., and R.M. Smith. 1982. *Critical Stability Constants, Volume 5: First Supplement.* New York, NY: Plenum Press.

Martinot, L. and J. Fuger. 1985. "The Actinides," *Standard Potentials in Aqueous Solution.* Eds. A.J. Bard, R. Parsons, and J. Jordan. New York, NY: Marcel Dekker. 631-674.

McCarthy, J.F., and J.M. Zachara. 1989. "Subsurface Transport of Contaminants," *Environmental Science & Technology.* Vol. 23, no. 5, 496-502.

Moore, R.C. Feburary 22, 1996. "Model Parameters for Deprotonation of Lactic Acid, Citric Acid, Oxalic Acid, and EDTA and Complexation of Acetate, Lactate, Citrate, Oxalate, and EDTA with Mg^{2+}, NpO_2^{+}, Am^{3+}, Th^{4+}, and UO_2^{2+} in NaCl Media." Memorandum to C.F. Novak. (Copy on file in the Sandia WIPP Central Files A:1.1.1.1.4: TD:QA; WPO 35307).

Nash, K.L., and G.R. Choppin. 1980. "Interaction of Humic and Fulvic Acids with TH(IV)," *Journal of Inorganic and Nuclear Chemistry.* Vol. 42, no. 7, 1045–1050.

National Institute of Standards and Technology. 1995. *NIST Standard Reference Materials Catalog, 1995-1996.* Washington, DC: Commerce Department, Technology Administration, National Institute of Standards and Technology. 25-38.

Neck, V., J.I. Kim, and B. Kanellakopulos. 1992. "Solubility and Hydrolysis Behavior of Neptunium (V)," *Radiochimica Acta.* Vol. 56, no. 1, 25-30.

Neck, V., W. Runde, and J.I. Kim. 1995. "Solid-Liquid Equilibria of Np(V) in Carbonate Solutions at Different Ionic Strengths: II," *Journal of Alloys and Compounds.* Vol. 225, 295-302.

Neretnieks, I. 1982. *The Movement of a Redox Front Downstream From a Repository for Nuclear Waste.* KBS Report TR 82-16. Stockholm: Svensk Kärnbränsleforsorjning AB.

Nitsche, H. 1987. "Effects of Temperature on the Solubility and Speciation of Selected Actinides in Near-Neutral Solution," *Inorganica Chimica Acta.* Vol. 127, no. 1, 121-128.

Nitsche, H., and N.M. Edelstein. 1985. "Solubilities and Speciation of Selected Transuranium Ions. A Comparison of a Non-complexing Solution with a Groundwater from the Nevada Tuff Site," *Radiochimica Acta.* Vol. 39, no. 1, 23-33.

Nitsche, H., K. Roberts, R.C. Gatti, T. Prussin, K. Becraft, S.C. Leung, S.A. Carpenter, and C.F. Novak. 1992. *Plutonium Solubility and Speciation Studies in a Simulant of Air Intake Shaft Water from the Culebra Dolomite at the Waste Isolation Pilot Plant.* SAND92-0659. Albuquerque, NM: Sandia National Laboratories. WPO 23480.

Nitsche, H., K. Roberts, R. Xi, T. Prussin, K. Becraft, I. Al Mahamid, H.B. Silber, S.A. Carpenter, R.C. Gatti, and C.F. Novak. 1994. "Long Term Plutonium Solubility and Speciation Studies in a Synthetic Brine," *Radiochimica Acta, Special Issue: Chemistry and Migration Behaviour of Actinides and Fission Products in the Geosphere, Proceedings of the Fourth International Conference, Charleston, SC, December 12-17, 1993.* Munich: R. Oldenbourg Verlag. Vol. 66/67, 3-8. WPO 21107.

Novak, C.F. 1995. *The WIPP Actinide Source Term: Test Plan for the Conceptual Model and the Dissolved Concentration Submodel.* SAND95-1985. Albuquerque, NM: Sandia National Laboratories. WPO 27860.

Novak, C.F., and R.C. Moore, March 28, 1996. "Estimates of Dissolved Concentrations for III, IV, V, and VI Actinides in Salado and Castile Brine Under Anticipated Repository Conditions." SNL Tech Memo. (Copy on file in the Sandia WIPP Central File A: WBS 1.2.0.7.1; WBS 1.1.10.1.1: WPO 36207.)

Novak, C.F., R.C. Moore, and R.V. Bynum. 1996. "Prediction of Dissolved Actinide Concentrations in Concentrated Electrolyte Solutions: A Conceptual Model and Model Results for the Waste Isolation Pilot Plant (WIPP)," *Proceedings of the International Conference on Deep Geological Disposal of Radioactive Waste, Winnipeg, Manitoba, Canada, September 16-19, 1996.*

Papenguth, H.W. 1996a: H.W. Papenguth to Christine T. Stockman: "Parameter Record Package for Colloidal Actinide Source Term Parameters" May 7, 1996: Attachment A: Rationale for Definition of Parameter Values for Actinide Intrinsic Colloids." WPO 35852.

Papenguth, H.W. 1996b: H.W. Papenguth to Christine T. Stockman: "Parameter Record Package for Colloidal Actinide Source Term Parameters" May 7, 1996: Attachment A: Rationale for Definition of Parameter Values for Microbes." WPO 35856.

Papenguth, H.W. 1996c: H.W. Papenguth to Christine T. Stockman: "Parameter Record Package for Colloidal Actinide Source Term Parameters" May 7, 1996: Attachment A: Rationale for Definition of Parameter Values for Humic Substances." WPO 35855.

Papenguth, H.W. 1996d: H.W. Papenguth to Christine T. Stockman: "Parameter Record Package for Colloidal Actinide Source Term Parameters" May 7, 1996: Attachment A: Rationale for Definition of Parameter Values for Mineral Fragment Type Colloids." WPO 35850.

Papenguth, H.W., and Y.K. Behl. 1996. "Test Plan for Evaluation of Colloid-Facilitated Actinide Transport at the Waste Isolation Pilot Plant." SNL Test Plan TP 96-01. (Copy on file in the Sandia WIPP Central File A:1.1.10.2.1. PUB:QA; WPO 31337.)

Pitzer, K.S., ed. 1991. *Activity Coefficients in Electrolyte Solutions.* 2nd ed. Boca Raton, FL: CRC Press.

Pryke, D.C., and J.H. Rees. 1986. "Understanding the Behaviour of the Actinides Under Disposal Conditions: A Comparison between Calculated and Experimental Solubilities," *Radiochimica Acta.* Vol. 40, no. 1, 27-32.

Rai, D., and R.G. Strickert. 1980. "Chemical Aspects of Medium- and Long-Term Radioactive Waste Disposal," *Transactions of the American Nuclear Society and the European Nuclear Society.* Vol. 35, 185-186.

Rai, D., and J.L. Swanson. 1981. "Properties of Plutonium(IV) Polymer of Environmental Importance," *Nuclear Technology.* Vol. 54, no. 1, 107-111. WPO 30420.

Rai, D., R.J. Serne, and D.A. Moore. 1980. "Solubility of Plutonium Compounds and Their Behavior in Soils," *Soil Science Society of America Journal.* Vol. 44, no. 3, 490-495.

Rai, D., R.G. Strickert, and G.L. McVay. 1982. "Neptunium Concentrations in Solutions Contacting Actinide-Doped Glass," *Nuclear Technology.* Vol. 58, no. 1, 69-76.

Rai, D., A.R. Felmy, and R.W. Fulton. 1995. "Nd^{3+} and Am^{3+} Ion Interactions with Sulfate Ion," *Journal of Solution Chemistry.* Vol 24, no. 9, 879-895.

Rao, L., and G.R. Choppin. 1995. "Thermodynamic Study of the Complexation of Neptunium(V) with Humic Acids," *Radiochimica Acta.* Vol. 69, no. 2, 87-95.

Rao, L., D. Rai, A.R. Felmy, R.W. Fulton, and C.F. Novak. 1996. "Solubility of $NaNd(CO_3)_2 \cdot 6H_2O$ in Concentrated Sodium Carbonate and Sodium Bicarbonate Solutions." *Radiochimica Acta.* In press. WPO 36484.

Reed, D.T., D.G. Wygmans, and M.K. Richman. 1996. "Actinide Stability/Solubility in Simulated WIPP Brines." Interim Report under SNL WIPP Contract AP-2267. (Copy on file in the Sandia WIPP Central files.)

Refait, Ph. and J.-M.R. Génin. 1994. "The Transformation of Chloride-Containing Green Rust One Into Sulphated Green Rust Two by Oxidation in Mixed Cl^- and SO_4^{2-} Aqueous Media," *Corrosion Science.* Vol. 36, no. 1, 55-65.

Robinson, R.A., and R.H. Stokes. 1959. *Electrolyte Solutions, The Measurement and Interpretation of Conductance, Chemical Potential, and Diffusion in Solutions of Simple Electrolytes.* 2nd ed. (revised). London, England: Butterworths.

Ross, S., and I.D. Morrison. 1988. *Colloidal Systems and Interfaces.* New York. NY: John Wiley & Sons.

Runde, W. and J.I. Kim. 1994. *Untersuchungen der Übertragbarkeit von Labordaten natürliche Verhältnisse. Chemisches Verhalten von drei- und fünfwertigem Americium in salinen NaCl-Lösungen.* Report RCM-01094, Munich: Institut für Radiochemie, Technische Universität München. (Available from National Technical Information Service, 555 Port Royal Road, Springfield, VA, 22161, 703/487-4650 as DE 95752244.)

Sagoe-Crentsil, K.K., and F.P. Glasser. 1993. " 'Green Rust', Iron Solubility and the Role of Chloride in the Corrosion of Steel at High pH," *Cement and Concrete Research.* Vol. 23, no. 4, 785-791.

Sanchez, L.C., and H.R. Trellue. January 17, 1996. "Estimation of Maximum RH-TRU Thermal Heat Load for WIPP." WPO 31165.

Schnitzer, M., and S. I. M. Skinner. 1967. "Organo-Metallic Interactions in Soils: 7 Stability Constants of Pb^{++}, Ni^{++}, Mn^{++}, Co^{++}, Ca^{++}, and Mg^{++} - Fulvic Acid Complexes," *Soil Science*. Vol. 103, no. 4, 247-252.

Siegel, M.D. 1996. "Solubility Parameters for Use in the CCA NUTS and GRIDFLOW Calculations." SNL Technical memorandum dated 29 March 1996 to Martin S. Tierney. (Copy on file in the Sandia WIPP Central File A:WBS 1.2.0.7.1; WBS 1.1.10.61: WPO 35835.) Also WPO 37314.

Storz, L. June 24, 1996. "Estimate of the Amount of $Ca(OH)_2$ Contained in the Portland Cement Fraction of the Waste for Disposal in the WIPP," Memorandum to Yifeng Wang. (Copy on file in Sandia WIPP Central File A: WBS 1.1.09.1.1: WPO 40351.)

Stumm, W. 1992. *Chemistry of the Solid-Water Interface.* New York, NY: John Wiley & Sons, Inc.

Stumm, W. 1993. "Aquatic Colloids as Chemical Reactants: Surface Structure and Reactivity," *Colloids in the Aquatic Environment.* Ed. T.F. Tadros and J. Gregory. New York, NY: Elsevier Applied Science. (Reprinted from Colloids and Surfaces. Vol. 73, 1-18.)

Trauth, K.M., S.C. Hora, R.P. Rechard, and D.R. Anderson. 1992. *The Use of Expert Judgment to Quantify Uncertainty in Solubility and Sorption Parameters for Waste Isolation Pilot Plant Performance Assessment.* SAND92-0479. Albuquerque, NM: Sandia National Laboratories. WPO 23526

Vold, R.D., and M.J. Vold. 1983. *Colloid and Interface Chemistry.* Reading, MA: Addison-Wesley.

Wang, Y. March 18, 1996a. "Define Chemical Conditions for FMT Actinide Solubility Calculations," Memorandum to Malcolm D. Siegel, Sandia WIPP Central File A:WBS 1.1.09.1.1. WPO 37038.

Wang, Y. July 19, 1996b. "Evaluation of the Thermal Effect of Exothermal Chemical Reactions for WIPP Performance Assessment," memorandum to Richard Vann Bynum and Laurence H. Brush. (Copy on file in the Sandia WIPP Central File A:1.1.0.9.1.1.CO/COM:QA; WPO 39871.)

Wang, Y. and L. Brush. January 26, 1996. "Estimates of Gas-Generation Parameters for the Long-Term WIPP Performance Assessment." WPO 31943.

Weiner, R. 1996. "Documentation Package For: Oxidation State Distribution of Actinides in the Repository." SNL Technical memorandum dated 27 March 1996 to SWCF-A: Records Center, SWCF-A: WBS 12.1.10.1.1:PDD: QA: Dissolved Species: Oxidation State Distribution: Actinides: OX3: OX4: OX5: OX6 (WPO 35194).

WIPP Performance Assessment Department. 1992. *Preliminary Performance Assessment for the Waste Isolation Pilot Plant, December 1992. Volume 2: Technical Basis.* SAND92-0700/2. Albuquerque, NM: Sandia National Laboratories. WPO 20805.

WIPP Performance Assessment Department. 1995. *User's Manual for FMT, Version 2.0,* WPO 28119.

WIPP Performance Assessment Department. 1996. *User's Manual for NONLIN, Version 2.0,* WPO 30740.

Wolery, T.J. 1992. *EQ3/6, A Software Package for Geochemical Modeling of Aqueous Systems: Package Overview and Installation Guide (Version 7.0).* UCRL-MA-110662 PT 1. Livermore, CA: Lawrence, CA: Lawrence Livermore National Laboratory.

Wolery, T.J., and S.A. Daveler. 1992. *EQ6, A Computer Program for Reaction Path Modeling of Aqueous Geochemical Systems: Theoretical Manual, User's Guide, and Related Documentation (Version 7.0).* UCRL-MA-110662-Pt. 4. Livermore, CA: Lawrence Livermore National Laboratory.

Wood, J.R. 1975. "Thermodynamics of Brine-Salt Equilibria. I. The Systems NaCl-KCl-$MgCl_2$-$CaCl_2$-H_2O and NaCl-$MgSO_4$-H_2O at 25°C," *Geochimica et Cosmochimica Acta.* Vol. 39, no. 8, 1147-1163.

ATTACHMENTS

Attachment 1: WIPP Performance Assessment, User's Manual for FMT, Version 2.0. WPO 28119

Attachment 2: WIPP Performance Assessment, User's Manual for NONLIN, Version 2.0. WPO 20740

THIS PAGE INTENTIONALLY LEFT BLANK